Role of multiparametric MRI In post Transarterial Chemoembolisation response evaluation of Hepatocellular Carcinoma(HCC)

THESIS

SUBMITTED IN PARTIAL FULFILLMENT FOR DEGREE OF

DM CARDIOVASCULAR IMAGING AND VASCULAR INTERVENTIONAL RADIOLOGY

(2018-2020)

OF

SREE CHITRA TIRUNAL INSTITUTE FOR MEDICAL SCIENCES AND TECHNOLOGY, TRIVANDRUM, INDIA

DR. B MAHESH REDDY

DEPARTMENT OF IMAGING SCIENCES & INTERVENTIONAL RADIOLOGY

SREE CHITRA TIRUNAL INSTITUTE FOR MEDICAL SCIENCES AND TECHNOLOGY, TRIVANDRUM, INDIA

CERTIFICATE

This is to certify that the work incorporated in this thesis titled **"Role of multiparametric MRI In post-Transarterial Chemoembolisation response evaluation of Hepatocellular Carcinoma(HCC)"** *for the degree of* **DM CARDIOVASCULAR IMAGING AND VASCULAR INTERVENTIONAL RADIOLOGY** *has been carried out by* ***DR. B MAHESH REDDY*** *under our supervision and guidance. The work done in connection with this thesis has been carried out by the candidate himself and is genuine.*

Dr. Jineesh V
Assistant Professor
Chief Guide

Dr. Santhosh Kumar K
Associate Professor
Co-Guide

Dr. Anoop Ayyappan
Assistant Professor
Co-Guide

Dr. kapilamoorthy T. R
Professor
Co-Guide

Dr. Kesavadas C
Professor & HOD
Department of Imaging Sciences and Interventional Radiology,
SCTIMST, Thiruvananthapuram

DECLARATION

I hereby declare that this thesis titled **"Role of multiparametric MRI In post-Transarterial Chemoembolisation response evaluation of Hepatocellular Carcinoma(HCC)"** *has been prepared by me under the supervision and guidance of Dr. Jineesh V(Assistant Professor), Dr.Santhosh Kumar K (Associate Professor), Dr. Anoop A(Assistant Professor), Dr.Kapilamoorthy T.R(Professor), Department of Imaging Sciences and Interventional Radiology, Sree Chitra Institute for Medical Sciences and Technology, Trivandrum.*

B. Mahesh Reddy

Date: 31/08/2020
Place: Thiruvananthapuram

(Dr. B Mahesh Reddy)
Senior Resident

ACKNOWLEDGEMENT

- *I am deeply indebted to my teachers & guides especially Dr. Jineesh V, Dr. Santosh Kumar K, Dr. Anoop A, of Department of Imaging Sciences and Interventional Radiology, for their constant unwavering support, insightful criticism, expert supervision and immense patience throughout this study.*

- *I am profoundly grateful to Dr. Kesavadas C and Dr. Kapilamoorthy TR, for their omnipresent support and guidance during this tenure.*

- *I would especially like to acknowledge my gratitude to my past and present colleagues and the technologists of the Department of IS and IR and the advanced radiology technology trainees of the department for their valuable assistance at all times during this study.*

- *I would also especially like to acknowledge my gratitude to Jissa V. T and Mr. Shankar Sharma sir for assisting in carrying out the statistical analysis of the study.*

- *I would also like to extend my heartfelt gratitude to my family for being immensely supportive through my endeavors. I could not have achieved what I have without their prayers, love, and support.*

- *Finally, I am eternally grateful to all my patients & their relatives who have been very understanding and generous with their cooperation all through the study.*

ABBREVIATIONS

ADC- apparent diffusion coefficient

AF- Arterial Fraction

AHBF)-Arterial hepatic blood flow

BCLC- Barcelona clinic liver cancer

CLD- Chronic liver disease

D- D slow or true diffusion coefficient

D*- pseudodiffusion coefficient

DCE-Dynamic contrast enhancement

DV-distribution volume

EASL- European Association for the Study of the Liver

EES- Extravascular extracellular space

f- perfusion fraction

HCC-Hepatocellular carcinoma

IAUC -initial area under curve

k2=transfer constant from the tissue to the central vein,

ka=transfer constant from the arterial plasma to the surrounding tissue,

kp=transfer constant from the portal venous plasma to the surrounding tissue,

IAUGC- Initial area under Gadolinium concentration curve

LGU- Lipiodal good uptake

LPU- Lipiodal poor uptake

LR- liver resection

LT-liver transplantation

MTT- mean transit time

mRECIST- modified Response Evaluation Criteria in Solid Tumors

OATP - organic anionic transporting polypeptide

PHBF- portal venous hepatic blood flow

RECIST- Response Evaluation Criteria in Solid Tumors

ROI-region of interest

Signal to noise ratio(SNR)

Signal intensity(SI)

CONTENTS

Synopsis

Introduction- MR perfusion imaging of the liver computes the temporal changes in tissue enhancement after intravenous administration of contrast media. By this hemodynamical characteristics of the tumor changes with time can be assessed. Besides quantification of the parameters is also possible. IVIM imaging is a newer MRI which uses some principles similar to diffusion-weighted imaging using multiple b values but with a separate perfusion map. The imaging sequence can be done without contrast administration. The present study was done to know the feasibility and efficacy of MR perfusion, IVIM imaging, and the role of multiparametric MRI in post TACE response assessment of HCC.

Aims and Objectives- To assess the feasibility and efficacy of imaging sequences like MR perfusion, Intravoxel incoherent motion (IVIM) imaging in post trans-arterial Chemoembolization(TACE) response evaluation of HCC. To compare the changes in HCC between preTACE and postTACE values in MR perfusion and Intravoxel incoherent motion (IVIM) imaging.

Methods and materials - 26 patients with 32 lesions underwent MRI on a 3T MRI machine() 1-2 weeks before and 6weeks after TACE. Values of MR perfusion like Ktrans, Kep, Ve, max slope, IAUGC, and IVIM parameters like D, D*,f, ADC were measured. Lesions were divided into complete response lesions (group 1) and residual or viable or nonresponding lesions(group 2). The values of MR perfusion and IVIM parameters before and after TACE were compared using paired T-tests. Mean differences between complete response lesions (group 1) and residual or viable or nonresponding lesions(group 2) were compared using the T-test of unequal variances. ROC curve analysis was done for calculating sensitivity and specificity and also for proposing cutoff values.

Results- In complete responding (group 1) lesions, significant differences between mean preTACE and postTACE values of Ktrans, Kep, IAUGC, D, D*, f, ADC was noted . There was no significant differences between preTACE and postTACE values of Ve and max slope were noted. In nonresponding (group 2)lesions, no significant difference between mean preTACE and postTACE values of MR perfusion and IVIM parameters was noted. In complete responding(group 1) lesions and nonresponding (group 2)lesions, mean differences between preTACE and postTACE values were significant in Kep and D. In ROC curve analysis, among MR perfusion parameters, Kep has highest AUC with a sensitivity and specificity of 77.27% and 60% respectively. Ktrans and Kep have the highest sensitivity of 77.27%. Ktrans and max slope have the highest specificity of 80%. 'Ve' and Kep has less specificity of 60%. Among IVIM D has the highest AUC with a sensitivity and specificity of 77.27% and 60%. Combined D and f have a

specificity of 90% which is similar to ADC and combined D and D* sensitivity have a sensitivity of 63.2% which is higher than ADC.

Conclusions: MR perfusion and IVIM imaging are feasible to assess the response in HCC lesion after TACE . It is the change in the values between preTACE and postTACE parameters but not the absolute values that indicate the response. MR perfusion has adjunct value in assessing the response after TACE. However, it cannot be used as standalone in the assessment of response because of relatively less sensitivity and specificity compared to contrast MRI. Ktrans, Kep, and IAUGC can be used as an adjunct to the visual assessment especially useful in equivocal cases. IVIM parameters can be used as an adjunct to contrast enhancement and as standalone in cases where contrast injection is contraindicated. Thus multiparametric MRI imaging especially IVIM parameters provides better assessment in the evaluation of postTACE response for HCC.

INTRODUCTION

INTRODUCTION

Hepatocellular carcinoma(HCC) is the fourth most common cause of cancer-related death in the world(1). Risk factors for HCC include chronic hepatitis B, chronic hepatitis C, chronic alcohol intake, metabolic liver disease (particularly non-alcoholic fatty liver disease), exposure to dietary toxins, etc.(1). There are several staging or classification systems for management of HCC of which Barcelona clinic liver cancer (BCLC) staging is the most commonly used system(2).In this classification system of treatment, Trans-arterial chemoembolization (TACE) is done in intermediate stage(BCLC B) as a palliative treatment or to downstage the tumor to be within Milan's criteria in patients planning for liver transplantation. TACE can also be done in early-stage HCC and also in advanced stage HCC when recommended treatments are not feasible(2,3). Based on technique TACE can be of two types: conventional TACE (c-TACE) which uses lipiodol as a carrier for the chemotherapeutic agent and drug-eluting bead TACE (DEB-TACE) where special particles are used for carrying the chemotherapeutic agent. In terms of survival benefit, no difference exists between the two techniques; however, DEB-TACE provides better patient tolerance (4). Tumor response is crucial as it decides the further management. Various criteria for response assessment like WHO criteria, RECIST criteria, EASL criteria, m-RECIST criteria are used. While the former two criteria assess the decrease in the overall size of the tumor, the latter two criteria access the viable(enhancing) portions of the lesion after treatment with m-RECIST which followed widely criteria for response assessment. Recently Liver imaging and Reporting data system (LIRADS) also addresses treatment response(5,6).

Persistent hyperaemia and inflammatory changes in peritumoral areas confound the early assessment of tumor response. Moreover in TACE or antiangiogenic treatment, there is a decrease in contrast enhancement without obvious tumor necrosis as these treatments affect tumor microvasculature and permeability. So conventional CT/ MRI sequences take at least a delay of 4-6 weeks to determine response after TACE. Routine CT and MRI give only qualitative analysis without any quantitative parameters. In CT lipoidal staining in postTACE may interfere with contrast enhancement assessment whereas, in MRI, post-treatment T1 hyperintensities due to coagulative necrosis(postRFA), haemorrhage (in post embolization) may interfere with contrast enhancement assessment. Functional imaging techniques like CT/MR perfusion, DWI, and IVIM, CEUS may help in identifying and quantifying the perfusion and permeability changes not only to assess but also for earlier detection of response. CT perfusion is a good tool, however, MRI is preferred due to lack of radiation, superior soft-tissue resolution, higher contrast to noise ratio, non-interference of lipiodol with enhancement features, and its multiparametric capability (7).

MR perfusion imaging of liver computes the temporal changes in tissue enhancement after intravenous administration of contrast media. By this how hemodynamical characteristics of the tumor changes with time can be assessed. Besides quantification of the parameters is also possible. IVIM imaging is a newer MRI which uses some principles similar to diffusion-weighted imaging using multiple b values but with a separate perfusion map. The imaging sequence can be done without contrast administration. The present study was done to know the feasibility and efficacy of MR perfusion, IVIM imaging, and the role of multiparametric MRI in post TACE response assessment of HCC.

Review of literature

Review of literature

Hepatocellular carcinoma is the fourth most common cause of cancer-related death in the world(1). According to the Global Burden of Disease Study, there were 854,000 incident cases and 810,000 deaths due to liver cancer globally contributing to 20,578,000 disability-adjusted life years (DALYs) in the year 2015. Globally, hepatitis B virus (HBV) is estimated to account for 33% of liver cancer deaths, alcoholism for 30%, hepatitis C virus (HCV) for 21%; these relative figures show substantial variation between countries(8). Data on the incidence of HCC in India as reported by various population-based registries show a marked (>30-fold) variation in crude and age-adjusted incidence rates of HCC. Estimates based on these data suggest that the crude incidence rate of HCC in India is 2.8 cases per 100,000 population per year (males: 3.9, females: 1.6), with mortality rate 2.7 per 100,000 population per year. The registry data also suggest a slight increase in the incidence of HCC over time, but whether this reflects a true increase remains uncertain. An Indian study showed the incidence of HCC as 1.6 per 100 person-years of follow-up in patients with cirrhosis, with fairly wide confidence intervals (0.55-2.64)(9).

Liver circulation in HCC

The knowledge of liver blood flow is paramount in the interpretation of the CT and MRI of the liver. The liver is a highly vascular organ that contains sinusoids (porous channels) with fenestrae through which hepatic artery (25%)and portal venous(75%) blood diffuse into adjacent interstitial space called space of Dissie. Space of Disse contains stellate cells and collagen III fibers. Stellate cells play a major role in fibrogenesis in various liver pathologies. Hepatocytes were arranged in the form of rows called hepatic cords adjacent to the space of Dissie. There is usually a free exchange of low molecular weight compounds between sinusoids and the space of Dissie due to the large size of fenestrae. But in cirrhosis capillarization of sinusoids occurs due to deposition of the basement membrane and new formation of capillary tight junctions. Space of Dissie also enlarges due to the deposition of fibers by the increased number of stellate cells. This causes a decrease in the transfer of low molecular weight compounds from sinusoids into interstitial space. After a long period of chronic liver disease, cirrhosis develops which contains different types of nodules ranging from benign to malignant. Thus HCC is a multistep process with sequential development of regenerative nodules, low-grade dysplastic nodules, high-grade dysplastic nodules, well-differentiated, poorly differentiated, and undifferentiated HCC. The nodules initially show dominant portal venous flow and normal arterial flow. But with sinusoidal

capillarization and hepatic neo-angiogenesis, it gets its supply completely from the hepatic artery. In this process, cell density increases, Kupffer cells decrease, hemodynamic changes occur, and also OATP (organic anionic transporting polypeptide) transporters of bile salts decreases. Hemodynamical changes in tumor sequentially in which there is portal flow dominance (in low-grade dysplastic nodules), followed by the codominant flow of both hepatic arterial and portal flow (in high-grade dysplastic nodule). HCC takes the blood flow only from the hepatic artery(10).

Diagnosis of HCC

When a nodule >1cm is detected in surveillance or random ultrasonogram in a cirrhotic liver dynamic CT/ MRI are recommended as first-line diagnostic tools for HCC as per AASLD guidelines(10). The classical features of HCC (arterial phase enhancement and washout in the portal-venous phase) can only be applied to cirrhotic patients having nodule(s) ≥1 cm. In nodules of size <1 cm, a three-monthly follow-up is recommended for one year using ultrasound to detect any increase in size. Multiphase CT/ MRI should be done if there is an increase in the size of the lesion. If CT/MRI imaging is typical of HCC in cirrhotic liver, no tissue diagnosis is required. Based on this, all guidelines (AASLD Guideline, the National Comprehensive Cancer Network (NCCN) Guideline, EASL guideline, Japan Society of Hepatology (JSH) Guideline) has approved the imaging diagnosis of HCC ≥1cm in cirrhotic patients if arterial enhancement with portal venous washout is presently obviating the need of liver biopsy(11,12). Lesion showing the atypical pattern for HCC in one of the dynamic cross-section multiphasic scans(CT/MRI) should undergo other multiphasic scans (CT/MRI). If in the second cross-sectional imaging the features are typical of HCC then a biopsy is not necessary. If in both modalities of imaging(contrast CT and MRI) the features are atypical of HCC, then histological confirmation for diagnosis of HCC is required(9). In patients with renal failure (eGFR<30ml/min), contrast-enhanced ultrasound with SonoVue is recommended for a lesion detected on Ultrasound(13,14). Tissue diagnosis is indicated when imaging and other findings are equivocal or not typical or suspected HCC which are smaller than 2 cm and in lesions in non-cirrhotic livers(9).

Tumor markers

AFP(alpha-fetoprotein), PIVKA II(Protein induced by vitamin K antagonist-II) are used as tumor markers for HCC. Of these only AFP is extensively studied. Serum AFP estimation is a useful test for the management of HCC. However, AFP alone is not recommended for surveillance or diagnosis of HCC. But it can be used in monitoring response to locoregional therapy(9,15). However, it is not included in the BCLC guidelines but baseline AFP is recommended by the Indian National Association for Study of the Liver (INASL) before locoregional therapy. PIVKA II is also a biomarker for HCC diagnosis and

prognosis. PIVKA II along with AFP has a sensitivity and specificity of 94% and 98% respectively in detecting HCC. Japanese clinical guidelines recommended the use of both AFP and PIVKA II for diagnosis of HCC, management of the high-risk population, the prognosis of anticancer treatment(16).

Classification systems in HCC

There are several classification systems used for the management of HCC like Okuda staging system, Hong Kong Liver classification system, American joint committee on cancer/TNM staging system, and Barcelona clinic Liver cancer classification(BCLC) system. Of these BCLC is the best and most widely used one(17)(fig 1). The patients under BCLC B were subclassified by Bolondi et al into B1-B4 since this group comprised a wide spectrum and greater heterogeneity. They have proposed alternative lines of management in sub-categories of BCLC B(18)(Table 1)

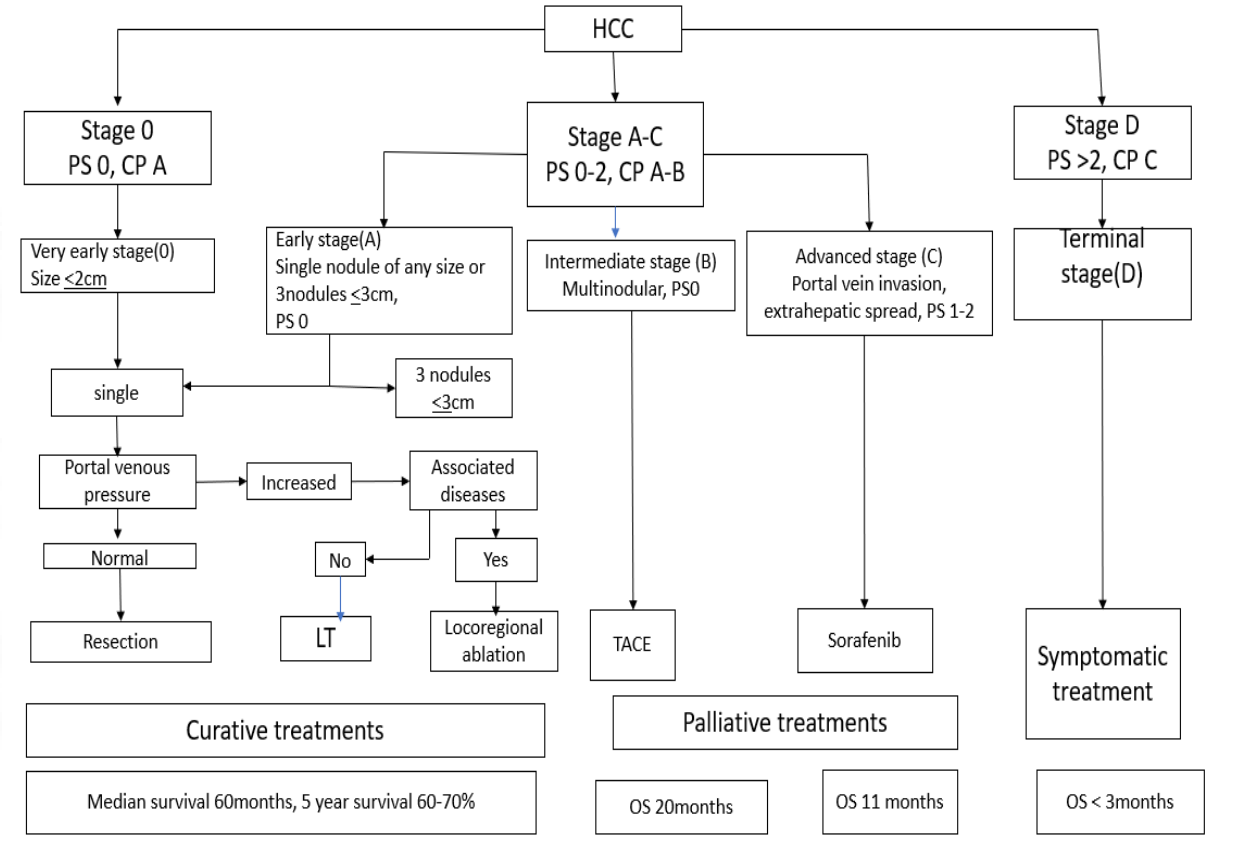

Figure 1. BCLC classification system

CP- Child-Pugh score, PS- performance status, LT -Liver transplantation, OS overall survival

Table 1- BCLC stage B subclassification

Substage		B1	B2	B3	B4
Child Pugh score		5-6-7	5-6	7	8-9(with severe /refractory ascites and /or jaundice)
Beyond Milan and within Ut-7		In	Out	Out	Any
ECOG(tumor related) PS		0	0	0	0-1
Portal vein thrombosis		-	-	-	-
Treatment	1st option	TACE/LT	TACE	Research trials	LT (only if Ut 7IN and PS 0)
	Alternative	TACE+ Ablation	TARE or Sorafenib	TACE +/-sorafenib	-

Ut -7 -Upto 7 criteria, LT -Liver transplantation

Up to 7 criteria are defined as the sum of the size of the largest tumor in cm and the total number of tumors in the absence of tumor microvascular invasion.

Management protocol in HCC

In very early (≤2cm)and early-stage HCC (≤ 3cm), liver resection(LR) is the treatment of choice in the non-cirrhotic liver with favorable outcomes provided an R0 resection with clear margin can be carried out with adequate future liver remnant (FLR)(19). In cirrhotics in early disease (BCLC) treatment options include liver transplantation or loco-ablative procedures like RF ablation, microwave ablation. In resectable HCC, both resection and RFA were having comparable results in terms of overall survival and disease-free progression(20,21). In cirrhotic patients, liver transplantation(LT) is the ideal treatment option if it is within Milan's criteria or University of California San Francisco (UCSF) extended criteria(solitary tumor < 6.5 cm, or patients having ≤3 nodules, with the largest lesion being ≤4.5 cm, or having a total tumor diameter <8.5 cm without vascular invasion)(22). Other treatments like Percutaneous alcohol ablation, microwave ablation, and Irreversible electrophoresis also can be done in the early stage. In cases where LT or LR cannot be done, RFA is preferred if lesion ≤ 3cm and in a favourable location. If the lesion is between 3 cm and 5cm, combined RFA and TACE can be offered. However long term survival outcomes and recurrence rates are inferior to liver resection(23) in early HCC.

The treatment recommended in the intermediate stage [(BCLC B) which is large or multinodular, non-invasive, confined to the liver, with good liver function (Child-Pugh A or B), and good clinical status (performance status ≤2)]is TACE. However, the reach of TACE has progressed to other stages including early and late stages. It can be done in patients of early HCC (BCLC stage A), when there are technical limitations for local ablation and also for downstaging the lesion size and stage in patients awaiting transplant(9). TACE can also be done as combination therapy with RFA(24,25) or antiangiogenic treatment (sorafenib) in large and advanced tumors(26,27). However TACE is contraindicated in patients with poor liver function (Child-Pugh C), hepatic encephalopathy, poor performance status (ECOG>2), un-correctable coagulopathy, main portal vein thrombosis, and in pregnancy(9). In advanced HCC (BCLC C), TARE or sorafenib is recommended treatment(28). In a very advanced stage or BCLC D, best supportive care is the treatment recommended. However, depending on the tumor burden, macrovascular invasion, and extrahepatic spread, other treatments like immunotherapy, hormonal therapy, and radiotherapy also can be considered(9,29).

Imaging and response evaluation

There are many in response assessment criteria in post TACE lesions like WHO criteria, RECIST & RECIST 1.1, EASL, mRECIST, Choi criteria(Table 2). WHO and RECIST assessment is based on the residual size of the lesion whereas mRECIST and EASL criteria (fig 2) are based on the residual arterial enhancing lesion. Choi criteria are CT based which depends on the size of the lesion and Hounsfield units(HU) which is initially proposed for GIST and later extended to HCC. Residual Size-based criteria are poor predictors of patient survival after TACE (30). RECIST first introduced the concept of measurable disease but was not able to account for lesion enhancement characteristics. Besides features like irregular, confluent or circumferential tumor morphology, asymmetric size changes, and differential lesion response were also not appropriately addressed. They also did not consider multiplanar length or tumor volume for response assessment. Both mRECIST and EASL criteria introduced the concept of 'viable tumor' which corresponds to the arterial enhancing portion of the tumor after intravenous contrast administration (excluding necrotic [non-enhancing] areas). Tumor viability is determined by arterial enhancement alone in the mRECIST criteria whereas in EASL criteria takes into consideration both arterial and portal venous phase images. mRECIST measures the single largest diameter of the enhancing area whereas EASL criteria measure the largest axial bidimensional diameters of the enhanced area of the lesion. Meta-analysis showed no difference between mRECIST and EASL criteria for the assessment of tumor response(31). Thus mRECIST or EASL criteria have a better reproducibility and predictability of survival and is used to assess response in thermal ablation, TACE and also in systemic targeted therapies(like

sorafenib,) where predominantly tissue necrosis with decreased perfusion occurs with or without much decrease in size(32–35). Among these mRECIST criteria is most widely used across the world.

Table 2- Criteria for response assessment after locoregional therapy in patients with HCC

Type of tumor response	WHO criteria	RECIST criteria	EASL criteria	mRECIST criteria
Complete response(CR)	The disappearance of all target lesions	The disappearance of all target lesions	The complete absence of enhancing tumor regions	The complete absence of enhancing tumor regions in all target lesions
Partial response(PR)	≥50% decrease	≥30% decrease	≥50% decrease of enhanced areas	≥30% decrease in the sum of diameters of enhancing areas of target lesions
Stable disease(SD)	Cases in between partial response and progressive disease	Cases in between partial response and progressive disease	Cases in between partial response and progressive disease	Cases in between partial response and progressive disease
Progressive disease(PD)	≥25% increase or new lesions	≥20% increase or new lesions	≥25% increase in enhancing lesions or new enhancing lesions	>20% increase in sum of the diameters of enhancing target lesions

LI-RADS CT/MRI treatment response algorithm

The Liver Imaging Reporting And Data System (LI-RADS) is a comprehensive system to standardize the terminology, technique, interpretation, reporting, and data collection of liver lesion imaging. The LI-RADS also includes an algorithm for assessing treatment response which can be applied to patients with liver malignancies treated by ablation techniques, intra-arterial therapies, or external beam radiation therapy. This is based on the assessment of tumor viability visually and is defined as nodular, mass-like,

or thick, irregular tissue in or along the treated lesion showing arterial enhancement or delayed washout appearance, or enhancement characteristics similar to that observed before treatment. It includes viable tumor,(LR TR viable), nonviable tumor(LR TR non- viable), and also category of "equivocal enhancement" when the tumor shows atypical enhancement which does not meet criteria for probable or definite viability(36).

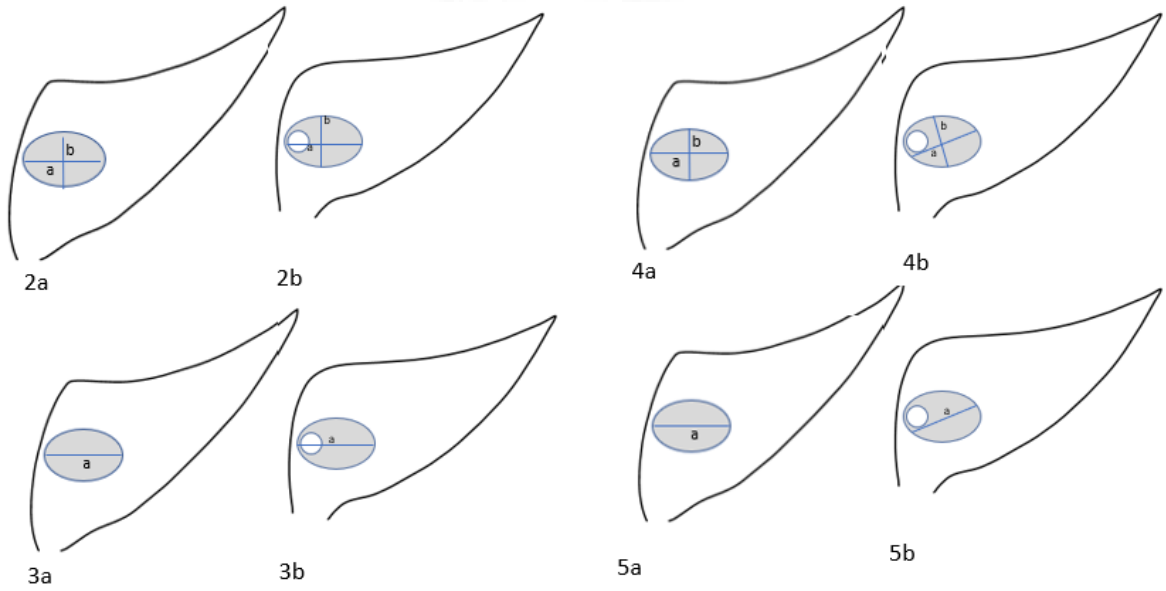

Fig 2 -5 Various response assessment criteria

Fig 2 showing WHO response assessment criteria 2a showing enhancing tumor before treatment with diameters a and b, 2b showing smaller tumor before treatment with diameters a and b irrespective of tumor enhancement

Fig 3 RECIST criteria, 3a showing enhancing tumor before treatment with a maximum diameter 'a', 3b showing smaller tumor after treatment with maximum diameter 'a' irrespective of tumor enhancement

Fig 4 EASL criteria 4a showing enhancing tumor before treatment diameters with 'a' and 'b', 4b showing the tumor before treatment with diameters a and b including only enhancing tumor portion

Fig 5 mRECIST criteria 5a showing enhancing tumor before treatment with maximum diameter 'a', 5b showing tumor after treatment with a maximum diameter an including only tumor enhancement

Limitations of the present response assessment criteria

mRECIST and EASL are used widely in post TACE response with good effect. However, there are some issues in the criteria. They include

a)Lipoidal deposition after TACE which appears hyperdense in CT may cause difficulties in differentiating tumor enhancement versus lipiodol hyperattenuation. Since mRECIST and EASL criteria assume that tumor areas containing lipiodol are necrotic and also that several studies have shown a strong correlation between the amount of lipiodol deposition, the extent of tumor necrosis, and the degree of tumor devascularisation**,** homogenous lipiodol deposition in CT helps to identify tumors with major necrosis. Lipiodol having iodine can hinder the assessment of arterial enhancement in CT and may cause underestimation of residual disease in CT(37). MRI which is relatively insensitive to lipiodol is a better modality than CT in response evaluation.

b) MRI is not full proof in post-TACE/RFA evaluation since coagulative necrosis after thermal ablation, liquefactive necrosis, haemorrhage may also appear T1 hyperintense in precontract images creating difficulties in assessing post-contrast enhancement. This can be overcome by using arterial subtracted images(arterial – baseline scan)(38,39). However since the pixels are threshold-based, if the precontract T1 signal is very high, the arterial enhancement may be missed even in subtracted arterial images

c)Infiltrative and non-enhancing HCC (around 20% of HCC) may present as an ill-defined lesion with infiltrative margins and develop with a predominantly intravascular growth pattern without arterial enhancement in imaging. In such cases, the response cannot be evaluated by the mRECIST criteria. m-RECIST and EASL criteria have stated that response in such cases should be done using RECIST criteria and consider them as non-target lesions and reporting only as to whether the disease is present or absent or progressive(30).

d) These criteria are usually applied after 4-6weeks which causes delays in response assessment which further will delay the management.

e) Another challenge using these criteria is in post TARE response assessment in which severe post-inflammatory changes and fibrosis associated with delayed shrinkage cause a delay in response assessment.

f) The arterial enhancement is subjective and qualitative

Since the current criteria are based on arterial enhancement, there are some limitations a few groups of cases there is a need for exploring alternate properties of the tumor other than arterial enhancement in addressing these niche situations. This opens the realm of functional imaging

Functional Imaging

Viable tumor based criteria only assesses the visual appearance of enhancement which is qualitative The microvascular and capillary level changes that indicate perfusion and permeability changes occur can occur than 6 weeks can be assessed by using functional imaging techniques. As these changes occur before morphological changes, early response assessment is possible with these techniques.

Techniques of functional imaging include

- Diffusion-weighted and IVIM imaging
- Perfusion imaging- MR perfusion/CT perfusion/ CEUS perfusion
- Metabolic imaging using PETCT or PETMR

Using functional imaging techniques treatment induced tumor modification(like necrosis, devascularisation, perfusion, and permeability changes) can be objectively quantified. This may be especially useful particularly in treatments like TACE or antiangiogenic treatments where obvious necrosis might not be present with the only decrease in contrast enhancement. Functional imaging can identify responses earlier than morphological criteria which are very useful in planning further treatment as early as possible(40). As the use of novel treatments like newer antiangiogenic drugs and immunotherapy is on the rise, new response criteria including functional imaging are need of the hour.

MR Perfusion imaging

The principle of MR perfusion imaging of the liver is based on dynamic contrast-enhanced imaging (DCE) that compute the temporal changes in tissue enhancement after intravenous administration of contrast media. Different types of techniques like T2 susceptibility-weighted imaging, T1 weighted imaging, and arterial spin labeling are used for perfusion imaging. In liver T1 weighted imaging is the most commonly used technique((41). In this technique, when contrast passes from intravascular to extravascular extracellular (EES) compartment within tumor tissue, T1w signal intensity in MRI. This rate of contrast extravasation is determined by the vessel leakiness(permeability) and blood flow.

A variety of imaging protocols have been proposed for this perfusion imaging and the protocol selection should be made on the availability of the scanner technology and the pertinent physiologic parameter of interest. But there is no consensus regarding standard scanning protocol or computational model in MR perfusion. HCC having predominant hepatic artery supply with a negligible portal supply, a single input model is applied to simplify the calculations. Besides dual compartment model is more appropriate to be used in tumors and cirrhotic liver for calculations, as

compartmentalization occurs due to the capillarization of sinusoids preventing the free flow of contrast into interstitial space(11).

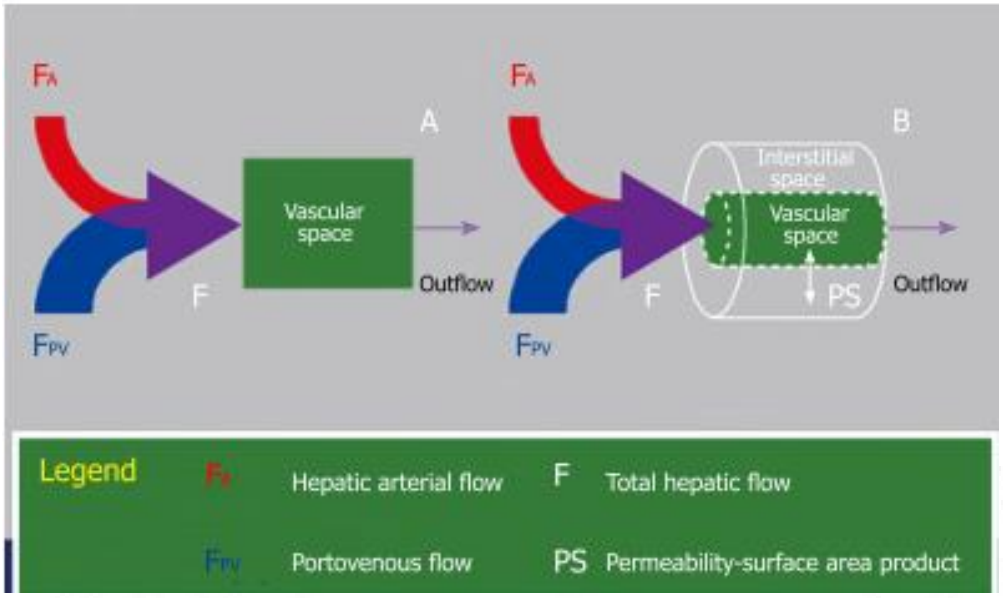

Fig 6. Schematic diagram illustrating the key difference between a single-compartment model (A) and a dual-compartment tracer kinetic model (B). Using a single-compartment model, only the vascular compartment is considered and kinetic properties related to this (e.g. blood flow, F) can be estimated. The behavior of the normal liver can be approximated by a single-compartment model. Using a dual-compartment model, kinetic properties that describe the interstitial space (e.g. PS) can be quantified besides. In disease states (e.g. liver cirrhosis and tumors), the vascular behavior of these tissues are better described using a dual-compartment model

In MR perfusion imaging, vascular permeability changes, blood flow, and extravascular extracellular space can be calculated depending on the model used. To capture the change of signal intensity in tumor high temporal resolution is needed which can be quantified using semiquantitative(model-free) or quantitative(model-based) analysis. The semi-quantitative analysis is based on time-signal intensity curves whereas quantitative analysis needs technically demanding and laborious computational algorithms. However, there is a good correlation between parameters from both analysis methods and tumor angiogenesis(7).

Semiquantitative parameters used are initial area under the curve (IAUC), peak enhancement ratio, distribution volume(DV), maximum wash in slope, mean transit time (MTT). (1) the area under the curve (AUC): expresses the amount of enhancement over a defined period (usually from starting increment of the SI-time curve to 60 or 90 s); (2) maximum of SI or peak enhancement ratio (SI maximum-SI baseline/SI baseline) of the enhancing curve; (3) wash-in slope: determines the velocity of enhancement. It is calculated as the maximum change in enhancement per unit

time, usually from 20% to 80% range of the increment curve; and (4) mean transit time (MTT): represents the meantime for blood to perfuse a region of tissue and is affected by the blood volume and blood flow in the region under analysis. Even though easy to calculate, these parameters were affected by volume and rate of the contrast media injected and also by the gain factor of the acquisition systems as the true concentration of contrast agent in the tissues is not estimated. True physiologic understanding of the microvasculature and behavior of the tumor tissue is not possible with these models (7).

Model-based or quantitative analysis is based on definite mathematical models and depends on fitting the time SI curves voxel by voxel with the changes in concentration of the contrast agent using several kinetics models such as dual-compartmental model (intravascular and interstitium) vs mono-compartmental (only vascular space like in normal liver, single input (only arterial) vs dual input (arterial and portal) and conventional compartment (CC) models vs distributed parameters (DP) models(7,11). Parameters calculated from these models are Ktrans, Kep, Ve. (1) KTrans (forward volume transfer constant) determines the diffusion of the contrast agent from the intravascular space to the EES. It predominantly represents vascular permeability in a permeability-limited (high flow) situation, but also represents the blood flow into the tissue in a flow-limited situation; (2) Kep (reverse reflux rate constant): determines the return diffusion process of the contrast agent from the EES to the intravascular space, and (3) Ve (volume fraction of EES): an indirect measure representing the cellular density of the tissue(7). Many pharmacokinetic models can be used to calculate these parameters. The single input system is used in models proposed by Tofts et al(42), Brix et al (43), and Larsson et al(44). As HCC receives blood supply predominantly from the hepatic artery, this single input model is frequently used in the literature. In a liver parenchymal and metastatic disease where both arterial and portal vein supply is present, it is more recommended to use dual input one-compartment model proposed by Materne et al (45). However, till now there is no consensus regarding the standard protocol, the model used for calculating parameters, the definition of ROI to be drawn, and the cut off values(6).

MR perfusion is used for diagnosis and characterization of liver lesions, grading of liver tumors, and in response assessment to TACE and locoregional therapies(40,46). Studies by Chen et al and Yang et al showed that in HCC, a significant reduction in perfusion parameters is seen after TACE (47,48). In MR perfusion parameters, k trans is the most accepted quantitative surrogate endpoint from compartment models. Studies in preclinical animal models showed significant differences in pre and post-treatment perfusion values which provided a platform to study perfusion changes in HCC in humans (49). Perfusion imaging shows less value addition in response assessment after ablation therapies as the information obtained from the morphological criteria assessment itself is reliable(50,51). However in

post TACE and antiangiogenic therapies that target the microvasculature of the tumor tissue they prove to be an adjuvant but lacks comprehensive evidence due to lack of large data and number of studies. Chen et al (52) compared differences of MR perfusion parameters including Ktrans, Kep, Ve, and AUC and found that DCE MRI derived Ktrans values were significantly negatively correlated with Ki-67 indices and histopathological grades(rho=-0.444, p=0.009) and Kep and Ve were significantly related with tumor microvascular density. Wang et al (53)compared MRI parameters of HCC before and after treatment with Thalidomide and found a statistically significant difference in peak enhancement, maximal enhancement, and enhancement slope percentage between two groups of the patients. Zhu et al(54) showed significant decreases in Ktrans and Kep after treatment with sunitinib(an anti-VEGF receptor sunitinib tyrosine kinase inhibitor).

Due to angiogenesis, the arterial fraction(AF) in tumors will be high when compared to normal liver parenchyma and so the AF also gets reduced after antiangiogenic therapy or embolization therapy like TACE(55). This was observed in a study by Taouli et al(56), who used 1.5T MRI with 3D volume coverage of liver and dual input single compartment model to assess perfusion parameters of 33 HCC lesions (treated and untreated) in 26 patients. The arterial fraction, the arterial hepatic blood flow, distribution volume(DV) and portal venous hepatic blood flow were calculated and found that HCC, when compared to normal liver, showed significantly higher arterial fraction and arterial hepatic blood flow; significantly lower DV and portal venous hepatic blood flow without any indifference in MTT. Lower arterial fraction and higher portal venous hepatic blood flow noted in treated HCC(with TACE) when compared to untreated HCC. Similarly, Pahwa et al also used a dual input single compartment model and showed a statistically significant difference in arterial fraction and distribution volume in HCC when compared to normal liver parenchyma in volunteers(57).

Pokuri et al(58) studied 16 patients with HCC who underwent sunitinib and TACE combination therapy and found that Ktrans and viable tumor percentage after combination therapy decreased significantly. Similarly, another study done by Saito et al(59) showed a significant reduction in Ktrans and DV after TACE and sorafenib combination therapy in the responder group. Ippolito et al(60) assessed 54 patients with biopsy-proven HCC who underwent TACE or RFA with an MRI examination 1 month after treatment. They analyzed perfusion parameters including relative arterial, venous, and late enhancement; maximum enhancement; maximum relative enhancement, and time to peak. A significant difference was found in these parameters between residual viable tumor tissue and effective treated lesions. In a study by Xiangyu Chen et al(61), post TACE response was assessed by using MR perfusion Time- signal intensity curves(TSC). TSC before TACE showed a pattern of a fast decrease and slow increase in the ROI of tumor in 34 patients with HCC whereas slow decrease and a slow increase were noted in normal liver tissue. After TACE, the fluctuating range of TSC was significantly reduced in

31 patients with HCC, slightly reduced in three, and no significant change in one. This study showed that MR perfusion imaging can also assess the hemodynamic characteristics of liver tumors before and after TACE and thus provide guidance for further management. In a study by Kim et al(62), after concurrent chemoradiotherapy for HCC, cut off values for perfusion parameters like Ktrans, Kep, Ve, and diffusion parameter ADC were estimated depending on the shorter or longer progression-free survival(PFS). Optimal cut-off values to differentiate between shorter and longer PFS were trans, Kep, Ve, ADC-0.108 min^{-1}, 0.570min^{-1}, 0.298 %, 1.008 x 10-3mm^2s^{-1} respectively.

Antonacci et al (55) evaluated 28 patients with 52 HCCs (size: 10–104 mm) and showed that time to peak increased from 62.5 ± 18.2 s before to 83.3 ± 12.8 s after treatment (P< 0.01). For equivocal or viable tumors (n=25), time to peak and mean transit time significantly increased (from 54.4 ± 24.1 s to 69.5 ± 18.9 s, P < 0.01 and from 14.2 ± 11.8 s to 33.9 ± 36.8 s, P=0.01, respectively) and the transfer constant(K2) from the extracellular and extravascular space to the central vein significantly decreased from 14.8 ± 14.1 s^{-1} to 8.1 ± 9.1 s^{-1} after treatment (P=0.01). Wang et al(63) used TRIP (Transcatheter intraarterial perfusion) MRI for monitoring intraprocedural tumor perfusion reductions during TACE in 28 patients with 29 tumors. After that MR imaging follows up was done 1-3 months after TACE. There was a significant reduction in intraprocedural tumor perfusion after TACE(324.1vs 158.6, p value-<0.001) which is also associated with future tumor response.

The studies in MR perfusion though a few have shown a reduction in MR perfusion post-TACE. However, there is no comparison between the perfusion values between responders and non-responders to TACE. Besides a cut-off value of the perfusion parameters to differentiate responders from non-responders to TACE is not mentioned in the literature. This would be helpful in cases where there is a dilemma in assessing the response by contrast enhancement alone as it provides an objective value.

DWI and IVIM

DWI is an MR imaging technique based on the random movement of the protons in the tissue. In highly cellular tissues and thick collections like an abscess, movement of the protons get restricted and gives the high signal intensity at high b- values (800-1000 s/mm^2). Free diffusion of the protons causes signal decay whereas, in high cellular and thick collections due to restriction of diffusion of protons, no signal decay occurs causing hyperintense signal. This hyperintense signal corresponds to hypointense signal in ADC maps which can also be quantified. Thus DWI measures both qualitative (signal intensity) and quantitative (apparent diffusion coefficient [ADC]) variables which reflect tissue cellularity and cellular membrane integrity.

Table 3 Different studies on MR perfusion

Study	Parameters	Model used	MRI	Therapy	Conclusion
Taouli et al(56)	AF, AHBF, DV, PHBF	dual input single-compartment model		TACE	Lower AF, higher PVBF in treated HCC
Zhu et al(54)	Ktrans, Kep	Single compartment Toft's model	1.5-T MRI system (Avento; Siemens, New York, NY)	Sunitinib	Decrease in Ktrans and Kep
Pokuri et al(58)	Ktrans,	Single compartment Toft's model	1.5T(GE)	Sunitinib and TACE	Significant reduction in Ktrans
Saito et al(59)	Ktrans, DV	Single compartment Toft's model	1.5 T(Avanto, Siemens Medical Systems, Erlangen, Germany)	TACE and sorafenib	Significant reduction in Ktrans and DV
Antonacci et al (55)	TTP, MTT, Ka, Kp, K2, DV, AF	dual-input single-compartment model	3.0 T MRI system (Achieva TX, Philips Healthcare, Best, The Netherlands)	TACE	Increased TTP, decreased K2

AF- arterial fraction, AHBF- arterial hepatic blood flow, DV- Distribution volume, PHBF- portal hepatic blood flow, ktrans – transfer constant, Kep- reverse reflux rate constant, TTP- Time to peak, MTT- mean transit time, ka-transfer constant from the arterial plasma to the surrounding tissue, kp-transfer constant from the portal venous plasma to the surrounding tissue, k2-transfer constant from the tissue to the central vein.

ADC is recently investigated to predict treatment response for TACE using pretreatment values[49]. But there is conflicting data in the literature regarding the tumor response after TACE whether low ADC values or high ADC values are associated with good response [49, 84, 85]. In many studies, a better outcome was observed in lesions with lower pre-treatment ADC values. The lesions with higher vascularity exhibit a more restricted diffusion with low ADC values as suggested by Padhani et al(64). Necrotic lesion indicating its aggressiveness and poor perfusion has higher ADC value. As they are poorly perfused, TACE is not effective and has poor response after treatment. ADC also confounded by haemorrhage and motion artifacts When compared to DCE-MRI, DWI and ADC have demonstrated lower sensitivity for tumor detection (65).

Signal decay in DWI routinely uses a mono-exponential model which takes into account both diffusion of water molecules in interstitial space and movements of blood molecules in microcapillaries. But diffusion signal intensity decay follows a biexponential pattern at low b value(66). Intravoxel incoherent motion (IVIM) imaging allows the separation of pure molecular diffusion parameters from microcapillaries perfusion related parameters within a tissue (40) by imaging at multiple different low b values. By using b values < 200 s/mm², perfusion related parameters can be calculatedfig .

IVIM signal attenuation is modeled according to the Equation

SI(b) =SI0[(1-PF)·exp(-b·Dslow) + f·exp(-b·Dfast)],

where SI(b) and SI0 denote the signal intensity acquired with the b-factor value of b and b = 0, respectively. PF (perfusion fraction) is the fraction of the pseudo-diffusion linked to microcirculation, Dslow (or D) is the true diffusion coefficient representing the pure molecular diffusion (a slow component of diffusion), and D-fast (D*) is the pseudo-diffusion coefficient representing the incoherent microcirculation within the voxel (perfusion related diffusion, or fast component of diffusion).

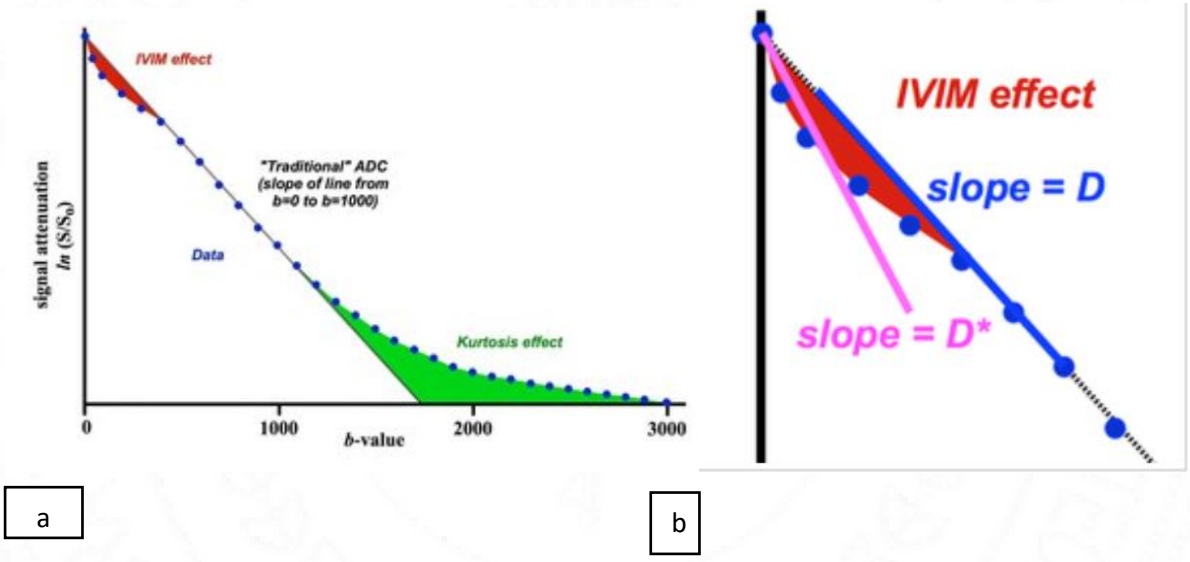

Fig 7a Deviation of expected MR signal in DWI image from the monoexponential model. At low b values, < 200 s/mm², IVIM effects due to microscopic perfusion should be considered and at high b values kurtosis effect should be considered. Fig 7b – D represents true diffusion coefficient , D* represents pseudodiffusion due to blood flow in microcapillaries.

In tumors or liver pathology, diffusion or perfusion may be altered which can be detected by using the IVIM technique. D slow measured at high b value measures the diffusion of free protons giving tissue cellularity (different from ADC calculation in that ADC is calculated from the assumption of monoexponential fit including both diffusion and perfusion characteristics). D* (pseudodiffusion

coefficient) measures the velocity of protons in the microcapillaries perfusing the tissue and f (perfusion fraction) measures the tissue blood volume. For IVIM to be used in clinical settings, accuracy, and reproducibility in different settings is needed. Accurate quantification is also challenging because of limited sampling and low signal to noise ratio for fast data acquisition of the liver. There is no consensus on the standard values of D* and f values, protocol, and the number of b values to be used in normal liver, cirrhotic liver, and liver tumors (67). D slow appears to be better than ADC for assessing necrosis as ADC contains combined information of tissue cellularity and perfusion(microcirculation) in the tumor tissue. These have opposite effects in measuring ADC resulting in decreased sensitivity and specificity. IVIM can be used to assess the response of the HCC after TACE or other treatments without using contrast injection(5). However, there are only a few articles published evaluating the post TACE response assessment by IVIM imaging.

In a study by Wagner et al(68) 48 patients with 51 HCC were assessed by using DW imaging with 11 b values (0-500 s/mm²) and gadolinium-enhanced three-dimensional gradient-echo T1-weighted imaging. D slow showed significant difference between regions of viable tumor tissue and fibrosis (1.16 × 10(-3) mm(2)/sec ± 0.29 and 1.48 × 10(-3) mm(2)/sec ± 0.31, respectively; P = .016) and between regions of viable tumor tissue and necrosis (1.16 × 10(-3) mm(2)/sec ± 0.29 and 1.70 × 10(-3) mm(2)/sec ± 0.49, P = .002). Significant lower perfusion fraction was seen in necrotic regions (14% ± 6) compared to viable tumor regions (21% ± 8, P = .005); however no significant difference was observed in perfusion fraction of the fibrous regions (21% ± 7) from necrotic and viable regions. Kakite et al(66), used IVIM parameters to compare HCC and liver parenchyma and between a viable and necrotic portion of the tumors. D, PF, and ADC were significantly higher in HCC when compared to the liver. There were weak significant positive correlations between D/PF and Enhancement ratio(ER. Among diffusion parameters, D had the highest area under the curve for predicting complete tumor necrosis. ER outperformed diffusion parameters for the prediction of complete tumor necrosis. They concluded that D is better for predicting complete tumor necrosis but lower when compared to contrast-enhanced imaging.

Peng et al(69) reported 20 patients who underwent IVIM imaging 1-3 days before TACE and 4-6weeks after TACE. Post TACE, ADC, and D-slow values in tumor increased significantly whereas the values of D* decreased significantly with no significant changes in f values. They also compared responsive and nonresponsive groups wherein ADC values were significantly higher in responsive groups and D fast values significantly lower in nonresponsive groups. However, D slow and f values were not significantly different between the two groups. They concluded that IVIM parameters can be used as potential markers for response assessment of HCC after TACE

Imaging in 3T

3T MRI has the advantage of increased signal to noise ratio(SNR) that can improve the contrast resolution and lower the acquisition time by decreasing Nex values. The dynamic study has a major advantage because of the significant increase in T1 relaxation times with only minimal changes in gadolinium T1 shortening effects. This leads to the higher liver to lesion contrast making the lesion more conspicuous.

However, there are also disadvantages like longer acquisition times because of longer T1 relaxation times which can be overcome by parallel imaging techniques, susceptibility artifacts which may cause image distortion, higher radiofrequency energy deposition(7).

Lacunae in literature

There are several lacunae in the literature of both MR perfusion and IVIM parameters in assessing the treatment response of HCC after TACE.

MR perfusion

- No standardization of protocol and sequences to be used
- Timing of MR perfusion to be done. MR perfusion can pick up microvascular changes, which occur very early after treatment. So MR perfusion can be used to assess response as early as possible. But there is no standard consensus regarding the timing of MR perfusion to be done.
- No definite cutoff values were present in the literatiure to assess the response
- Very few studies comparing MR perfusion characteristics and histopathological features.

IVIM

In IVIM also lacks standardization of protocol and sequences to be used with no standard consensus regarding the timing of MR perfusion . Thers is no definite cutoff values and very few studies for assessing the response after TACE.

AIMS AND OBJECTIVES

AIMS AND OBJECTIVES

1. To assess the feasibility and efficacy of imaging sequences like MR perfusion, Intravoxel incoherent motion (IVIM) imaging in post trans-arterial Chemoembolization(TACE) response evaluation of HCC
2. To compare the changes in HCC between preTACE and postTACE values in MR perfusion and Intravoxel incoherent motion (IVIM) imaging.

Hypothesis

MR perfusion parameters can assess the microvasculature characteristics and also the cellular density of the tumor tissue, early response is predicted. Besides the quantification of the parameters can be done.

IVIM can assess the microvasculature characteristics and cellular density of the tumor tissue without using contrast which can be used for assessing treatment response.

Methodology and materials

Methodology and materials

This is a prospective study done in 34 consecutive patients referred to the radiology department for TACE according to BCLC criteria. Of the 34 patients, 31 patients with inclusion criteria BCLC A or B and Child-Pugh A or B were selected. 5 patients were excluded as per exclusion criteria and 26 patients were selected. These 26 patients with 32 lesions were included in the study. Informed consent was obtained from all the patients. Pre-TACE MRI was done before TACE(within 1-2weeks) and postTACE MRI was done 6weeks after TACE (fig 8).

Inclusion criteria

- BCLC A or B
- Child-Pugh A or B

Exclusion criteria

- Liver lesion size < 1cm
- Patients not giving consent
- Contraindications for undergoing MRI

Pre and post-TACE Imaging was done in 3T MRI machine (Discovery; General electric GE healthcare; USA). Informed consent was taken from all patients. Patients were given breathing training before scanning. Breath-hold sequences without respiratory navigation were used for MR perfusion and IVIM imaging . MR sequences with details were given in Table 4.

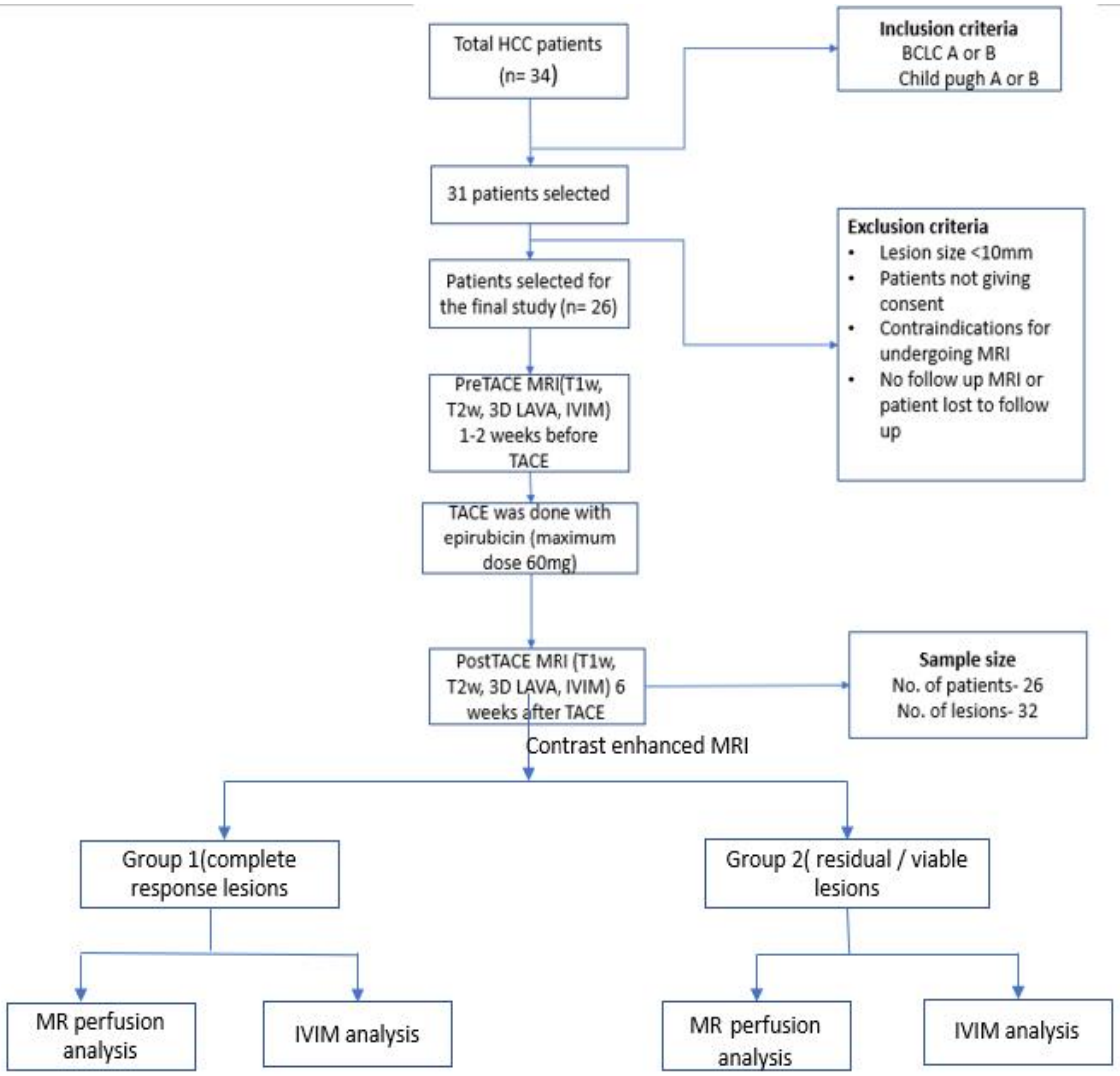

Fig 8. Study Design

Table 4 MR parameters and Sequences obtained

Parameter	T1W Axial	T2W axial	T1 perfusion	IVIM
Sequence used	3D, in/out phase gradient echo sequence (GRE)	fast spin-echo sequence	dynamic 3D lava (3D T1 spoiled gradient echo)	single shot spin echo echo planar imaging
TR	10ms	9230ms	3.8ms	2500ms
TE	2.3ms(in)/4.6ms(out)	102ms	1.1ms and 2.2ms	69.6ms
NEX	2	2	-	Multiple (2-8)
Matrix	150x236	384x256	180x180	128x128
FOV	As small as possible	38cm	42cm	40cm
Flip angle	15°	-	12°	-
Slice thickness	4mm	5mm	3.8mm	8mm
Slice gap	0.5mm	2mm	-	2mm
Scan time	16 sec	2.06min(varies with respiratory rate)	5.20min	6.35min
Parallel imaging	-	-	Arc	Asset
Bandwidth	-	-	142.86	250
Others	-	Fast suppression: Frequency selective Respiratory gating-Navigator	Breath-hold	No. of directions-3 Free-breathing

MR perfusion protocol

For MR perfusion, images were acquired over 20 consecutive breath-holds at end-expiration extending up to approximately 5 min after injection. One mask volume acquisition of the liver was done before contrast injection. Each phase was scanned for a time of 11 sec with a breath-hold gap of 4sec(fig 9).

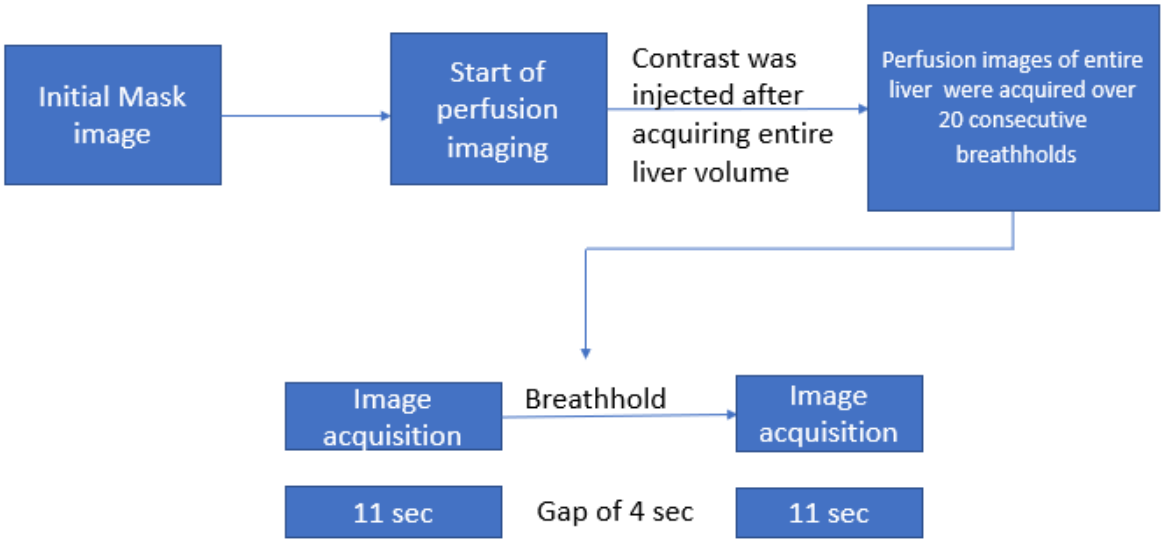

Fig . 9 MR perfusion acquisition algorithm

IVIM protocol

IVIM with 7 b values acquired in free-breathing as given in fig 10.

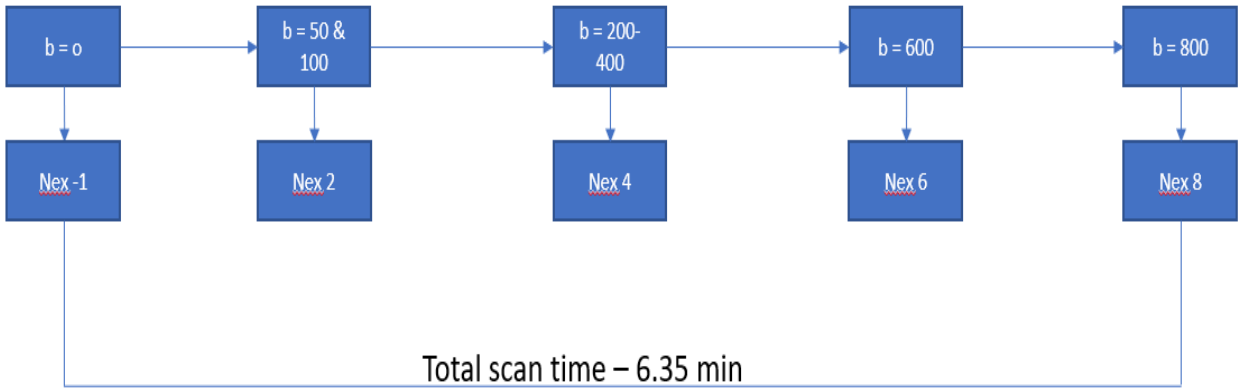

Fig 10 IVIM acquisition algorithm

MRI analysis :

MR Perfusion

All visible lesions on preTACE images were analyzed if the size exceeded 10 mm, 3D ROI was drawn in enhancing the area of the lesion in preTACE MRI, and in post-TACE MRI. ROI was drawn in the entire tumor region in complete response lesions or in the visible enhancing region in viable/residual lesions.

Population averaged Arterial input function (AIF) was taken. Post-processing of perfusion MRI data was performed on the GenIQ software (by General electronics) to calculate perfusion parameters using a single-input dual-compartment model based on the extended Toft's General kinetic model. A motion correction was done before processing. Mean values of quantitative perfusion parameters like Ktrans(min-1), Kep(min-1), Ve(%); and semiquantitative parameters like maximum slope(mMol/sec) and IAUGC(no units) were measured after generating coloured parametric map(fig 11).

IVIM

2D ROI was drawn in the corresponding area as drawn in perfusion imaging for calculating IVIM. Post processing of IVIM was performed by loading the 8 b values in Osirix MD software by using two-stage IVIM fit asymptomatic method(fig 12). Parameters l D, D*, f, and ADC were generated in pre and post TACE cases (fig 13).

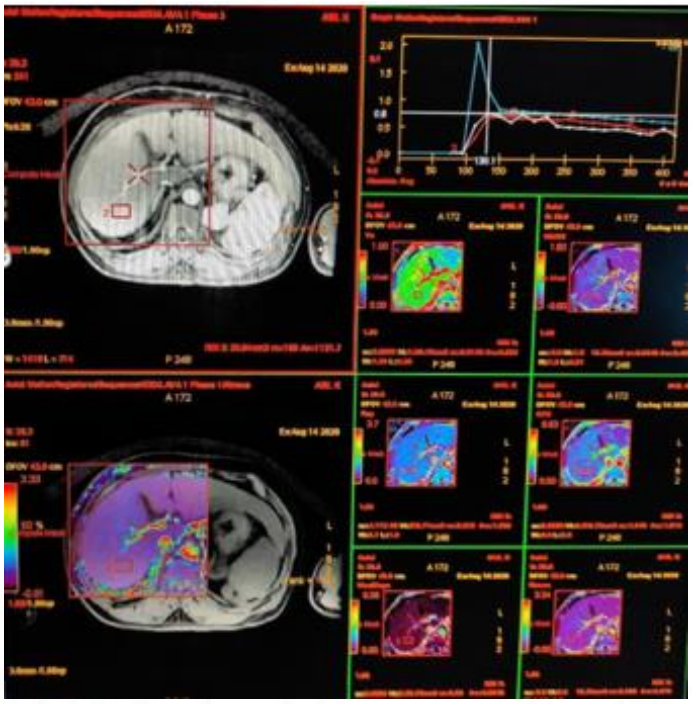

Fig 11 showing the method of acquiring the MR perfusion parameters

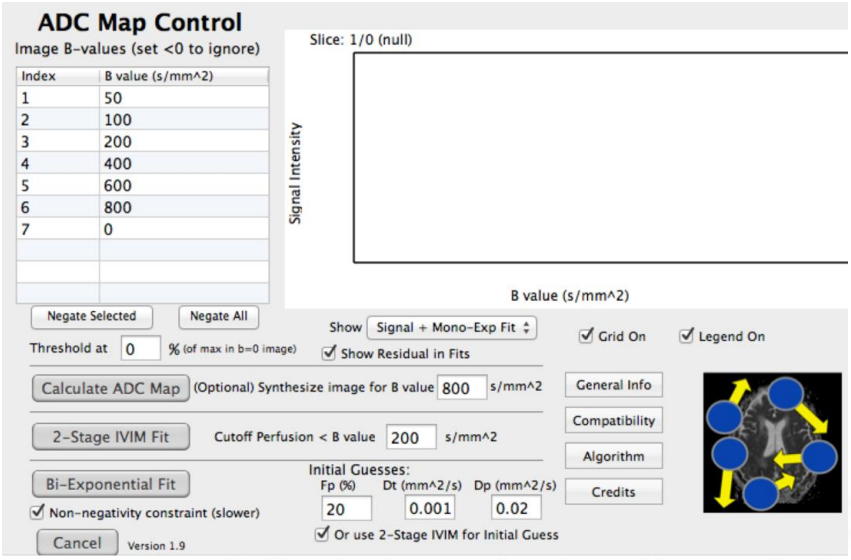

Fig 12– showing the method of acquiring the data of IVIM parameters

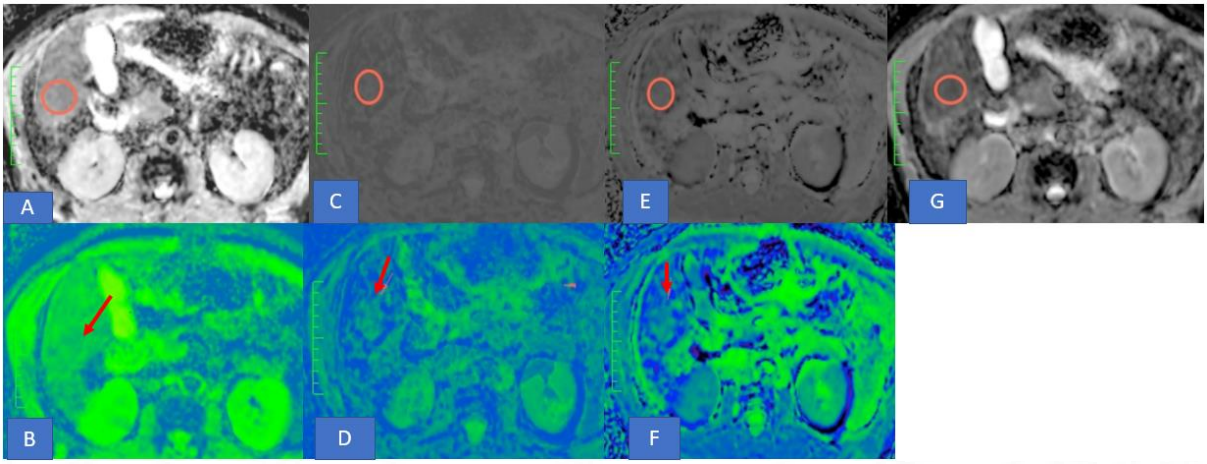

Fig 13. A, C, E, G represents D, D*, f, ADC respectively with circular ROI drawn over the lesion corresponding to enhancing lesion in DCE; B, D, F represents colour maps of D, D*, f respectively showing the lesion(arrows)

Lesions were divided into two groups depending on the presence or absence of contrast enhancement, Group 1 cases showed complete response lesions without any arterial enhancement and Group 2 cases were residual or viable or nonresponding lesions with a component of arterial enhancement and delayed venous washout.

Scatterplots and Box plots of preTACE and postTACE values of MR perfusion and IVIM were generated. Where appropriate, Pearson's correlation analysis was used to identify a relationship between preTACE

and postTACE parameters of the two MRI techniques (MR contrast perfusion and IVIM). PreTACE values of completer responding lesions (group 1) and nonresponding (group 2) were compared using the T-test of unequal variances to predict the response from pre-treatment values. Post TACE values of complete responding lesions(group 1) and nonresponding lesions(group 2) were also compared using the T-test of unequal variances. Correlation analysis was done for D & ADC, D* & Ktrans and D* and Kep. Mean differences of Both MR perfusion and IVIM parameters between preTACE and postTACE values in complete responding lesions(group 1) and nonresponding lesions(group 2) were compared using T-test of unequal variances.

The sensitivity and specificity of each parameter with the corresponding 95% confidence intervals (CI) were derived from ROC curve analysis and areas under the ROC curve (AUC) were computed. Differences in diagnostic performances were analyzed by comparing the ROC curves according to the method of Delong et al. All statistical analysis was carried out by MS excel and MedCalc software(MedCalc for Windows, version 19.4.1).

OBSERVATIONS AND RESULTS

OBSERVATIONS AND RESULTS

1.Demographics (Table 5)

32 HCC lesions in 26 patients were assessed. Of these, 23(88%) were male and 3(12%) were female(fig 14). The mean age was 61yrs and with a range of 48yrs to 76 yrs. Aetiology of CLD was alcoholism in 65% (n=17), HBV in 7.7% (n=2), HCV in 1.5% (n=3) and NASH in 15.3%(n = 4)(fig 15). The average number of lesions per patient was about 1.28 (range 1-4 per patient). The mean size of the lesions was 3.64cm (range of 1.5cm to 12cm). The most common lobe involved was segment VI.

Table 5 Demographics of the patients

Clinical characteristics	Value
Age in years(mean/range)	61yrs /48-76yrs
Sex	Male-23 Female- 3
Size in cm (mean/ range)	3.64/1.5-12
No. of lesions per patient(mean/range)	1.28/1-4
Aetiology	Alcohol-17 HBV-2 HCV-3 NASH-4
Distribution of lesions as per segment involvement	Seg II-2 segIII-3 seg IV-4 Seg V-0 Seg VI-14 Seg VII-4 Seg VIII-3 Multiple-1

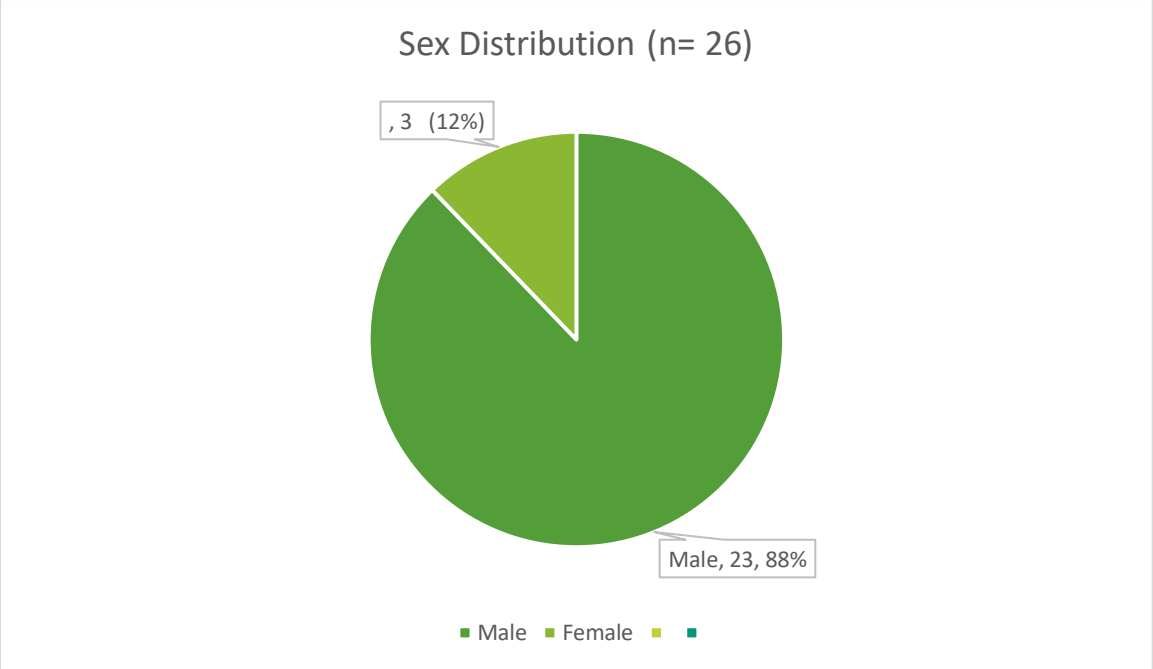

Fig 14.Distribution of lesions according to sex

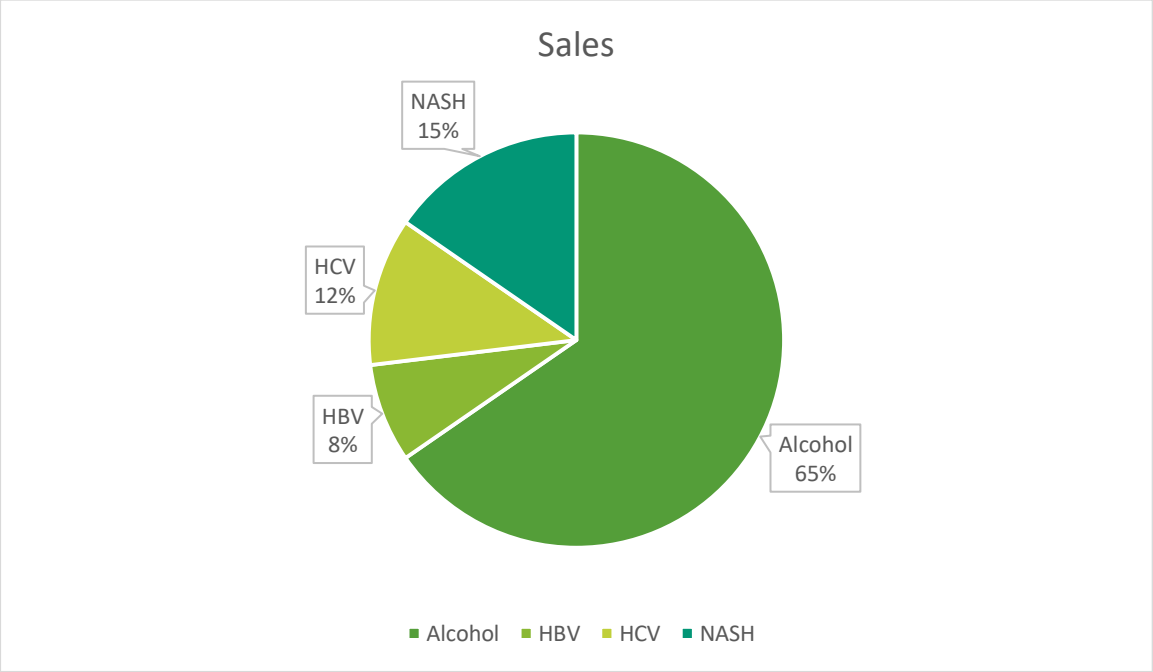

Fig 15. Distribution of lesions according to aetiology

2. Response assessment

Lesions with complete response were taken as group 1 and lesions with residual/ viable tumor were taken as group 2. Group 1(complete responder) included 22 lesions and group 2 (partial/non responder)include 10 lesions.The mean preTACE and postTACE values of MR perfusion and IVIM

parameters were calculated. The MR perfusion and IVIM parameters were analyzed in both the groups. Baseline mean preTACE values of MR perfusion and IVIM valiues were given in Table 6.

Table 6.Mean baseline preTACE of IVIM and MR perfusion (n= 32) for all lesions

Parameter	preTACE(mean+ SD)
D($10^{-3}mm^2/s$)	1.218 +/-0.4992
D*($10^{-3}mm^2/s$)	33.059+/-10.72
f(%)	19.487+/- 9.5
ADC($10^{-3}mm^2/s$)	1.335+/-0.46
Ktrans(min^{-1})	0.399+/-0.226
Kep(min^{-1})	2.136+/-1.55
Ve	0.239+/-0.124
Max slope(mmol/s)	0.025+/-0.015
IAUGC	0.29+/-0.123

2.1. MR perfusion Analysis

Group 1(complete responded lesions)

Perfusion parameters like Ktrans, Kep, Ve, max slope, IAUGC were calculated before and after TACE (Table 7 & fig 21)

2.1.Ktrans

Ktrans which represents permeability and leakiness of the tumor vasculature by determining the efflux of contrast from vascular space to EES usually decrease after TACE which indicates response. In 22 lesions with complete response, 17 lesions showed a decrease, 5 lesions showed an increase in mean values of Ktrans after TACE. The mean percentage changes from baseline values of Ktrans was 40%. There was a statistically significant decrease in Ktrans (0.38 vs 0.2, p value 0.011) after TACE. There was a weak positive correlation (r= 0.056) between preTACE and postTACE values which indicates that change is corresponding with preTACE values (fig 16)

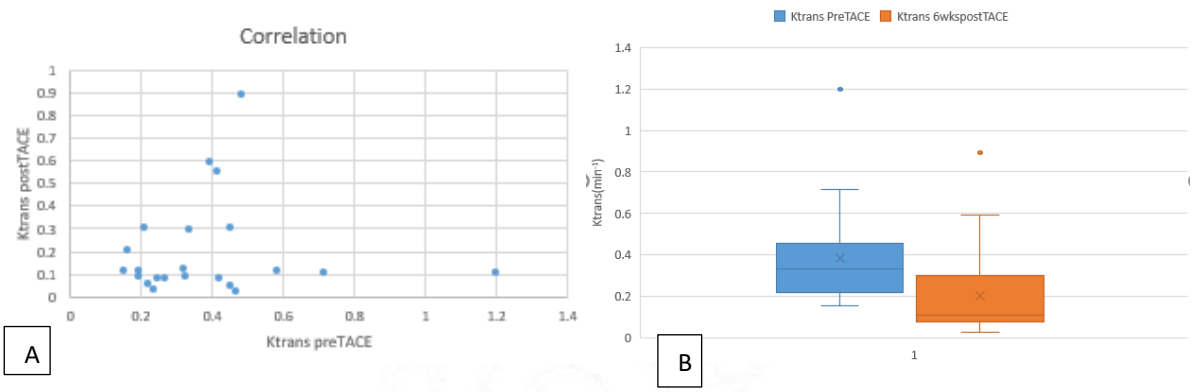

Fig 16

A. scatter plot showing a weak positive correlation between the reduction of Ktrans between preTACE and postTACE values

B. Box & whisker plot showing a significant difference between preTACE and postTACE values of Ktrans.There are outliers in both preTACE and postTACE values.

2.1.b Kep

Kep which determines the reverse efflux of contrast from EES to vascular space. Of the 22 lesions, 17 lesions showed a decrease, 5 lesions showed an increase in mean values of Kep after TACE. Although both Ktrans and Kep represent permeability, 5 lesions were showing a mismatch between Ktrans and Kep. The mean percentage changes from baseline values of Kep was 37%. There was a statistically significant decrease in mean Kep (2.09 vs 0.86, p value 0.007) after TACE. There was a mild negative correlation (r= -0.248) between preTACE and postTACE values which indicates that higher values were corresponding with greater change after TACE(fig 17).

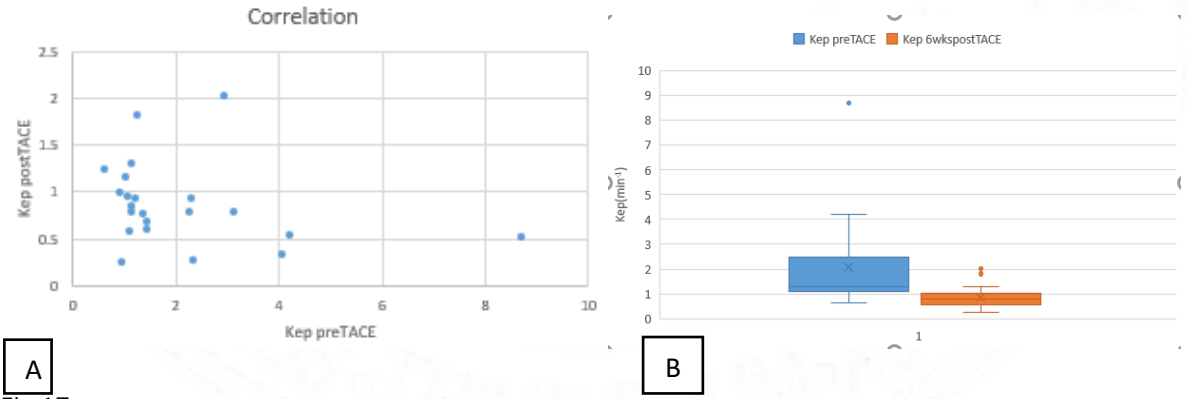

Fig 17

A. scatter plot showing a mild negative correlation between preTACE and postTACE values of kep

B. Box & whisker plot showing a significant difference between preTACE and postTACE values of Kep. No overlapping of n values was noted between preTACE and postTACE values.

2.1.c.Ve

Ve represents the volume fraction of EES which usually increases after TACE due to tumor necrosis. In this study, 13 lesions showed an increase, 9 lesions decrease in mean values of Ve after TACE. The mean percentage changes from baseline values of Ve was 64%. However, there was no statistically significant increase in mean Ve (0.23 vs 0.29, p value 0.207) after TACE. There was no correlation (r= 0.009) between preTACE and postTACE values(fig 18).

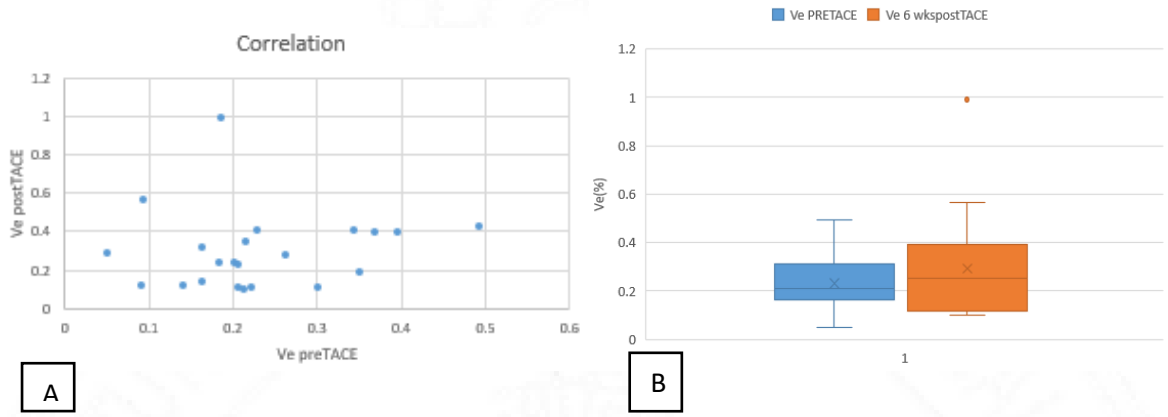

Fig 18

A. scatter plot showing no correlation between preTACE and postTACE values of Ve

B. Box & whisker plot showing no significant difference between preTACE and postTACE values. Significant overlapping of median values also noted between preTACE and postTACE values. There is an outlier in postTACE values.

2.1.d.Max slope

Max slope indicates the velocity of contrast enhancement in tumor tissue which has to decrease after treatment. In this study 14 lesions showed a decrease; 8 lesions showed an increase in mean values of the max slope. The mean percentage changes from baseline values of Max slope was 33%. However, there was no statistically significant decrease in mean max slope (0.024 vs 0.02, p value 0.48) after TACE. There was a moderate negative correlation (r= -0.364) between preTACE and postTACE values which indicates that higher values were corresponding with greater change after TACE(fig 19).

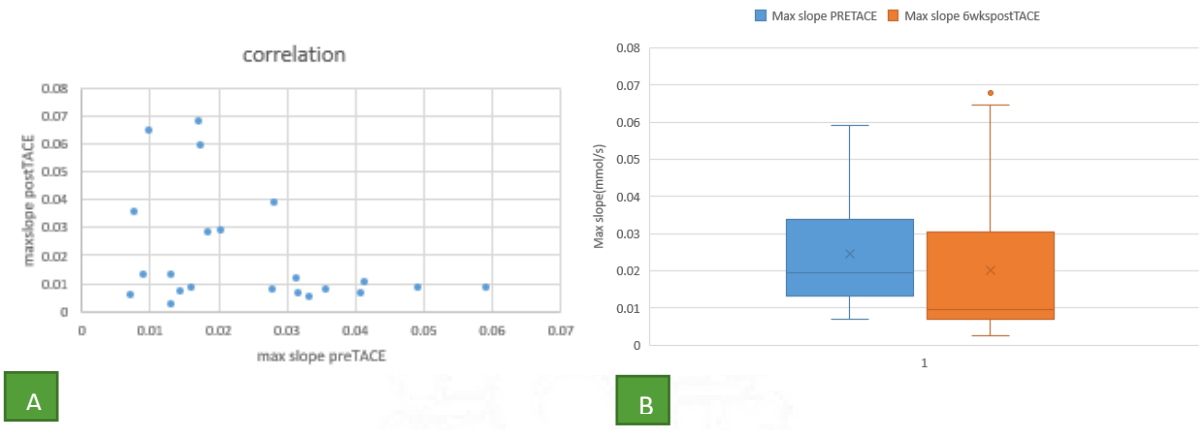

Fig 19

A. scatter plot showing a moderate negative correlation between preTACE and postTACE values of max slope

B. Box & whisker plot showing no significant difference between preTACE and postTACE values. Significant overlapping of median values also noted between preTACE and postTACE values. There is an outlier in postTACE values.

2.1.e.IAUGC

IAUGC indicates the amount of enhancement which usually decreases after TACE. Here 16 lesions showed a decrease, 6 lesions showed an increase in mean values after TACE. The mean percentage changes from baseline values of IAUGC was 43%. There was a statistically significant decrease in IAUGC (0.276 vs 0.154, p value 0.006) after TACE. There was a mild positive correlation (r=0.24) between preTACE and postTACE values which indicates that change is corresponding with preTACE values(fig 20)

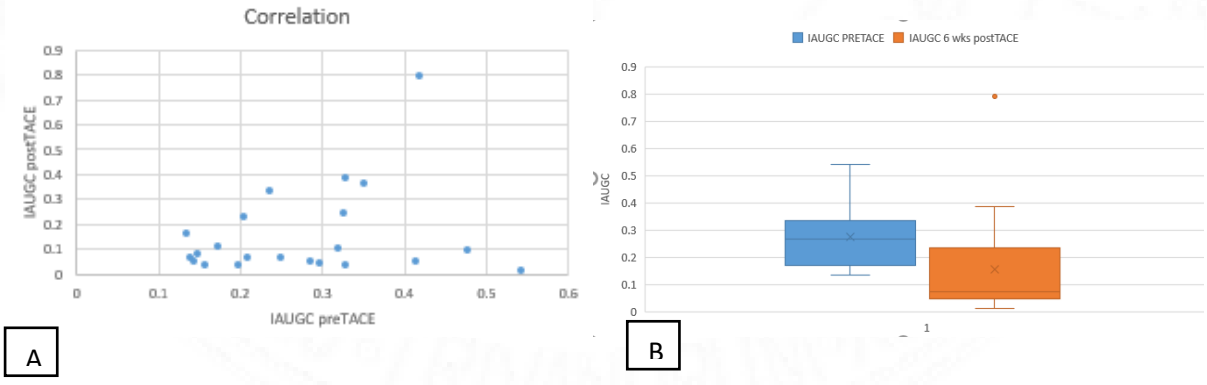

Fig 20

A. scatter plot showing a mild positive correlation between preTACE and postTACE values of IAUGC

B. Box & whisker plot showing a significant difference between preTACE and postTACE values of IAUGC. There is an outlier in postTACE values.

Table 7 Comparison between mean preTACE and postTACE values of MR perfusion in complete response(group 1) lesions(n=22)

Parameter	preTACE(mean+ SD)	postTACE(mean +SD)	P-value	Pearson correlation
Ktrans(min^{-1})	0.38+/-0.227	0.20+/-**0.214**	0.011	0.056
Kep(min^{-1})	2.09+/- **1.749**	0.86+/-**0.437**	0.007	-0.248
Ve	0.23+/-**0.105**	0.29+/-**0.199**	0.207	0.0099
Max slope(mmol/s)	0.024+/-**0.014**	0.020+/-**0.012**	0.48	-0.364
IAUGC	0.276+/-**0.113**	0.154+/- 0.177	0.006	0.24

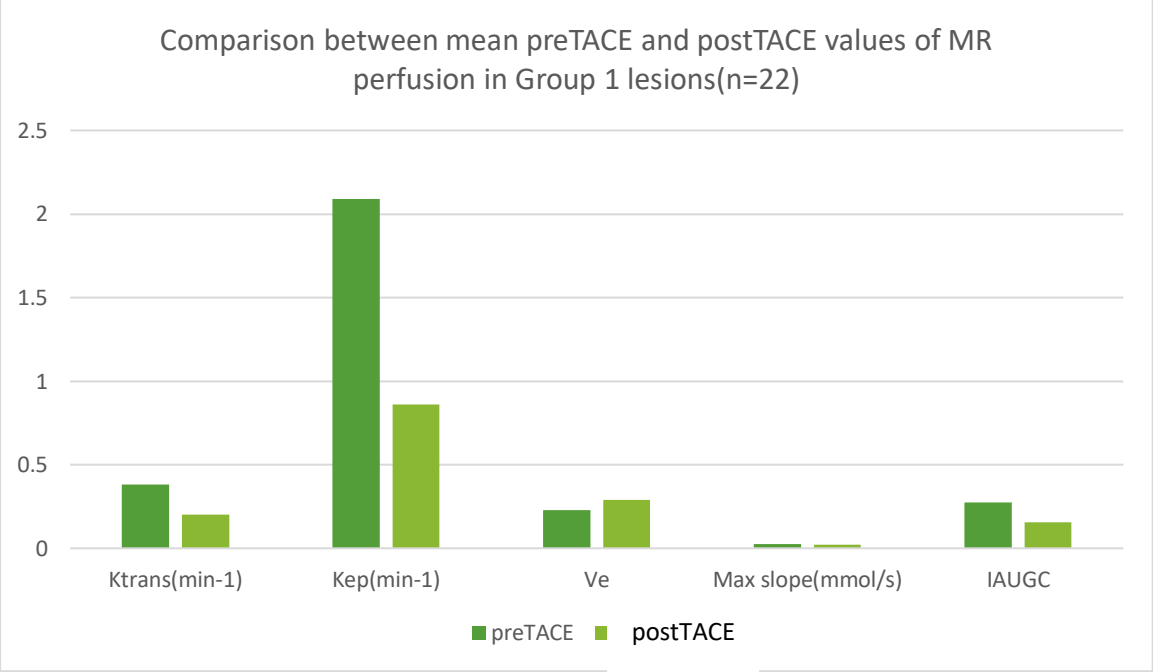

Fig. 21.Bar diagram showing a comparison between mean preTACE and postTACE values of MR perfusion imaging in Group 1(complete response) lesions

2.2.Group 2 (nonresponding/residual/viable) lesions

In group 2 lesions, mean preTACE and postTACE values of all MR perfusion and IVIM parameters were given in Table 8. Of 10 residual enhancing lesions, 5 lesions showing a decrease, and 5 lesions showing an increase in Ktrans value. Of the lesions showing decreased value, one lesion was showing a 76%

decrease; however, the lesion was very large about 12cm with mixed necrotic and enhancing areas after TACE. In one equivocal lesion, Ktrans is increased by about 76% which is showing no definite enhancement and washout (fig). The mean percentage changes from baseline values of Ktrans was a 5% decrease in which there was no statistical difference(p-value 0.79) in nonresponder lesions (fig 22)

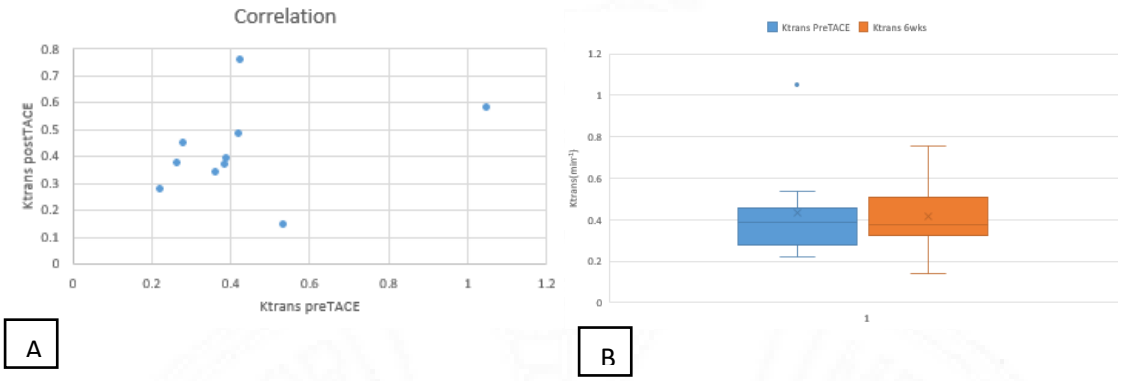

Fig 22

A. scatter plot showing a mild correlation between preTACE and postTACE values of Ktrans

B. Box & whisker plot showing no significant difference between preTACE and postTACE values. Significant overlapping of median values also noted between preTACE and postTACE values. There is an outlier in preTACE values.

2.2.a.Kep

Kep in residual enhancing portions is expected to be the same or increased in postTACE MRI. In this study, of 10 residual enhancing lesions, 5 lesions showing a decrease, and 5 lesions showing an increase in its value. The mean percentage changes from baseline values of Ktrans was a 7% increase. There was no statistical difference(p value 0.59) between mean preTACE and postTACE values (fig 23).

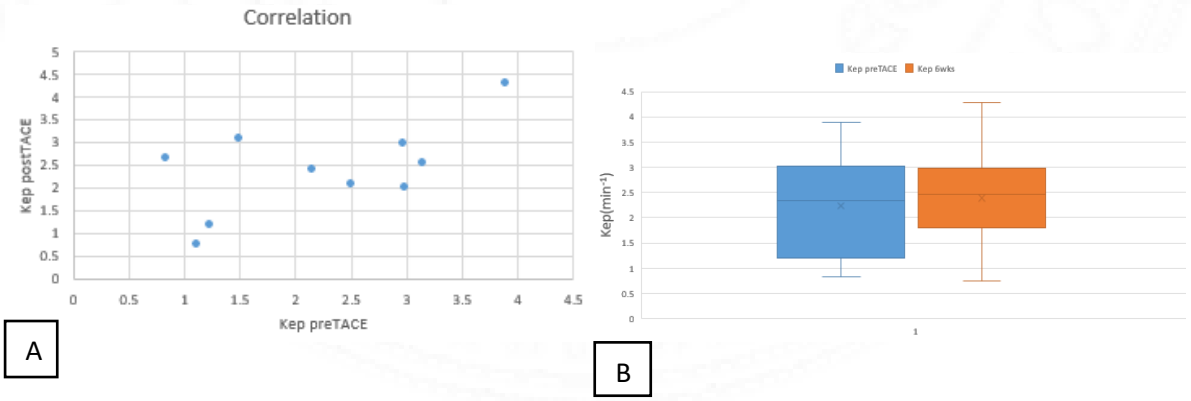

Fig 23 A. scatter plot showing good correlation between preTACE and postTACE values of Kep

B. Box & whisker plot showing no significant difference between preTACE and postTACE values. The significant overlap of median values was noted between preTACE and postTACE.

2.2.b.Ve

Of the 10 residual enhancing lesions, 5 lesions showing a decrease, and 5 lesions showing an increase in its value. The mean percentage changes from baseline values of Ve was 10% decrease. There was no statistical difference(p value 0.48) between mean preTACE and postTACE values. There was good correlation(r=0.605) between preTACE and postTACE values (fig 24)

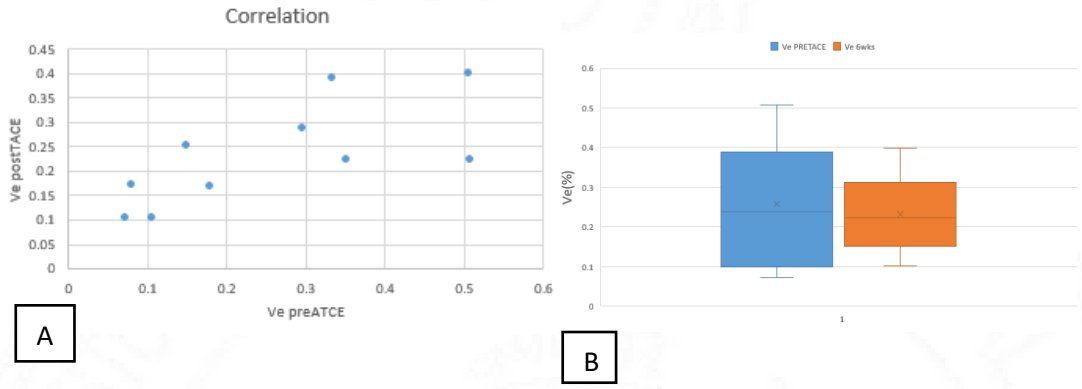

Fig 24 A. scatter plot showing good correlation between preTACE and postTACE values of Ve

B. Box & whisker plot showing no significant difference between preTACE and postTACE values. The significant overlap of median values was noted between preTACE and postTACE.

2.2.c.Max slope

Max slope in residual enhancing portions should be almost the same or increased in postTACE MRI. In this study, of 10 residual enhancing lesions, 2 lesions showing a decrease, and 8 lesions showing an increase in its value. The mean percentage changes from baseline values of Ve was 131% increase. There was no statistical difference(p value 0.28) between mean preTACE and postTACE values. There was very good correlation(r=0.932) between preTACE and postTACE values(fig 25)

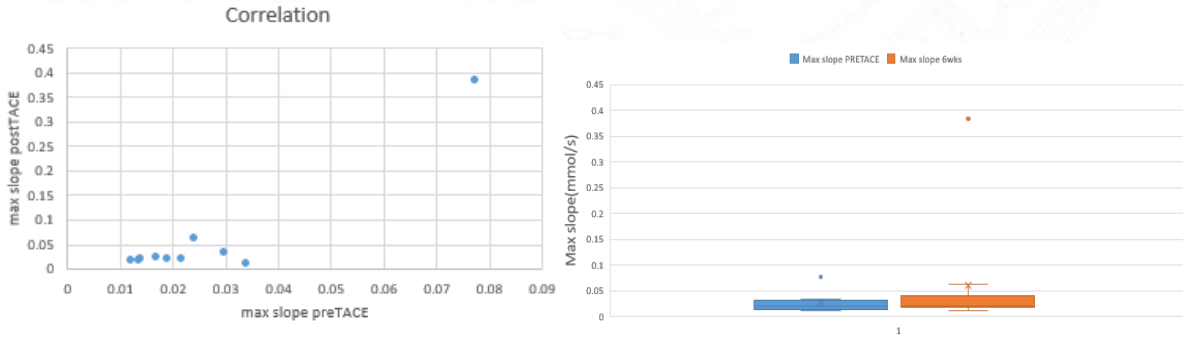

Fig 25

A. scatter plot showing a very good correlation between preTACE and postTACE values of max slope

B. Box & whisker plot showing no significant difference between preTACE and postTACE values. The significant overlap of median values was noted between preTACE and postTACE.

2.2.d.IAUGC

Of 10 residual enhancing lesions, 6 lesions showing decrease and 4 lesions showing an increase in its value. The mean percentage changes from baseline values of Ve was 5% decrease. There was no statistical difference(p value 0.81) between mean preTACE and postTACE values. There was mild negative correlation(r=-0.238) between preTACE and postTACE values (fig 26)

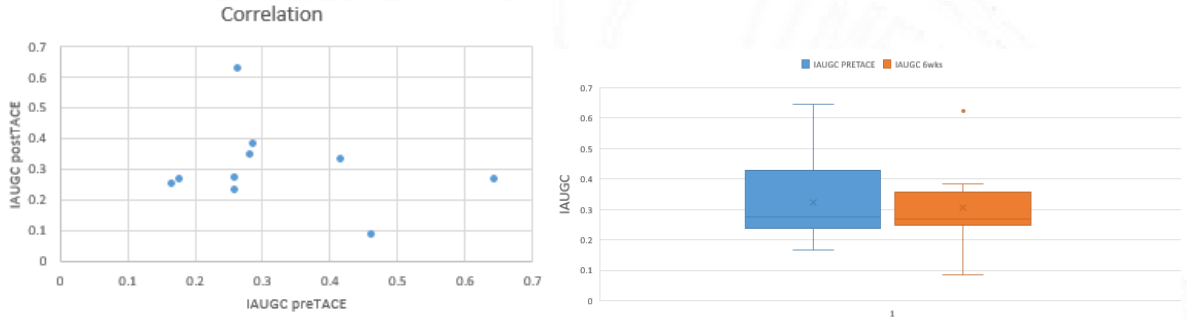

Fig 26

A. scatter plot showing a mild negative correlation between preTACE and postTACE values of IAUGC

B. Box & whisker plot showing no significant difference between preTACE and postTACE values. The significant overlap of median values was noted between preTACE and postTACE. There is an outlier in postTACE values.

Table 8 Comparison between mean preTACE and post TACE values of MR perfusion in nonresponding (Group 2) lesions (n=10)

Parameter	preTACE(mean+SD)	postTACE(mean+SD)	P-value	Pearson correlation
Ktrans(min^{-1})	0.435+/-0.223	0.414+/-0.159	0.79	0.315
Kep(min^{-1})	2.23+/-0.977	2.39+/-0.943	0.59	0.605
Ve	0.258+/-0.157	0.231+/-0.108	0.48	0.707
Max slope(mmol/s)	0.026+/-0.018	0.06+/-0.0984	0.28	0.932
IAUGC	0.322+/-0.138	0.305+/-0.131	0.81	-0.238

3.IVIM imaging

Group 1(complete response) lesions

In group 1 lesions, mean preTACE and postTACE values of all IVIM parameters were given in Table 9 and fig 31.

3.1.a. D (True diffusion coefficient)

D represents the true diffusion coefficient which usually increases after TACE due to tumor necrosis. In this study, 18 lesions showed an increase, 4 lesions showed a decrease in mean values of D after TACE. Of the 4 lesions decreased, 3 lesions showed very minimal change. The mean percentage changes from baseline values of D were 43%. There was a statistically significant increase in mean D **(1.208 vs 1.560; p value- 0.0207)** after TACE. There was mild correlation (r= 0.2865) between preTACE and postTACE values (fig 27)

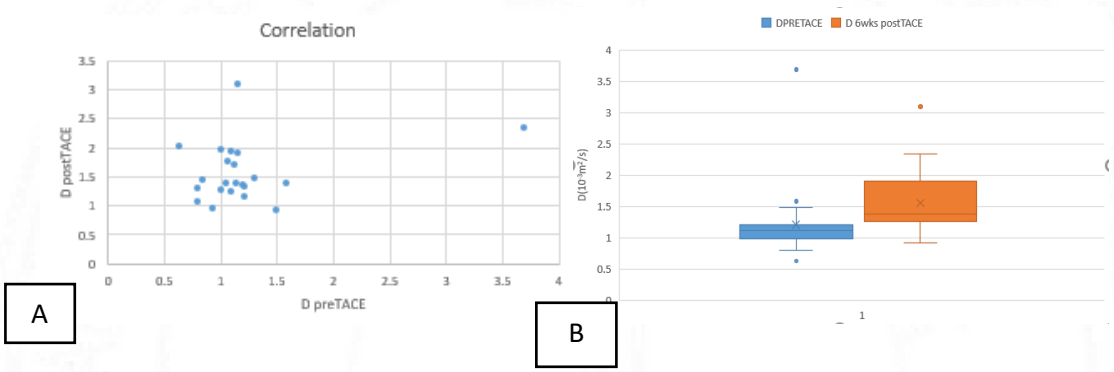

Fig 27

A. scatter plot showing a mild correlation between preTACE and postTACE values of D

B. Box & whisker plot showing a significant difference between preTACE and postTACE values. No significant overlap of median values was noted between preTACE and postTACE. There were 3 outliers in preTACE values and one outlier in posTACE values.

3.1.b. D*(Pseudodiffusion)

D* which represents perfusion related diffusion of tumor vasculature is usually expected to reduce after TACE. In this study, 20 lesions showed a decrease, 2 lesions showed an increase in mean values of D* after TACE. The mean percentage changes from baseline values of D* was 28%. There was a statistically significant decrease in mean D* **(33.7 vs 23.75; p value – 0.0005)**after TACE. There was good correlation (r= 0.506) between preTACE and postTACE values (fig 28).

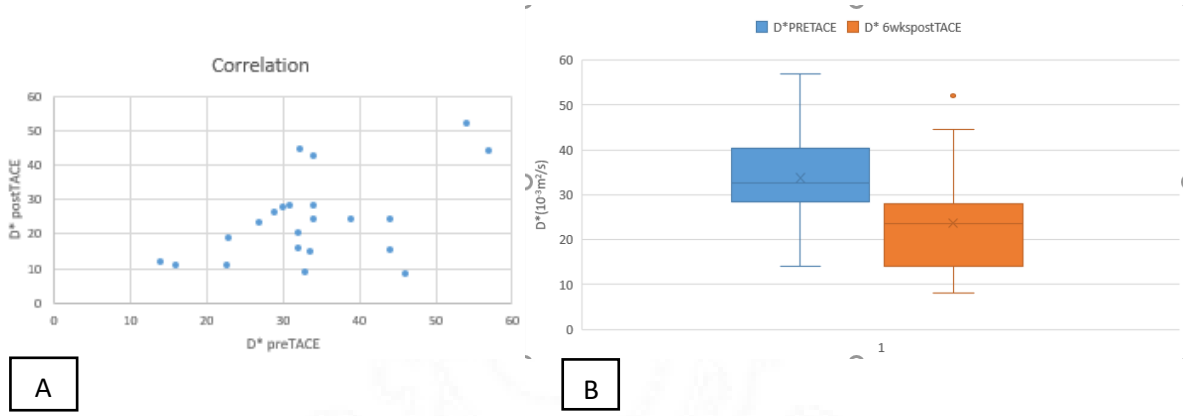

Fig 28

A. scatter plot showing good correlation between preTACE and postTACE values of D*

B. Box & whisker plot showing a significant difference between preTACE and postTACE values. No significant overlap of median values was noted between preTACE and postTACE. There was one outlier in posTACE values.

3.1. c. Perfusion fraction (f)

Of the 22 complete responders 17 lesions showed a decrease, 4 showed an increase, and one lesion showed no change in mean values of 'f' after TACE. The mean percentage changes from baseline values of 'f' were 20%. There was a statistically significant decrease in mean f (19.92 vs 12.9; p-value – 0.012) after TACE. There was mild correlation (r= 0.365) between preTACE and postTACE values(fig 29).

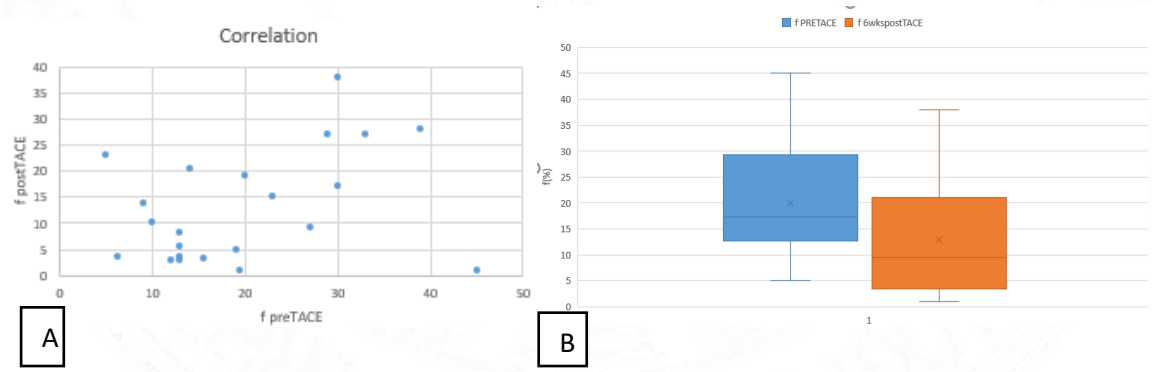

Fig 29

A. scatter plot showing a mild correlation between preTACE and postTACE values of perfusion fraction 'f'.

B. Box & whisker plot showing a significant difference between preTACE and postTACE values. Considerable overlap of median values noted between preTACE and postTACE.

3.1.d. ADC

ADC represents an apparent diffusion coefficient which usually increases after TACE due to tumor necrosis. In this study, 18 lesions showed an increase, 4 lesions showed a minimal decrease in mean values of D after TACE. The mean percentage changes from baseline values of ADC was 29%. There was a statistically significant increase in mean ADC **(1.37 vs 1.65; p-value- 0.016)**after TACE. There was moderate correlation (r= 0.464) between preTACE and postTACE values (fig 30).

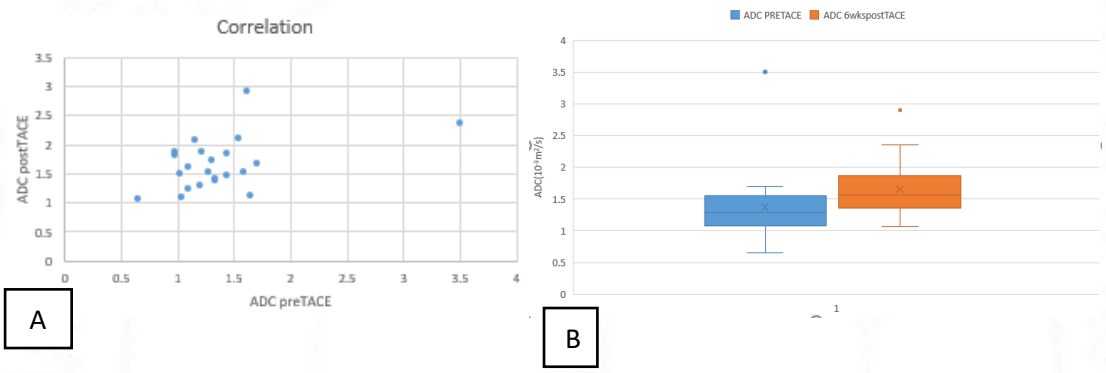

Fig 30

A. scatter plot showing a moderate correlation between preTACE and postTACE values of ADC

B. Box & whisker plot showing a significant difference between preTACE and postTACE values. No significant overlap of median values noted between preTACE and postTACE. There was one outlier in both preTACE and postTACE values.

Table 9. Mean preTACE and postTACE values of IVIM in complete response lesions(n=22)

Parameter	preTACE(mean+ SD)	postTACE(mean +SD)	P-value	Pearson correlation
D($10^{-3}mm^2/s$)	1.208+/-0.581	1.560+/-0.494	0.0207	0.2865
D*($10^{-3}mm^2/s$)	33.7+/-10.406	23.75+/-12.13	0.0005	0.506
f(%)	19.92+/-10.54	12.9+/-10.413	0.012	0.365
ADC($10^{-3}mm^2/s$)	1.37+/-0.5302	1.65+/-0.4287	0.016	0.464

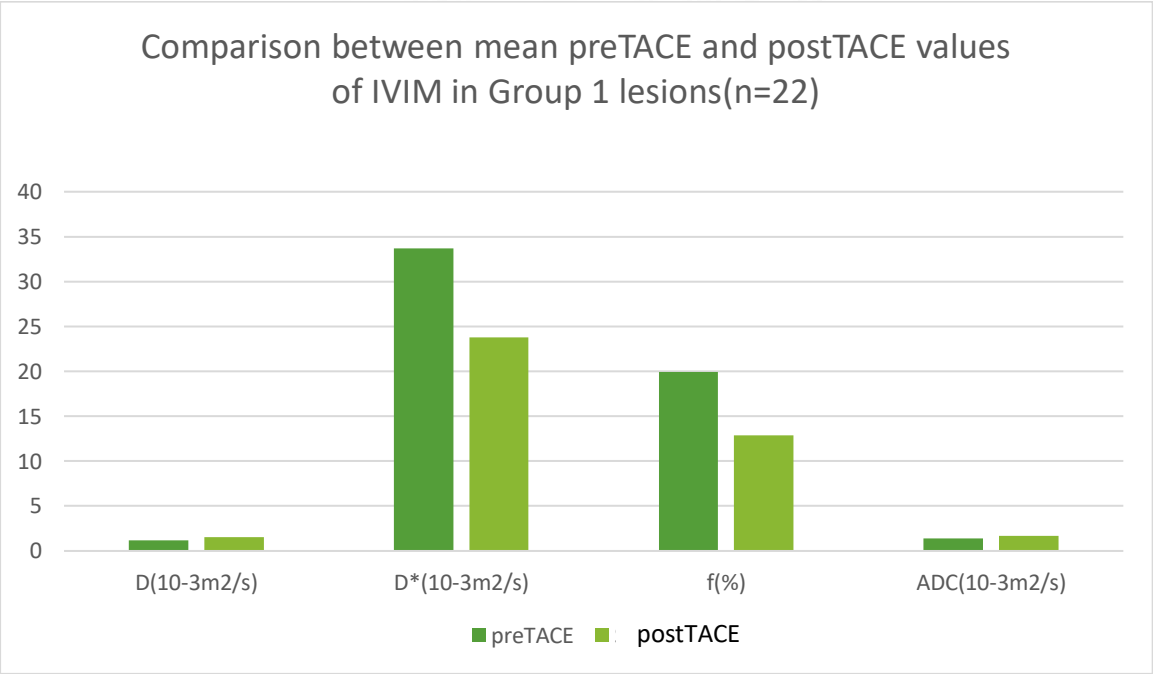

Fig.31. Bar diagram showing a comparison between mean preTACE and postTACE values of IVIM imaging in Group 1(complete response) lesions

3.2. Group 2 (Nonresponding/Residual/viable) lesions

In group 2 lesions, mean preTACE and postTACE values of all IVIM parameters were given in Table.10.

No IVIM parameters showed significant changes in group 2 lesions

3.2.a. D

Of 10 residual enhancing lesions, 5 lesions showing minimal decrease and 5 lesions showing a minimal increase in its value. The mean percentage changes from baseline values of D were 0.1%. There was no statistical difference (1.241 vs 1.247, P-value 0.94)between mean preTACE and postTACE values. There was mild correlation(r=0.26) between preTACE and postTACE values (fig 32).

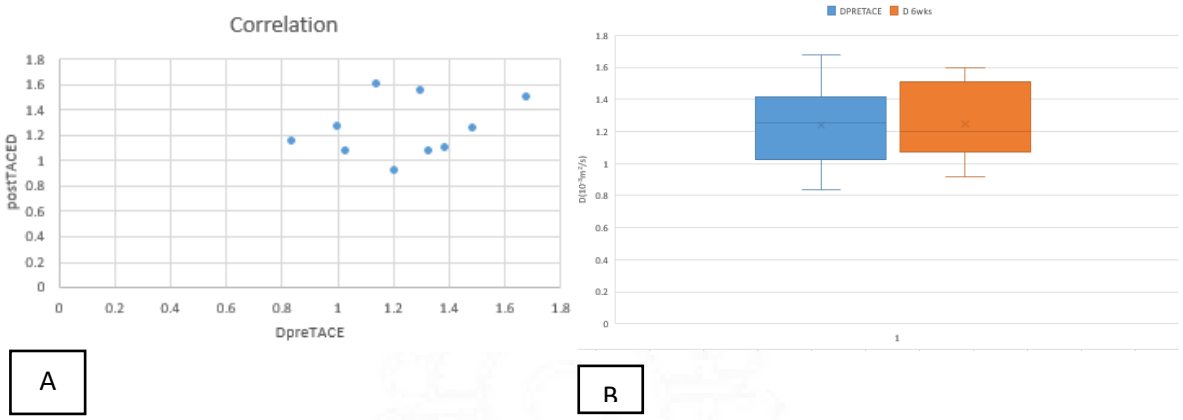

Fig 32 A. scatter plot showing a mild correlation between preTACE and postTACE values of D

B. Box & whisker plot showing no significant difference between preTACE and postTACE values. The significant overlap of median values was noted between preTACE and postTACE.

3.2.b. D*

D* in residual enhancing portions should be almost the same or increased in postTACE MRI. In this study, of 10 residual enhancing lesions, 5 lesions showing a decrease, and 5 lesions showing an increase in its value. The mean percentage changes from baseline values of D* was almost 0%. There was no statistical difference(31.63 vs 31.5, p-value 0.98) between mean preTACE and postTACE values. There was mild negative correlation(r= -0.131) between preTACE and postTACE values (fig 33).

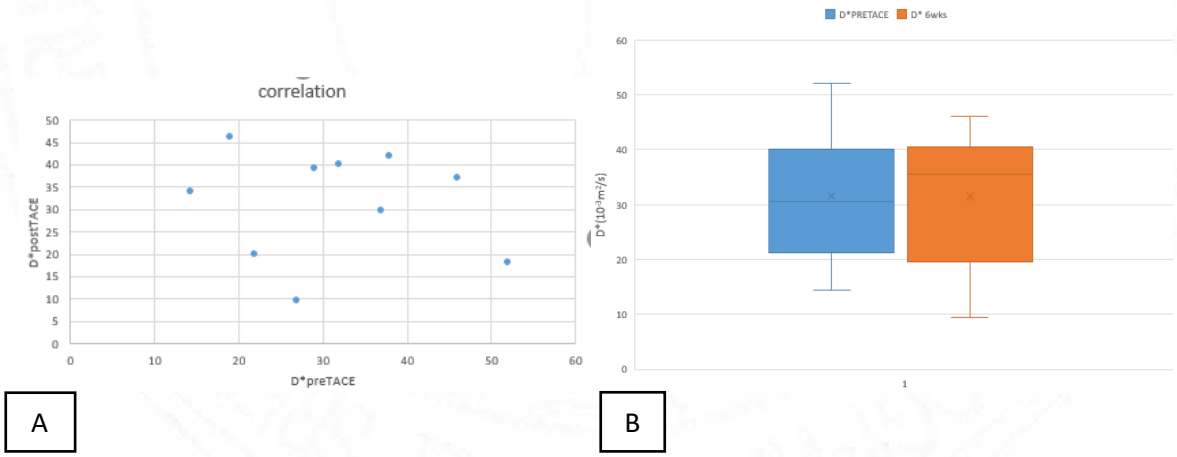

Fig 33

A. Scatter plot showing a mild negative correlation between preTACE and postTACE values of D*

B. Box & whisker plot showing no significant difference between preTACE and postTACE values. The significant overlap of median values was noted between preTACE and postTACE.

3.2.C. f

Of 10 residual enhancing lesions, 6 lesions showing minimal decrease and 4 lesions showing an increase in its value. The mean percentage changes from baseline values of 'f' were 0%. There was no statistical difference(18.52 vs 18.6, p-value 0.98) between mean preTACE and postTACE values. There was mild correlation(r= 0.211) between preTACE and postTACE values (fig 34).

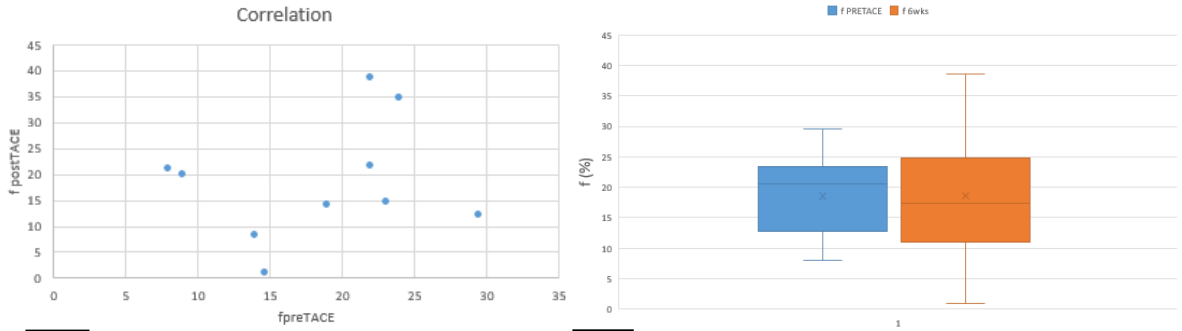

Fig 34

A. scatter plot showing a mild correlation between preTACE and postTACE values of perfusion fraction 'f'.

B. Box & whisker plot showing no significant difference between preTACE and postTACE values. The significant overlap of median values was noted between preTACE and postTACE.

3.2.d. ADC

Of 10 residual enhancing lesions, 2 lesions showing minimal decrease and 8 lesions showing a minimal increase in its value. The mean percentage changes from baseline values of D was a 9% increase. There was no statistical difference (1.258 vs 1.366, p-value 0.122) between mean preTACE and postTACE values. There was good correlation(r=0.725) between preTACE and postTACE values (fig 35).

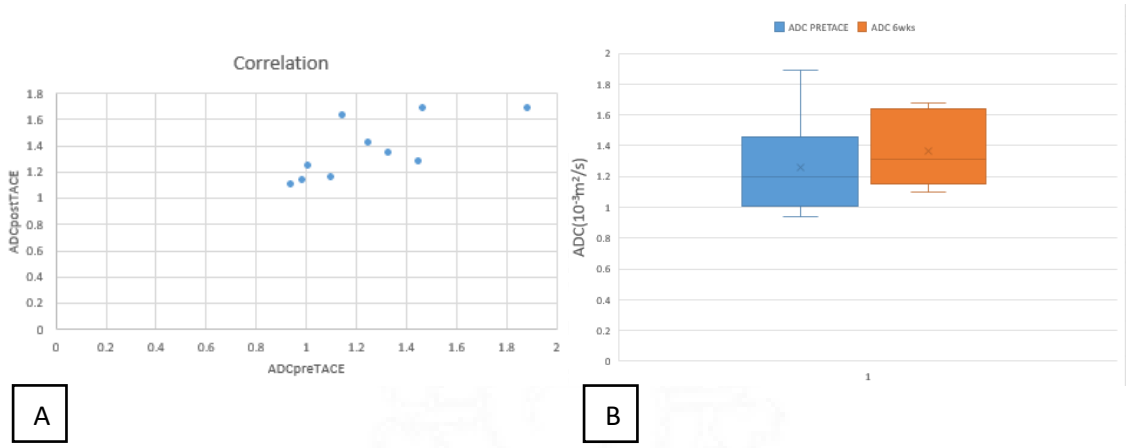

Fig 35

A. scatter plot showing good correlation between preTACE and postTACE values of ADC

B. Box & whisker plot showing no significant difference between preTACE and postTACE values. The significant overlap of median values was noted between preTACE and postTACE.

Table 10. Comparison between mean preTACE and post TACE values of IVIM in Group 2 lesions (n=10).

Parameter	preTACE(mean+ SD)	postTACE(mean +SD)	P-value	Pearson correlation
D($10^{-3}mm^2/s$)	1.241+/-0.237	1.247+/-**0.219**	0.94	0.26
D*($10^{-3}mm^2/s$)	31.63+/-11.266	31.5+/-**11.36**	0.98	-0.131
f(%)	18.52+/-6.58	18.6+/-**10.84**	0.98	0.2117
ADC($10^{-3}mm^2/s$)	1.258+/-0.275	1.366+/-**0.215**	0.122	0.725

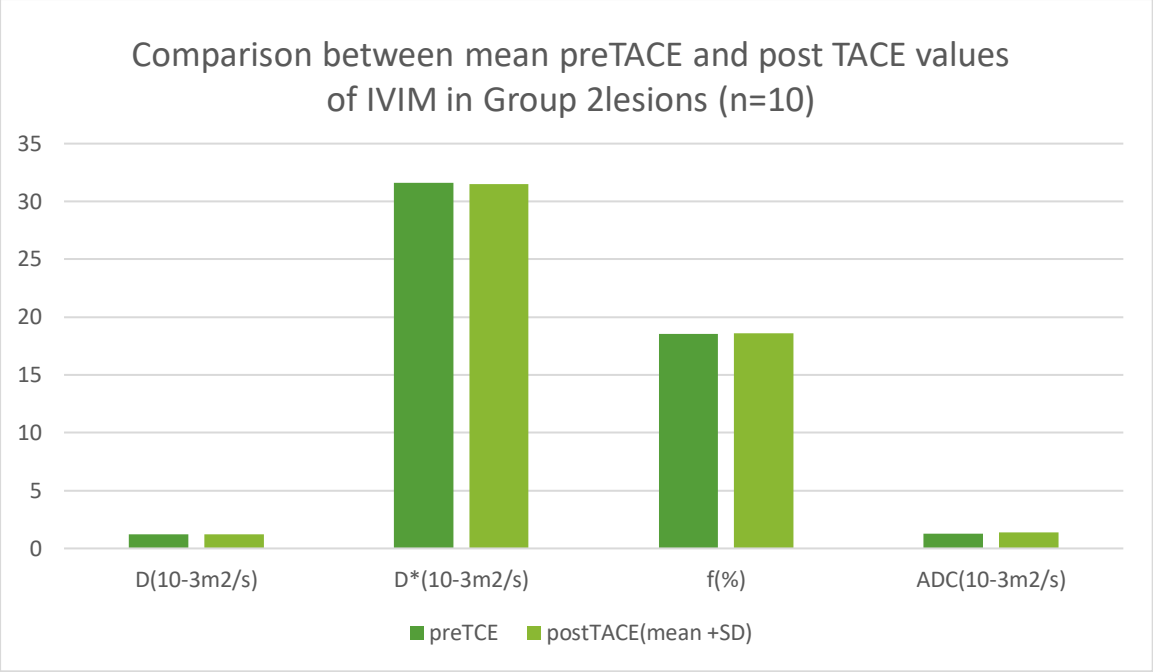

Fig 36. Bar diagram showing a comparison between mean preTACE and postTACE values of IVIM imaging in group 2 lesions

4.1. Comparison between D and ADC in complete responding (group 1) lesions

Four lesions showing a decrease in ADC after TACE in complete response lesions(group 1). Of these 4, 3 lesions also showing a corresponding decrease in D values. Only one lesion showing an increase in D value. Only one lesion which is showing a decrease in D is showing an increase in ADC. There was no statistical difference between mean D and ADC values in group 1(D- 0.35 vs ADC - 0.28, p-value 0.7). However, mean D values are higher than ADC values which may be due to the opposite effects of diffusion and perfusion while assessing monoexponential ADC. There was good correlation between D and ADC values(r= 0.834) (fig 37).

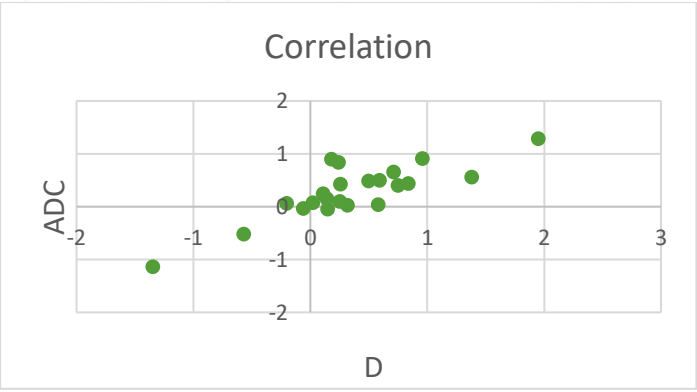

Fig 37 Scatter plot showing good correlation between D and ADC showing good correlation between D and ADC values in group 1 lesions

4.2.Comparison between D* and Ktrans & Kep in group 1 lesions

Four lesions showed an increase in Ktrans values after TACE. Of these, 3 lesions showed a decrease in D* values and one lesion showed an increase in D* value. 18 lesions showed a decrease in Ktrans after TACE. Of these, only one lesion showed an increase in D* after TACE. There was a statistical difference between mean differences of D* and Ktrans (D* 9.95 vs Ktrans 0.183, p-value- 0.00028). There was a weak correlation between D* and Ktrans(r= 0.076)(fig 38). 5 lesions showed an increase in Kep values after TACE. Of these, 4 lesions showed a decrease in D* values after TACE, and only one lesion showed an increase in D * value. 17 lesions showed a decrease in Kep value. Of these, only lesions showed an increase in D* and 16 lesions showed a decrease in D* after TACE. There was a statistical difference between mean differences of D* and Kep (D* 9.95 vs Kep 1.232, p-value- 0.0011). There was a weak correlation between D* and Kep(r= 0.057) (fig 39).

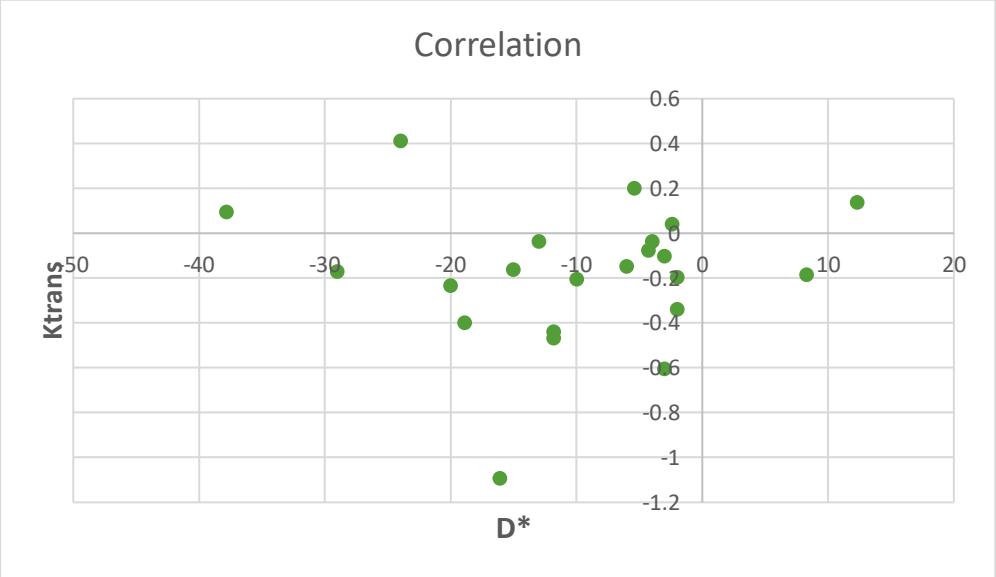

Fig 38 Scatter plot showing a weak correlation between D* and Ktrans in group 1 lesions

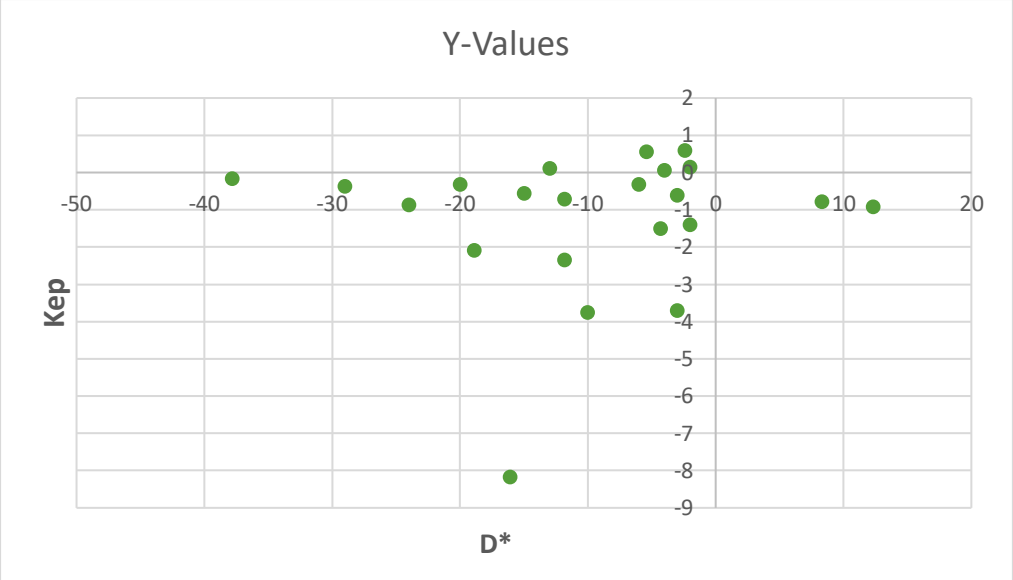

Fig 39 Scatter plot showing a weak correlation between D* and Kep in group 1 lesions

4.3.Comparison of preTACE values in-between group 1 and group 2

The comparison was made between preTACE values in group 1 and group 2 lesions to predict the lesions that may show a response after TACE. This showed no significant differences in MR perfusion and IVIM parameters between the two groups(Table 11)

Table 11. Comparison of preTACE values in-between group 1 and group 2

Parameter	Complete response group(group 1)(n=22)	Residual/ viable lesion group(group 2) (n=10)	P-value
D($10^{-3}mm^2/s$)	1.208+/-0.581	1.241+/-0.237	0.82
D*($10^{-3}mm^2/s$)	33.7+/-10.406	31.63+/-11.266	0.64
f(%)	19.92+/-10.54	18.52+/-6.58	0.66
ADC($10^{-3}mm^2/s$)	1.37+/-0.5302	1.258+/-0.275	0.45
Ktrans(min^{-1})	0.38+/-0.227	0.435+/-0.223	0.57
Kep(min^{-1})	2.09+/- 1.749	2.23+/-0.977	0.77
Ve	0.23+/-0.105	0.258+/-0.157	0.81
Max slope(mmol/s)	0.024+/-0.014	0.026+/-0.018	0.39
IAUGC	0.276+/-0.113	0.322+/-0.138	0.64

4.4.Comparison of postTACE values in between complete responding(group 1) and nonresponding (group 2) lesions

Comparison was also made between mean postTACE values in group 1 and group 2 lesions(Table 12). In this MR perfusion parameters like Ktrans(p value 0.005), Kep(p value 0.0007) and IAUGC (p value 0.01) showed significant difference and Ve (p value 0.27)and max slope(p value 0.29) showed no significant difference. In IVIM parameters, D (P value- 0.02)and ADC values (P value - 0.02) showed significant difference whereas D*(P value- 0.11) and f (P value 0.2) showed no significant difference between the two groups(Table 12). Mean differences with percentage changes between preTACE and postTACE values in group 1 and group 2 were given in Table 13

Table 12. Comparison of mean postTACE values in-between group 1 and group 2

Parameter	Complete response group(group 1)(n=22)	Residual/ viable lesion group(group 2)(n=10)	P-value
D($10^{-3}mm^2/s$)	1.560+/-0.494	1.247+/-0.219	0.02
D*($10^{-3}mm^2/s$)	23.75+/-12.13	31.5+/-11.36	0.11
f(%)	12.9+/-10.413	18.6+/-10.84	0.20
ADC($10^{-3}mm^2/s$)	1.65+/-0.4287	1.366+/-0.215	0.02
Ktrans(min^{-1})	0.20+/-0.214	0.414+/-0.159	0.005
Kep(min^{-1})	0.86+/-0.437	2.39+/-0.943	0.0007
Ve	0.29+/-0.199	0.231+/-0.108	0.27
Max slope(mmol/s)	0.020+/-0.012	0.06+/-0.0984	0.29
IAUGC	0.154+/- 0.177	0.305+/-0.131	0.01

Comparison of the mean difference between pre and postTACE values in group 1(complete response lesions) and group 2(nonresponding lesions)

Change in mean values between preTACE and postTACE values of both MR perfusion and IVIM parameters were compared between group 1(complete response lesions) and group 2(nonresponding lesions) (table 13 and fig 40&41). Mean differences of MR perfusion parameters were significant in Kep(1.23 min^{-1} vs 0.15, p – value 0.009) and nonsignificant in Ktrans(0.183 min^{-1}vs 0.021 min^{-1}, p-value

0.12) Ve(0.0614% vs 0.017%, p-value- 0.152), Max slope(0.0044mmol/s vs 0.027 mmol/s, p-value 0.24) and IAUGC (0.122 vs 0.034, p-value 0.22). Mean differences of IVIM parameters were significant in D(0.352 $X10^{-3}mm^2/s$ (43%) vs 0.006x $10^{-3}mm^2/s$ (0.4%), p- value 0.02) and nonsignificant in D*(9.95x$10^{-3}mm^2/s$ vs 0.13X $10^{-3}mm^2/s$), f(7.02% vs 0.07%, p-value 0.14), ADC (0.285X$10^{-3}mm^2/s$ vs 0.11X $10^{-3}mm^2/s$, p-value 0.17)

Table 13. Comparison of the mean difference between pre and postTACE values in group 1(complete response lesions) and group 2(nonresponding lesions)

Parameter	Group1-Complete response group(percentage change)	Group2-nonresponding/Residual/viable lesion group(percentage change)	p- value
D($10^{-3}mm^2/s$)	0.3524(43%)	0.006(0.4%)	0.02
D*($10^{-3}mm^2/s$)	-9.95(28%)	-0.13(0.4%)	0.13
f(%)	-7.0205(20%)	0.074((0.4%)	0.14
ADC($10^{-3}mm^2/s$)	0.2855(29%)	0.108(9%)	0.17
Ktrans(min^{-1})	-0.1838(40%)	-0.0209(5%)	0.12
Kep(min^{-1})	-1.232(37%)	0.1573(7%)	0.009
Ve	0.0614(64%)	-0.017(10%)	0.152
Max slope	-0.0044(33%)	-0.027(131%)-	0.239
IAUGC	-0.1217(43%)	-0.03454(5%)	0.217

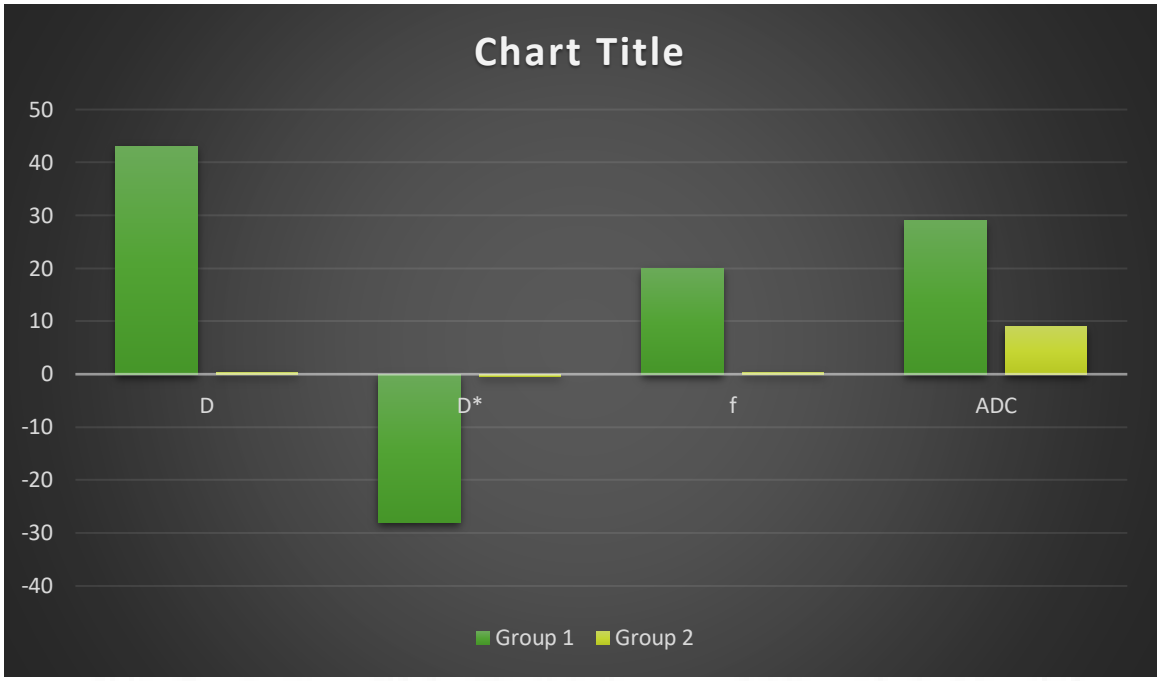

Fig 40 Comparison of mean difference in percentage between pre and postTACE IVIM values in group 1(complete response lesions) and group 2(residual/viable lesions

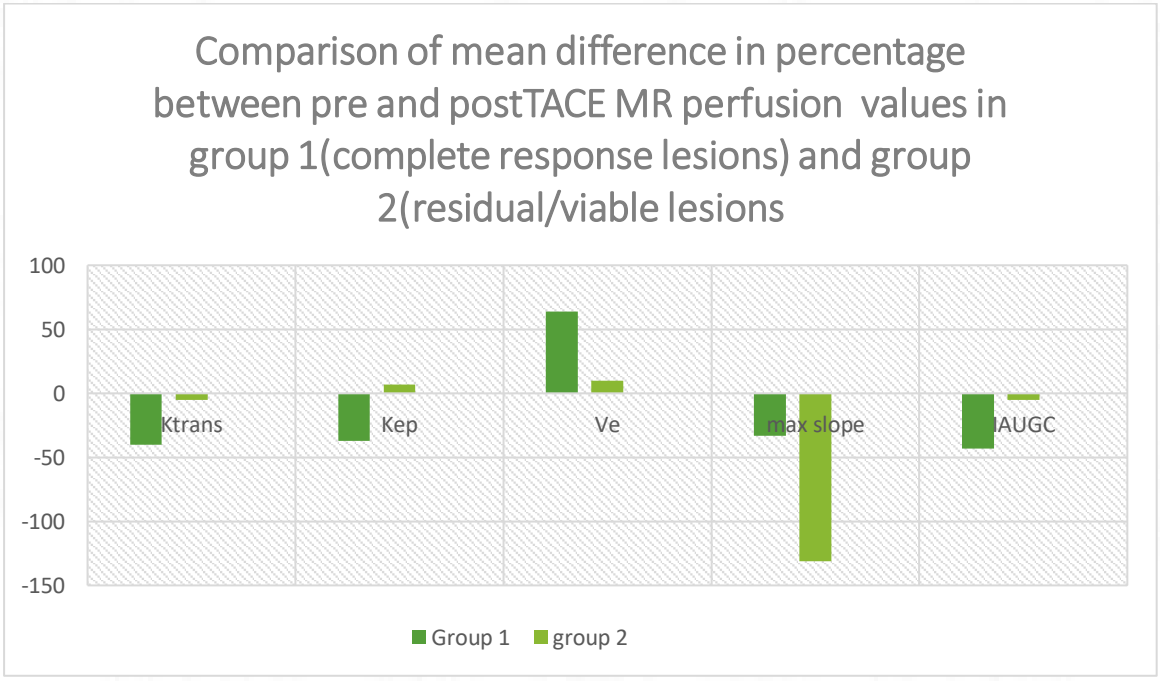

Fig 41 Comparison of mean difference in percentage between pre and postTACE MR perfusion values in group 1(complete response lesions) and group 2(residual/viable lesions

5.ROC curve analysis

Threshold, Area under the curve, sensitivity, and specificity of both IVIM and MR perfusion parameters were measured.. Among perfusion parameters, Kep means difference has the highest AUC with greater than 0.156 min^{-1} decrease between preTACE and postTACE values is having a sensitivity and specificity of 72.27% and 60% respectively(p-value 0.0073). Ktrans mean difference has AUC of 0.7 with greater than 0.038 decreases between preTACE and postTACE values having a sensitivity and specificity of 77.27 % and 80% respectively (p-value 0.072). The 'Ve' mean difference has AUC of 0.582 with greater than 0.003%increase between preTACE and postTACE values having a sensitivity and specificity of 59.09% and 60%respectively(p-value 0.455). Max slope mean difference has AUC of 0.677 with greater than 0.003decrease between preTACE and postTACE values having a sensitivity and specificity of 63.64% and 80%respectively (p-value 0.069)..IAUGC mean difference has AUC of 0.684 with greater than 0.068 decrease between preTACE and postTACE values having a sensitivity and specificity of 72.73% and 70% respectively (p-value 0.117). ROC curves for MR perfusion parameters were compared in fig 42.

Table 14. ROC curve analysis of mean differences between postTACE and preTACE values

Parameter	Threshold	AUC	Sensitivity	Specificity	P-value
$DX10^{-3}mm^2/s$ (increase)	>0.04	0.714	77.27	60	0.026
$D^*X10^{-3}mm^2/s$ (decrease)	> 2.4	0.691	81.8	60	0.106
f %(decrease)	>6	0.655	59.09	70	0.176
$ADCX10^{-3}mm^2/s$ (increase)	>0.23	0.645	54.55	90	0.141
$Ktrans min^{-1}$(decrease)	>0.038	0.7	77.27	80	0.072
Kep min^{-1} (decrease)	>0.156	0.745	77.27	60	0.0073
Ve%(increase)	>0.003	0.582	59.09	60	0.455
Max slope mmol/s(decrease)	>0.0003	0.677	63.64	80	0.069
IAUGC(decrease)	>0.068	0.684	72.73	70	0.117

Among IVIM parameters, D mean difference has the highest AUC with greater than 0.04 increase between preTACE and postTACE values having a sensitivity and specificity of 78 and 60% respectively(p-value 0.026). D* mean difference has AUC of 0.691 with greater than 2.4 decreases between preTACE and postTACE values having a sensitivity and specificity of 81.8% and 60% respectively(p-value 0.106). f mean difference has AUC of 0.655 with greater than 8 % decrease between preTACE and postTACE values having a sensitivity and specificity of 95.4% and 40%respectively(p-value 0.176). ADC mean difference has AUC of 0.645 with greater than 0.23 decrease between preTACE and postTACE values having a sensitivity and specificity of 54.55 % and 90% respectively(p-value 0.141). ROC curves for IVIM parameters were compared in fig 43.

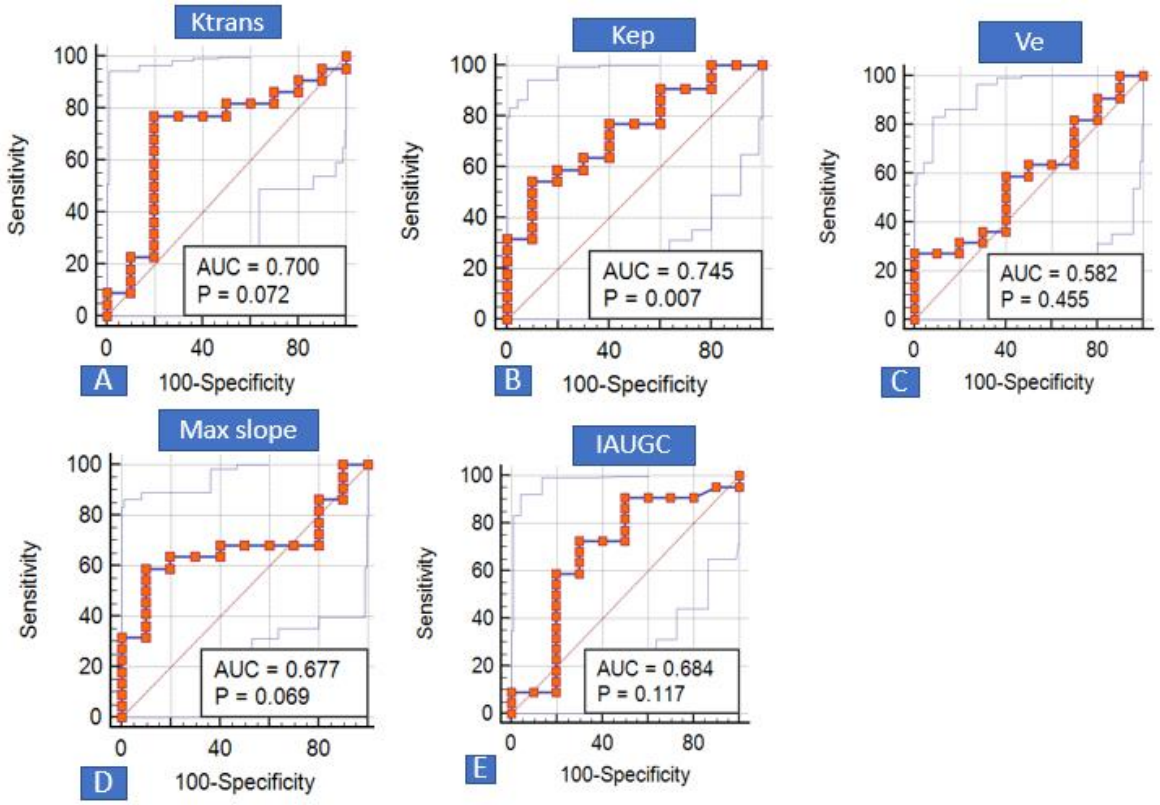

Fig 42.Comparison of ROC graphs of MR perfusion parameters

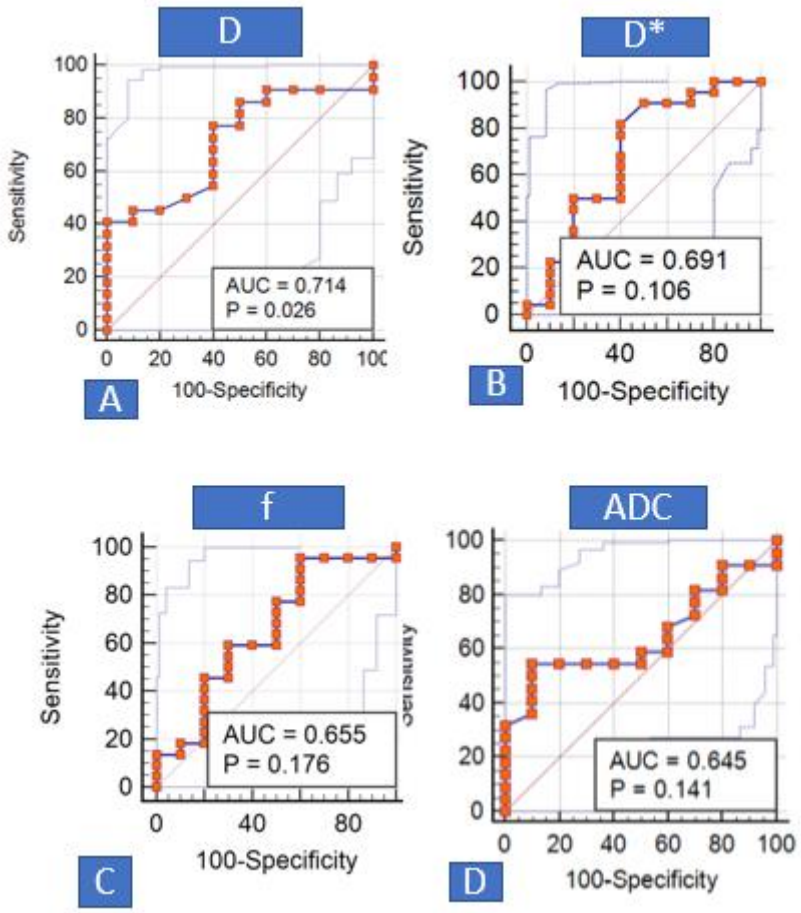

Fig 43 Comparison of ROC graphs of IVIM parameters

6. Comparison between BCLC category and response assessment

Of 16 BCLC A lesions, 14 had complete response and two were nonresponding. Of 16 BCLC B lesions, 8 a have complete response and 8 are nonresponding. The relationship between BCLC category and response is statistically significant(P-value- 0.02)(Table 15). This indicates complete response is high in BCLC A lesions

Table 15. Comparison between BCLC category and response assessment

Category	Complete response	Residual/nonresponse	Total
A	14	2	16
B	8	8	16
Total	22	10	32

7. Comparison between etiology and response assessment

Of 18 lesions with alcohol as etiology, 11 have a complete response and 7 have no response/ residual lesions and of 14 lesions with nonalcoholic etiology, 11 have a complete response and 3 have no response /residual lesion. The relationship between etiology and response is not significant (p-value-0.29) Table 16). This indicates that a high incidence of complete response in the nonalcoholic group is by chance.

Table 16 Comparison between etiology and response assessment

Etiology	Complete response	Residual/nonresponse	Total
Alcohol	11	7	18
Nonalcohol	11	3	14
Total	22	10	32

ILLUSTRATIVE CASES

1 Complete response lesion-

PreTACE MRI

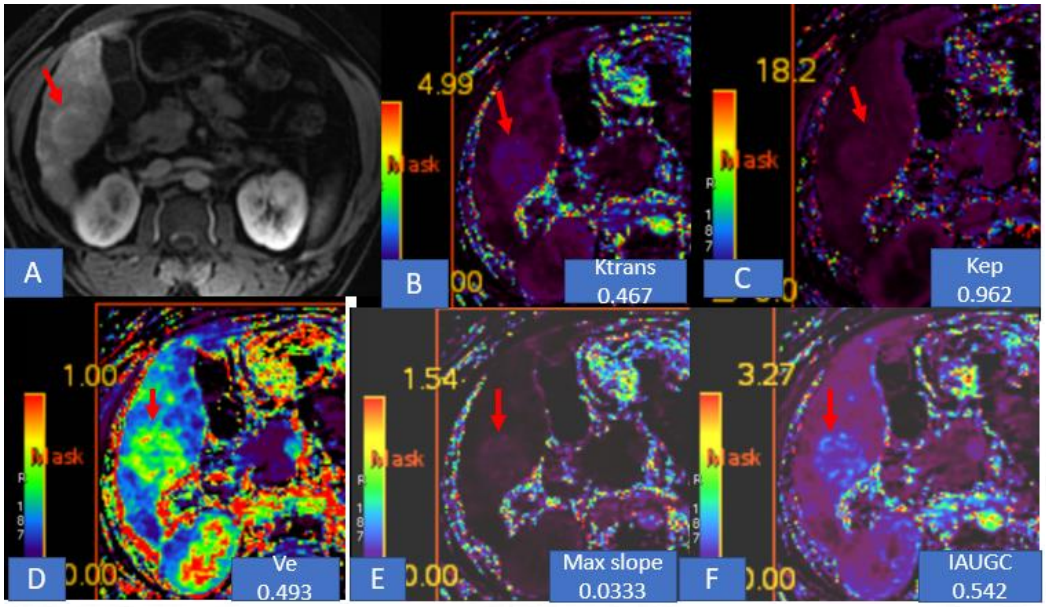

Fig 44. MR perfusion imaging A. showing arterial-enhanced lesion in seg VI (arrow). B- F- colour coded maps of Ktrans(B), Kep(C), Ve(D), Max slope(E), IAUGC(F) showing lesion(arrows)

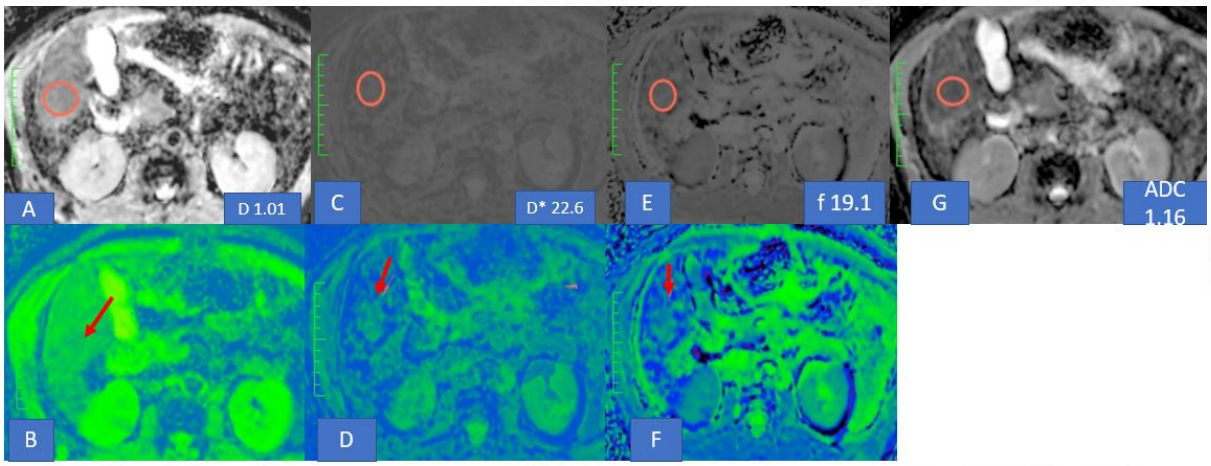

Fig 45 IVIM imaging showing the lesion - A., C, E, G represents D, D*, f, ADC respectively with circular ROI drawn over the lesion corresponding to enhancing lesion in DCE; B, D, F represents colour maps of D, D*, f respectively showing the lesion(arrows)

PostTACE MRI

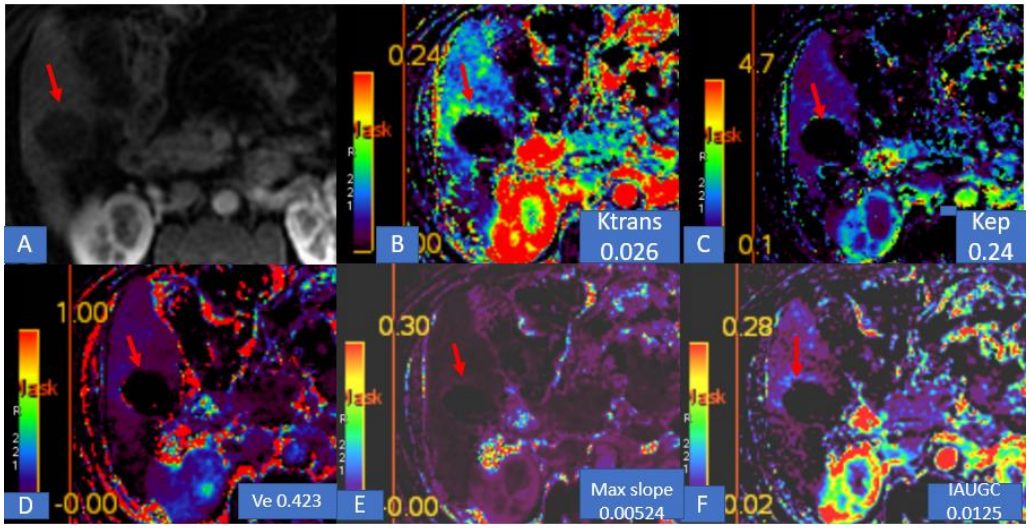

Fig 46. MR perfusion images in same patient with complete response. A- MR perfusion Contrast-enhanced image showing complete response with no enhancement in the lesion(arrow); B-F colour-coded maps of Ktrans(B), Kep(C), Ve(D), Max slope(E), IAUGC(F) (arrows) . Decreased Ktrans, Kep, max slope, IAUGC, and Ve noted in postTACE MRI indicating response.

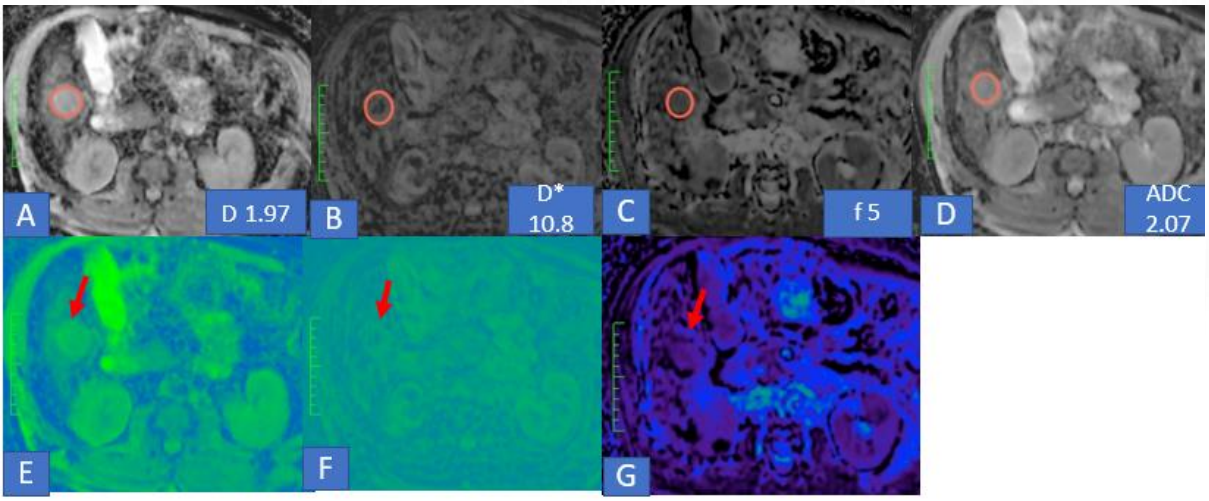

Fig 47. IVIM imaging showing lesion Fig A., C, E, G represents D, D*, f, ADC respectively with ROI drawn over the lesion corresponding to the lesion with no enhancement in DCE; B, D, F represents colour maps of D, D*, f respectively showing lesions (arrows) with decreased D* & f and increased D & ADC indicating response.

2. NON RESPONDER –

PreTACE

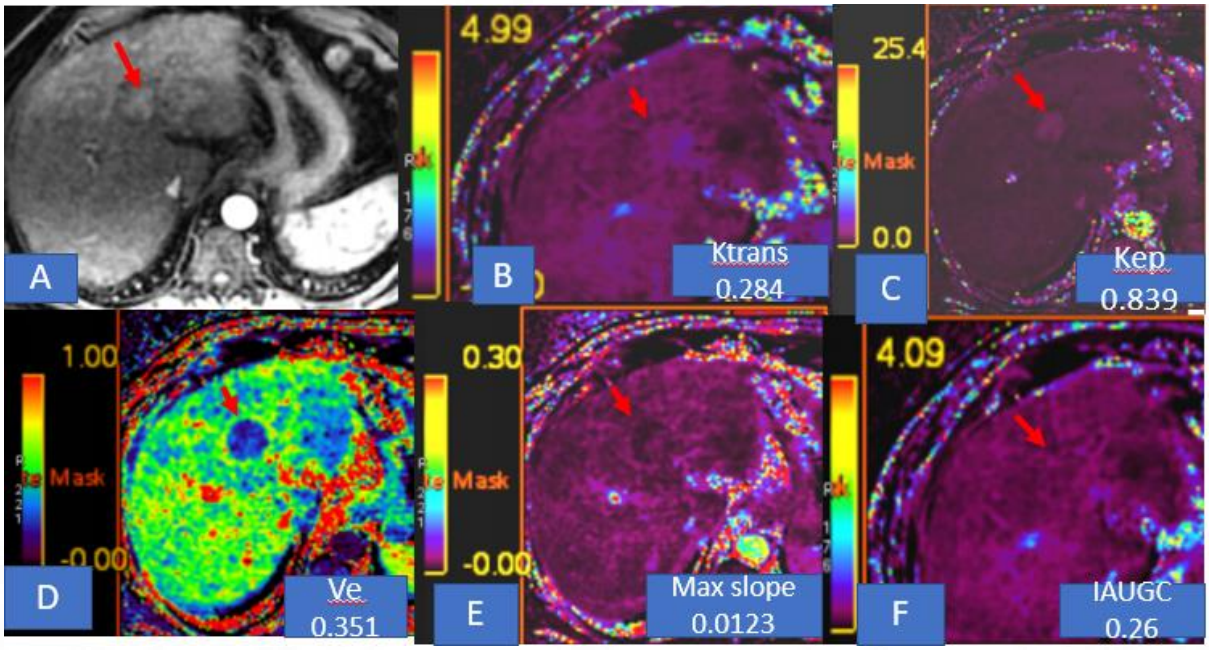

Fig 48 A HCC patient with seg IV lesion with preTACE MR perfusion images. A. DCE image showing enhancing lesion in seg IV(arrow), B – F colour maps of various MR perfusion parameters showing the lesion(arrows). B. Ktrans colour map, C. Kep colour map, D. Ve colour map, E. max slope colour map, E. IAUGC colour map

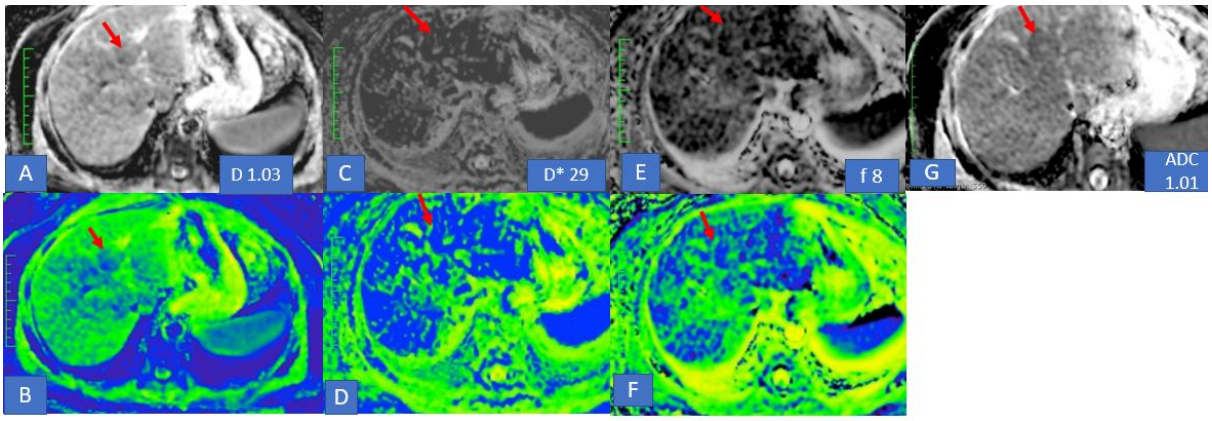

Fig 49. In the above patient IVIM preTACE IVIM images showing a lesion in seg IV (arrows), A. D map, B. D colour map, C. D* map, D. D* colour map, E. f map, F. f colour map, G. ADC map

postTACE

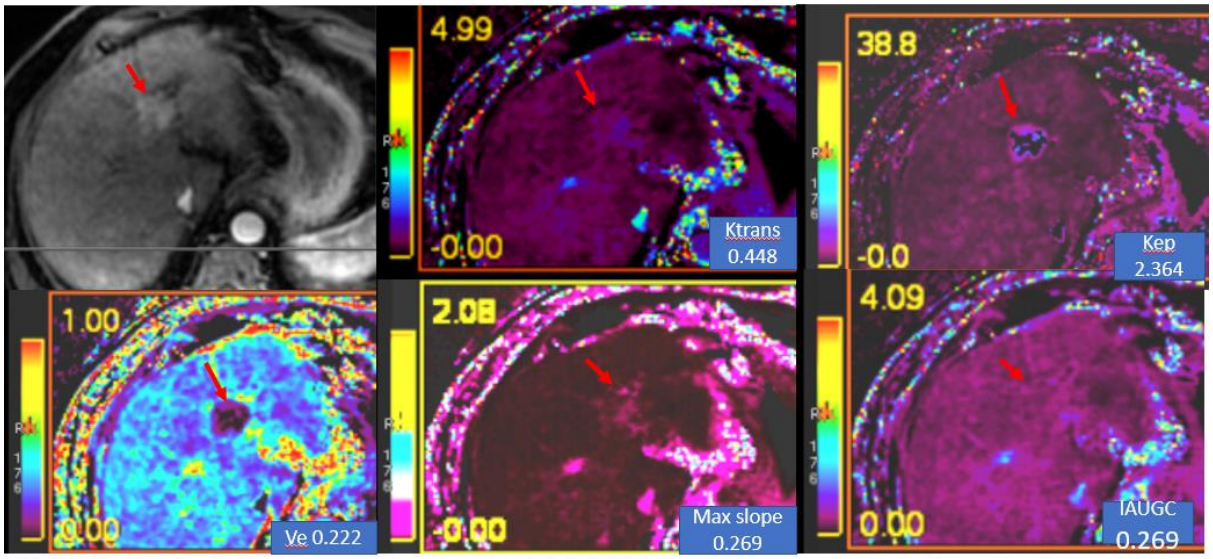

Fig 50. In thesame patient , seg IV lesion showing no response in postTACE in MR perfusion images. A.DCE image showing persistent enhancing lesion without any necrosis in seg IV(arrow), B – F colour maps of various MR perfusion parameters showing the lesion(arrows) with no significant chagnes in their values after TACE indicating no response. B. Ktrans colour map, C. Kep colour map, D. Ve colour map, E. max slope colour map, E. IAUGC colour map

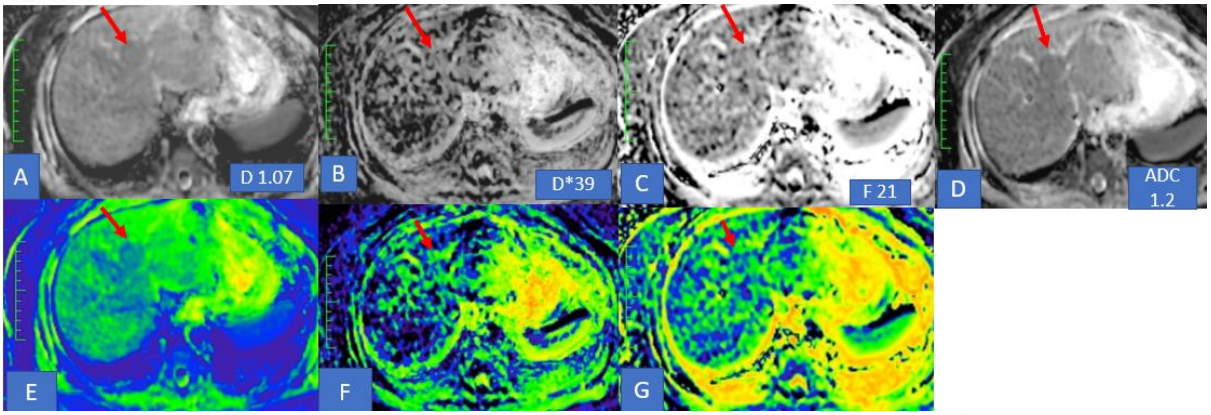

Fig 51. In the same patient , postTACE IVIM images showing a persistent enhancing lesion in seg IV with no response (arrows) with no significant changes in their values after TACE., A. D map, B. D colour map, C. D* map, D. D* colour map, E. f map, F. f colour map, G. ADC map

3. FALSE POSITIVE PERFUSION VALUES

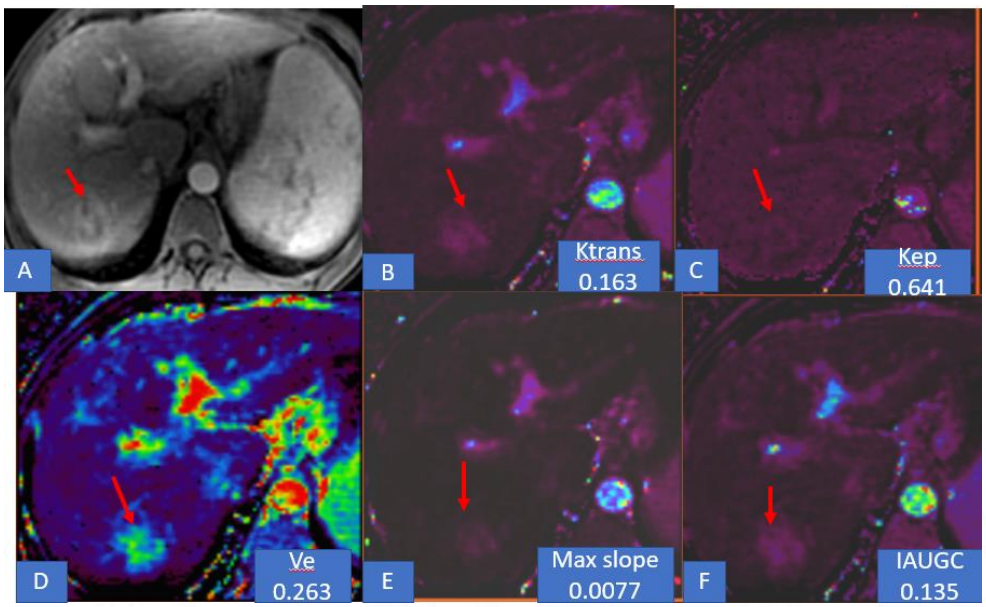

Fig 52. An HCC patient with seg VI lesion with preTACE MR perfusion images. A.DCE image showing enhancing lesion in seg VI(arrow), B – F colour maps of various MR perfusion parameters showing the lesion(arrows). B. Ktrans colour map, C. Kep colour map, D. Ve colour map, E. max slope colour map, E. IAUGC colour map preTACE Complete response lesion false negative perfusion parameters but IVIM parameters correctly showing response

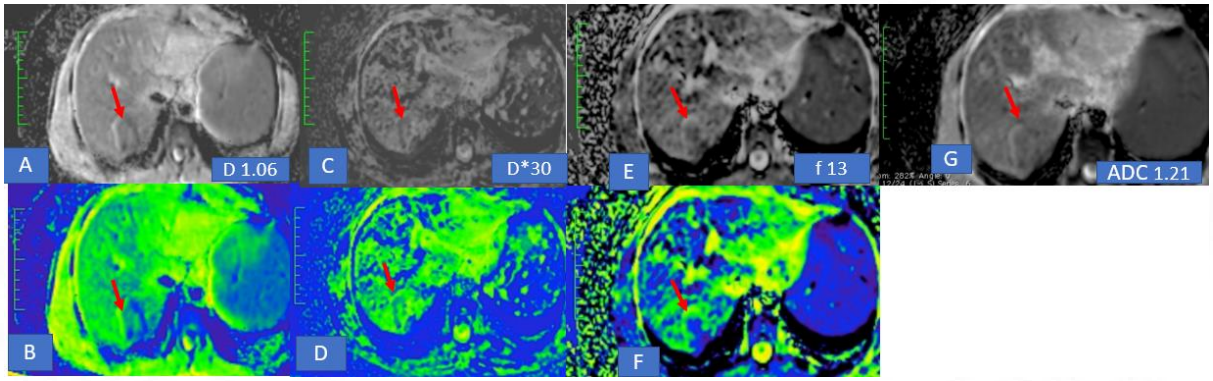

Fig 53. preTACE IVIM images showing a lesion in seg VI (arrows), A. D map, B. D colour map, C. D* map, D. D* colour map, E. f map, F. f colour map, G. ADC map

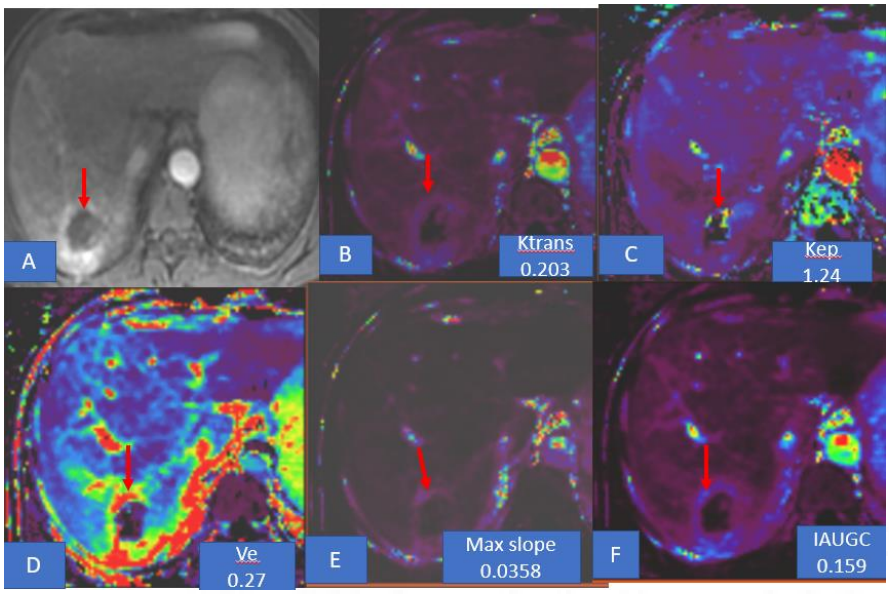

Fig 54. After TACE MR perfusion images. A.DCE image showing complete necrosis with no enhancement in the lesion in seg VI(arrow), B – F colour maps of various MR perfusion parameters showing the lesion(arrows) with increase in postTACE MRI values of K trans,, Kep, Max slope and IAUGC with no significant increase in Ve indicating false positive residual lesion. B. Ktrans colour map, C. Kep colour map, D. Ve colour map, E. max slope colour map, E. IAUGC colour map

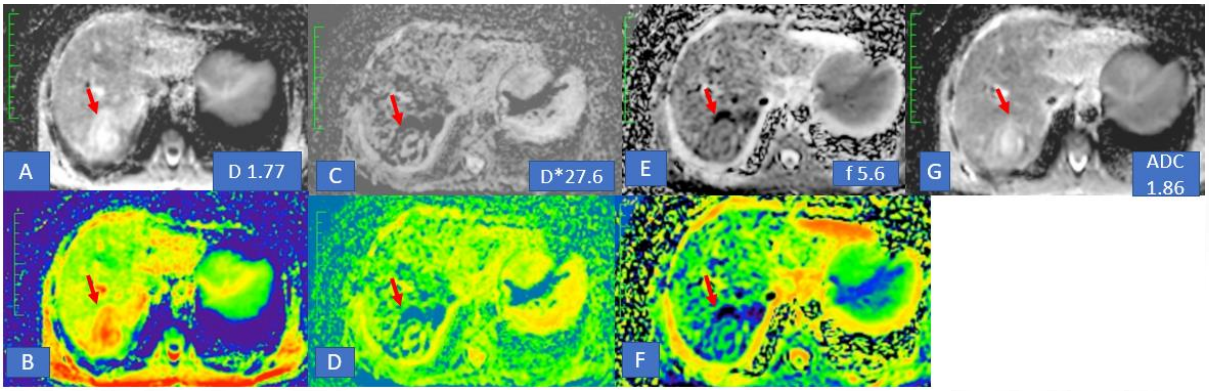

Fig 55. postTACE IVIM images showing lesion in seg VI (arrows), A. D map, B. D colour map, C. D* map, D. D* colour map, E. f map, F. f colour map, G. ADC map showing Decreased D* and f and increased D and ADCcorrectly identifying complete response.

4. FALSE POSITIVE MR PERFUSION VALUES of Ktrans and Kep

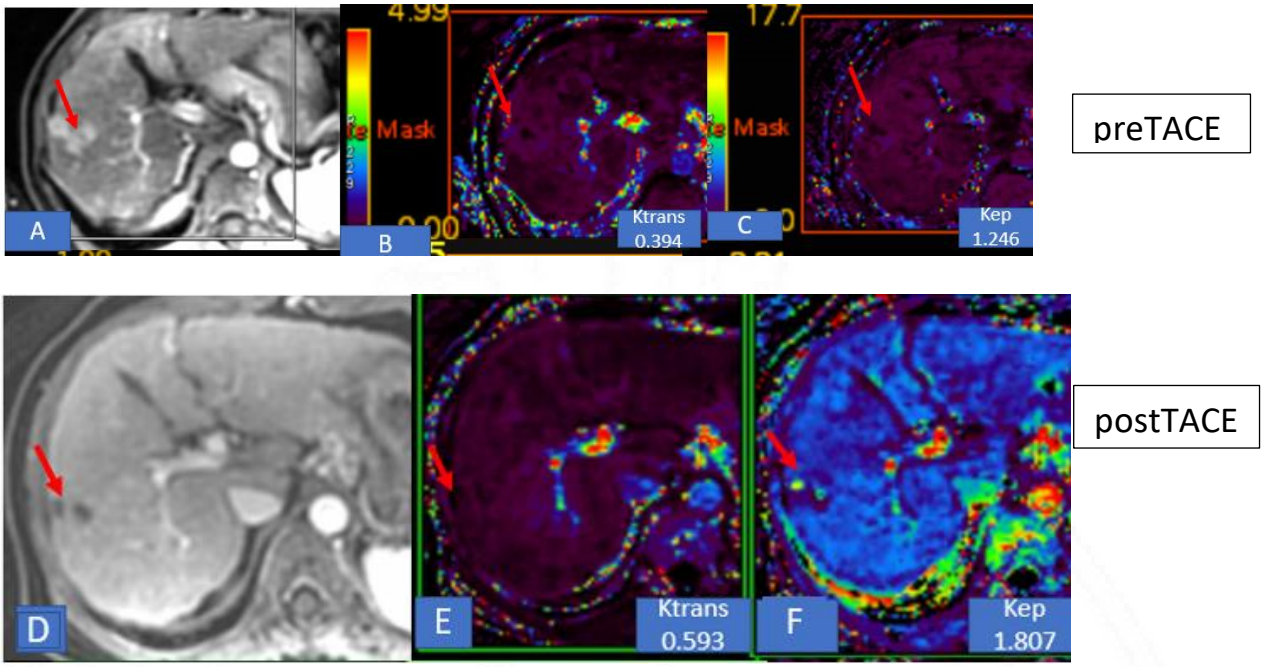

Fig 56 A HCV patient with complete response HCC lesion. DCE MRI showing lesion with contrast enhancement in preTACE MRI(A), which showed no enhancement and significant decrease in size with a complete response in postTACE DCE MRI. Paradoxical increase in Ktrans(B&E) and Kep values (C&F) after TACE which may be due to reduction in the size making it difficult to place ROI corresponding to the preTACE image(arrows).

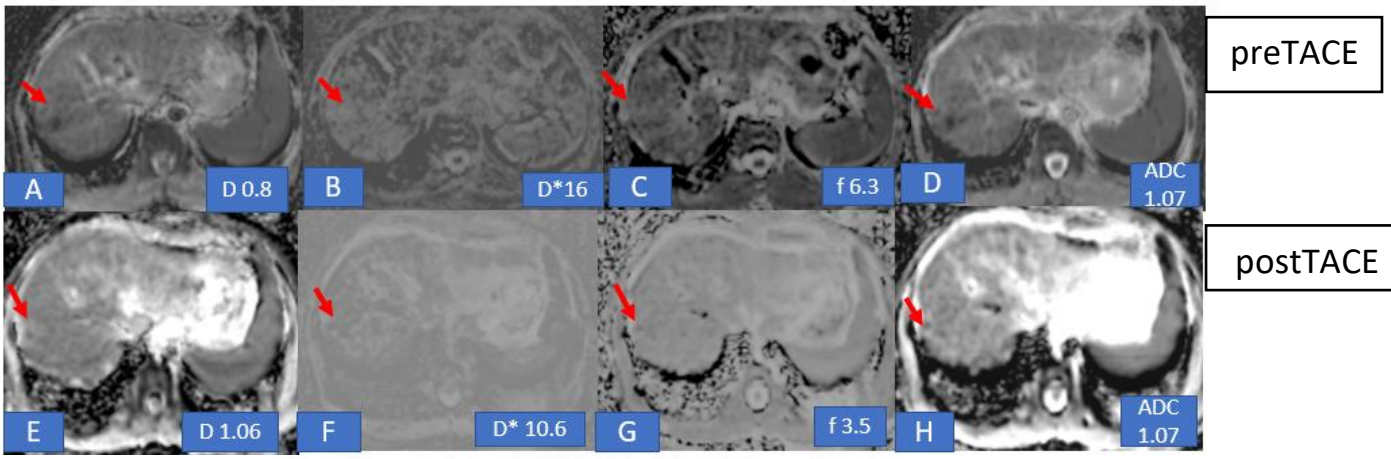

Fig 57 In the same patient shown above, the response of the lesionsis correctly identified by IVIM parameters. PostTACE showing an increase in D (A&E) and ADC (D&H), a decrease in D*(B&F), and f (C&G).

5. FALSE POSITIVE IVIM PARAMETERS

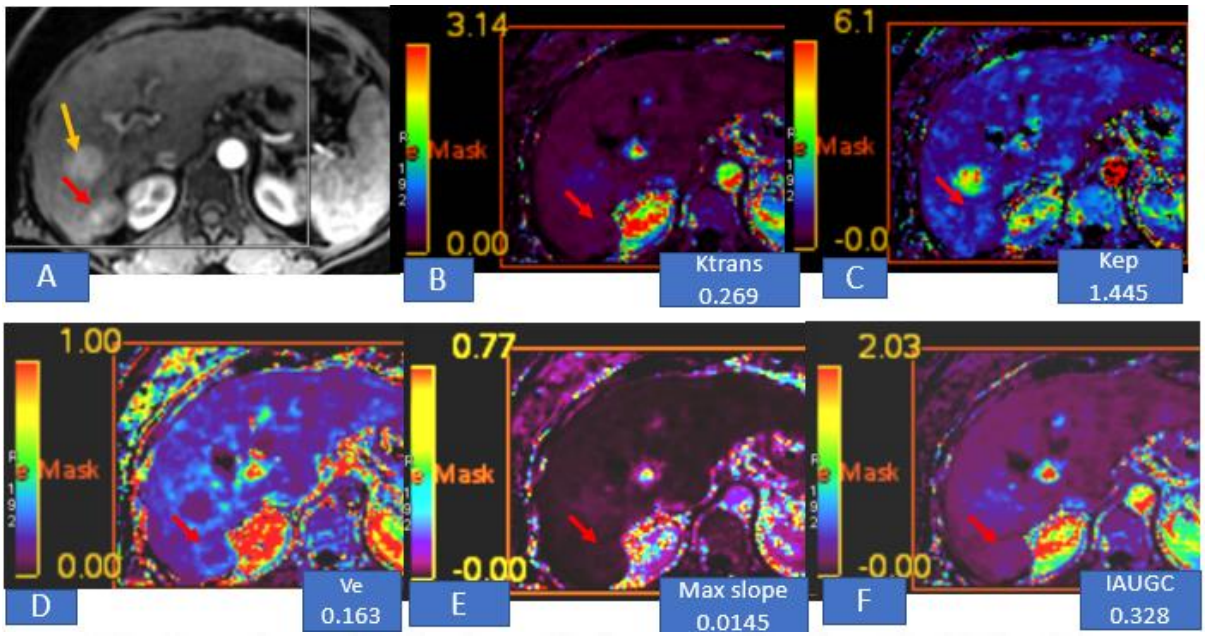

Fig 58. An HCC patient with enhancing lesions in seg VI (anterior lesion – yellow arrow and posterior lesion - red arrow). B – F colour maps of various MR perfusion parameters showing the lesion (red arrows) with values. B. Ktrans colour map, C. Kep colour map, D. Ve colour map, E. max slope colour map, E. IAUGC colour map

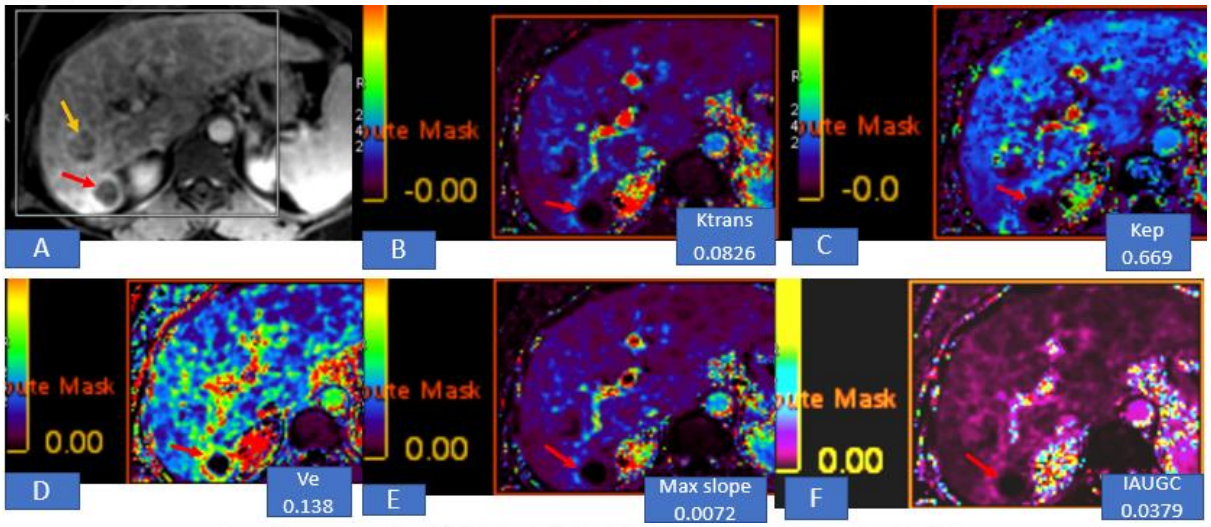

Fig 59. The same patient above with no enhancement in lesions in seg VI (anterior lesion – yellow arrow and posterior lesion - red arrow) after TACE indicating a complete response. B – F colour maps of various MR perfusion parameters showing the lesion (red arrows) with decreased Ktrans(B), Kep(B),

Max slope(E), IAUGC indicating a response. However, Ve (D) showing paradoxical decrease in its value

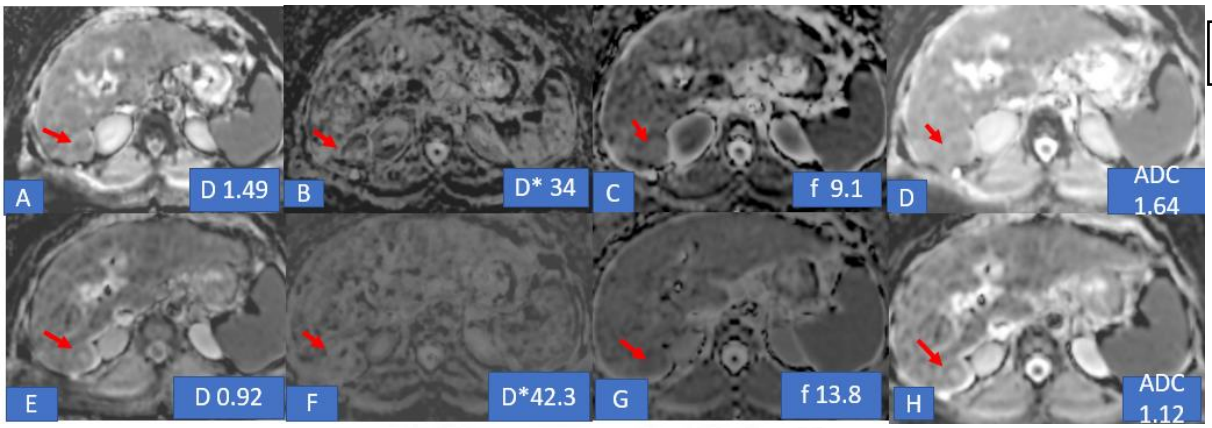

Fig 60. A patient with complete response HCC lesion showing false-positive IVIM parameters like decrease in D(A&E) and ADC(D&H) and increase in D*(B&F) and f(C&G)

6 AN EQUIVOCAL LESION WITH INCREASED MR PERFUSION VALUES

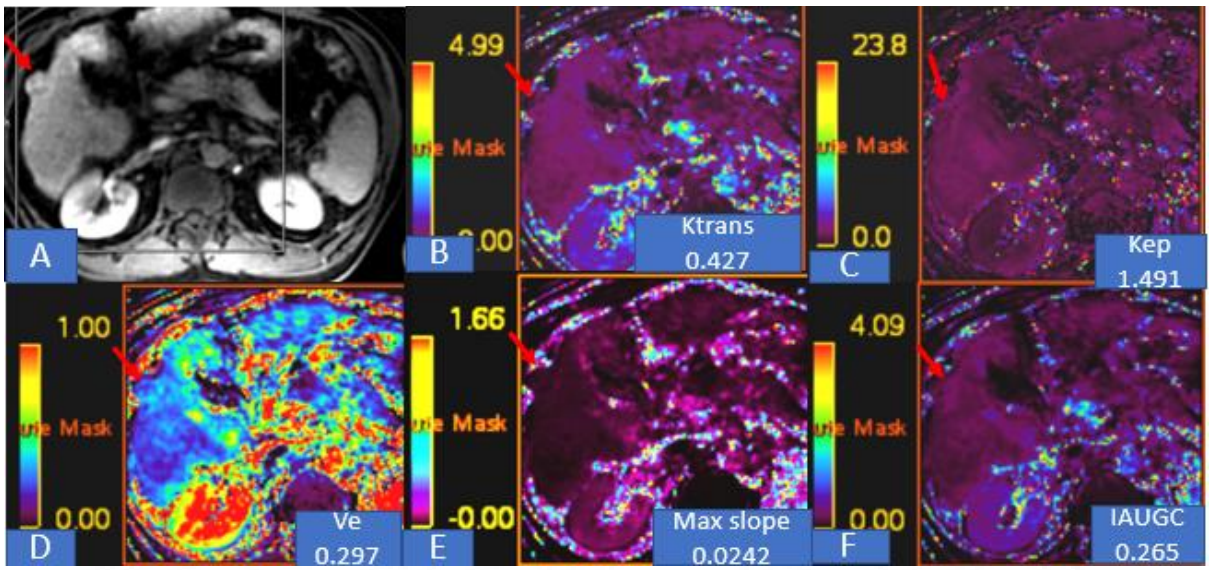

Fig 61. A patient with a small exophytic HCC lesion in seg VI showing arterial contrast enhancement(A). B-F : preTACE MR perfusion colour maps showing Ktrans (B), Kep(C), Ve(D), max slope(E), IAUGC(F)(arrows)

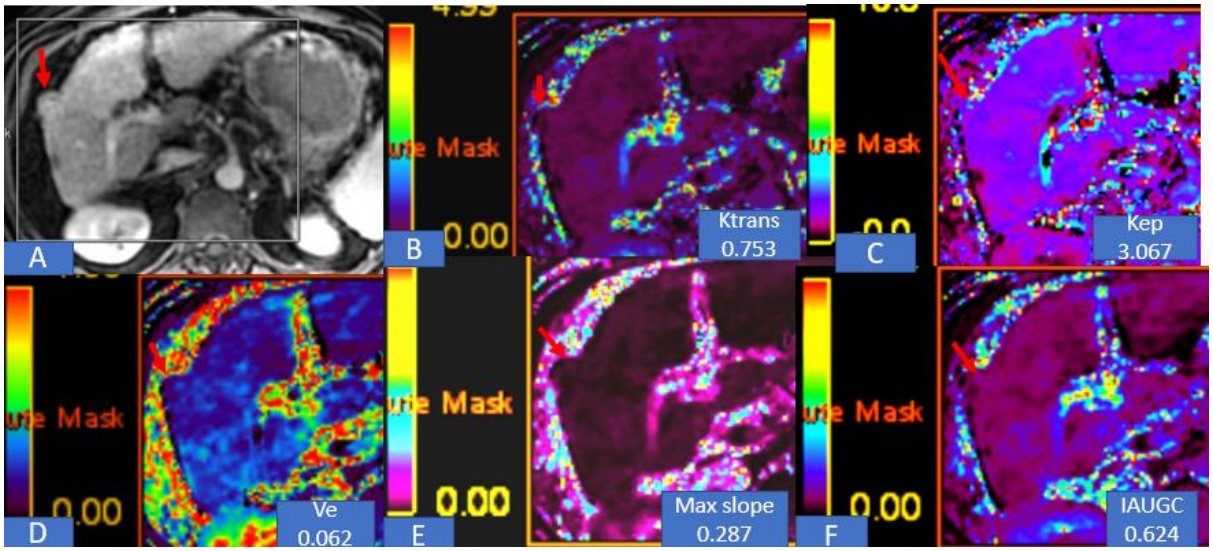

Fig 62. The same patient above showing the exophytic HCC lesion in seg VI with equivocal arterial enhancement and no definite washout indicating indeterminate response(A)with a rise in Alpha-fetoprotein(AFP) levels. B-F : postTACE MR perfusion colour maps showing an increase in Ktrans (B), Kep(C), max slope(E), IAUGC(F) and decrease in Ve(D) indicating residual lesion.

7 FALSE POSITIVE D AND ADC IVIM PARAMETERS

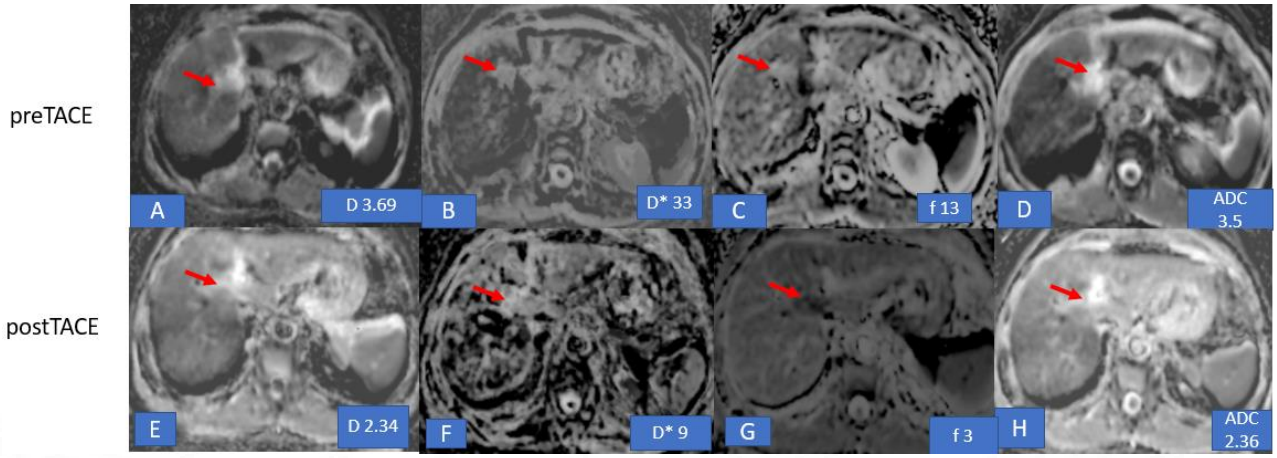

Fig 63. A HCC patient with lesion in segment IVb with complete response. A-D preTACE IVIM parameters, E-H postTACE IVIM parameters In this patient IVIM imaging showing high D(A) and ADC (D) values in preTACE with decreased D(E) and ADC (H)after TACE indicating false positive residual lesion. This was correctly identified as response by decreased D*(B & F) and f (C & G).

8 FALSE NEGATIVE MR PERFUSION VALUES

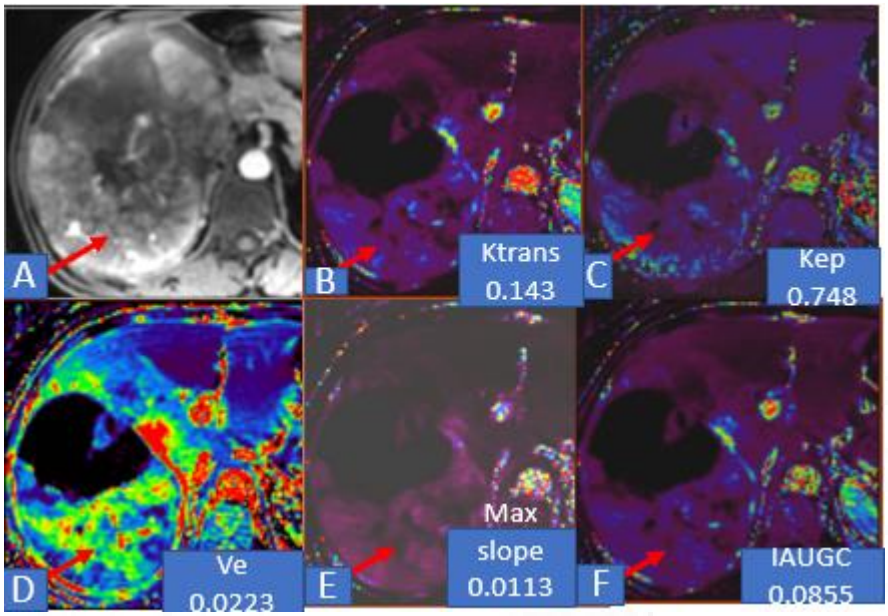

Fig 64. A. postTACE DCE MRI image showing a large HCC lesion with both necrotic and enhancing areas. In enhancing portion, mixed areas with enhancement and without enhancement noted.B-F colour maps of MR perfusion parameters showing decrease after TACE indicating false negative response.

9 Artifacts

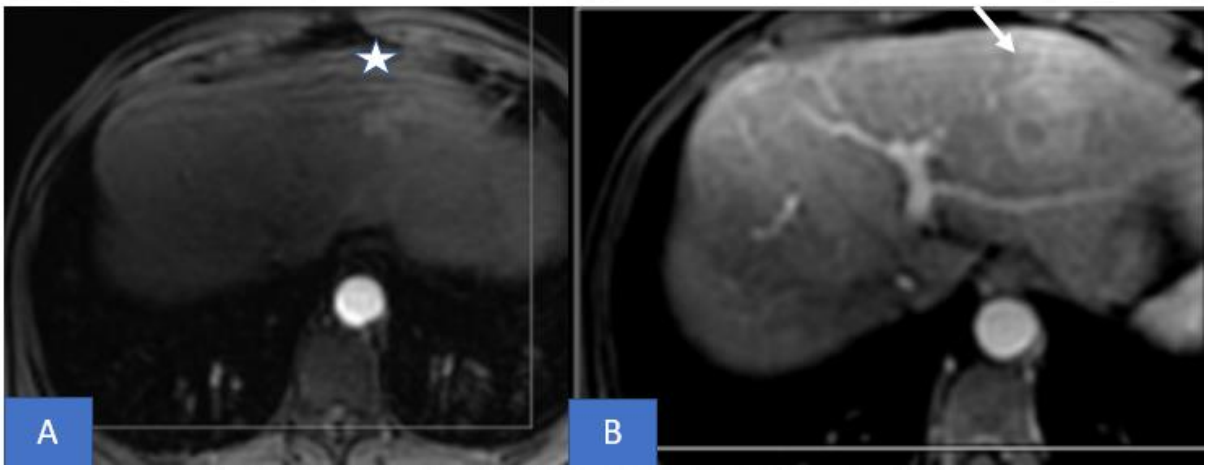

Fig 65`. MR perfusion images showing A. motion artifacts (asterisk) due to cardiac pulsations and B. blurring of the image(white arrow) due to inadequate breath-hold

Discussion

Discussion

In the present study, a comparison was made between preTACE and postTACE values of MR perfusion and IVIM imaging to assess the response of HCC lesions after the procedure. Conventional TACE shows complete response in 60-70 % of cases. Non responder account to around 30% and are due to drug related(lesion not responding to the drug injected), procedure related (failure to identify all feeders), hypoxia induced growth of the tumor(hypoxia induced by TACE in the periphery of the lesion causes increase in VEGF which further may cause the growth of the tumor). There are imaging criteria like WHO, RECIST, mRECIST, EASL in response assessment using size criteria or enhancement of the tumor. The most common followed criteria is mRECIST where the response is assessed by the presence or absence of arterial enhancement visually and by measuring the enhancement (5)(Table 2 and fig 5). In all these criteria only morphological assessment was done. Microvascular and capillary level changes indicated by perfusion and permeability changes occur early and are not routinely assessed in response to TACE and antiangiogenic drugs. These changes can be assessed only by using functional imaging techniques that can assess the physiologic properties of tissue at the microscopic level.

In recent years, the emergence of new imaging technology in MRI has made it possible to observe the response of tumors to treatment before any morphological changes. MR perfusion imaging can not only show the anatomical structure but also provide quantitative information on tumor angiogenesis and perfusion changes. IVIM technique which can separate perfusion and diffusion parameters by using multiple b values will be able to assess microvasculature and cell density/necrosis. In the present study, the feasibility of MR perfusion and IVIM imaging to assess treatment response after TACE was evaluated.

In this study, 32 HCC lesions in 26 patients were assessed. Of these, 23 were male and 3 were female. In literature male to female ratio varies between 2:1 to 4:1 across different populations(70). The male: female ratio for HCC in India is 4:1(71).Here we have a high male to female ratio of about 7:1. The age of presentation varies from 40 to 70 years(71). Here mean age was about 61yrs and was in the range of 48yrs to 76 yrs. In this study, etiology of CLD was associated most commonly with alcohol about 65%, (n=17) Other etiologies include HBV(7.7%, n=2), HCV(11.5%, n=3) and NASH (15.3%, n = 4). In India, HCC is associated with HBV in about 70%–80%, with HCV in about 15%, with both HBV and HCV in 5%, with alcohol in about 8%. The higher incidence of alcohol related CLD is likely due to the high prevalence of alcoholism in this area compared to the rest of the world. There is no significant relationship between etiology and response (p-value 0.29) (table 16). There are 16 BCLC A lesions and 16 BCLC B lesions. BCLC A lesions has significantly high incidence of complete response(n=14)than BCLC B lesions(n=8) (P-value- 0.02) .

.

MR perfusion

Analysis of MR perfusion showed there is significant difference between the values of Ktrans(0.38min^{-1} vs 0.20min^{-1} p-value 0.011), Kep(2.09min^{-1} vs 0.86min^{-1} P-value- 0.007), IAUGC (0.276 vs 0.154P-value-0.006))in post TACE cases in complete responders . However the the difference in the values of max slope(0.024mmol/s vs 0.020mmol/s P-value- 0.48) and Ve(0.23% vs 0.29%, P-value0.2) are not significant after TACE. This is in concurrence with the results of multiple studies by Pokuri et al(58) and Saito et al(59)which also showed a significant reduction in the Ktrans values in complete response cases and not in concurrent with the study by Antonacci et al(55) which showed no significant change in Ka and Kp in complete response cases. Among the perfusion values, Kep showed maximum significant correlation. One equivocal lesion with increasing AFP values after TACE, showed increasing MR perfusion parameters indicating residual lesion(fig 62-63)

In complete responded lesions, mean preTACE and postTACE values of Ktrans were 0.38min^{-1} and 0.20min^{-1}. Ktrans represents permeability and leakiness of the tumor vasculature by determining the efflux of contrast from vascular space to extravascular space (EES). In very high permeability lesions, due to fast leak into EES, Ktrans mainly reflects blood flow (72). In 22 lesions with complete response, 17 lesions showed a decrease, 5 lesions showed an increase in mean values of Ktrans after TACE. The possible explanation for an increase in K trans in 5 completely responded lesions could be leaky capillaries with a nonviable lesion which can occur in some stages of necrosis. Kep showed a statistically significant decrease in Ktrans(0.38min^{-1} vs 0.2min^{-1} p-value 0.011) after TACE in completely responding lesions..In 10 non responders, 5 lesions showing a decrease, and 5 lesions showing an increase in Ktrans value. one of the nonresponder lesion showed a 76% decrease in Ktrans likely due to the large size and presence of necrotic areas along with enhancing areas after TACE(fig 64). ROC curve analysis showed Ktrans having an AUC of 0.7 with greater than 0.038min^{-1} reduction having sensitivity and specificity of 77.27% and 80% respectively for correctly identifying complete response lesions. Pokuri et al(58) and Saito et al(59) also showed similar results with AUC values of 0.8 and 0.82. Antonacci et al(55) however have shown no significant difference between preTACE and postTACE values in Ktrans where he showed only TTP(Time to peak) as a significant indicator of complete response. Since our study used prolonged single input dual compartment (modified Toft's model) (11) which is more appropriate in HCC (because of compartmentalization) rather than dual input single compartment method [which was used by Antonacci et al(55), Pokuri et al(58) and Saito et al(59)] we had a lesser AUC for Ktrans values compared to studies by Pokuri et al and Saito et al. Besides, we assessed only the enhancing region in viable lesions. These may be the reasons for differences in values when compared to the study by Antonacci et al(55).

Kep which determines the reverse efflux rate of contrast from extravascular space to vascular space showed a statistically significant decrease in mean Kep (2.09 vs 0.86, p-value 0.007) after TACE. There was a mild negative correlation (r= -0.248) between preTACE and postTACE values which indicates that higher values were corresponding with greater change after TACE. In complete responded 22 lesions, 17 lesions showed a decrease while 5 lesions showed an increase in mean values of Kep after TACE. The mean percentage changes from baseline values of Kep was 37% in completely responded lesions. ROC curve showed Kep having AUC of 0.745 with greater than 0.156 min^{-1} decrease in mean difference between preTACE and postTACE values have a sensitivity and specificity of 77.27% and 60% respectively for correctly identifying complete response lesions. Although both Ktrans and Kep represent permeability, 5 lesions were showing a mismatch between Ktrans and Kep. Three lesions in which Ktrans was decreased showing an increase in Kep, whereas 2 lesions in which Ktrans was increased showing a decrease in Kep. This may be due to computational errors or capillaries on the venous side that may not be as permeable or leaky as capillaries on the arterial side.

Ve represents the volume fraction of EES showed a percentage change from baseline values of 64% in responders. However, there was no statistically significant increase in mean Ve (0.23 vs 0.29, p-value 0.207) after TACE. There was no correlation (r= 0.009) between preTACE and postTACE values. In ROC curve analysis, Ve has an AUC of 0.582 with greater than 0.0003% increase in mean difference between preTACE and postTACE values has a sensitivity and specificity of 59.09% and 60% respectively for correctly identifying complete response lesions. In a study by Saito et al(59), decreased EES was noted in responders 3 days and 10 days after TACE. In nonresponders, EES was decreased 3 days after TACE, but no significant decrease 10days after TACE. The decrease in Ve may be due to the edematous change of tumor cells which decreases intercellular space and lipiodol accumulation in the sinusoids which decrease contrast extravasation. Besides embolization of arteries causes decreased flow with decreased supply of contrast to the lesion.

IAUGC which indicates the amount of enhancement which usually decreases after TACE due to the embolization of vessels and tumor necrosis. Here 16 lesions showed a decrease, 6 lesions showed an increase in mean values after TACE. Increased may be due to artifacts or computational errors. Lesions which showed a decrease after TACE was also showing a corresponding decrease in Ktrans (except one lesion) and Kep(except two lesions). The mean percentage changes from baseline values of IAUGC was 43%. There was a statistically significant decrease in IAUGC (0.276 vs 0.154, p-value 0.006) after TACE. There was a mild positive correlation (r=0.24) between preTACE and postTACE values which indicates that change is corresponding with preTACE values. In residual/viable lesions(group 2), of 10 residual enhancing lesions, 6 lesions showing a decrease, and 4 lesions showing an increase in its value. The mean percentage changes from baseline values of IAUGC was 5% decrease. There was no statistical

difference(p-value 0.81) between mean preTACE and postTACE values. There was a mild negative correlation(r=-0.238) between preTACE and postTACE values. In ROC curve analysis, IAUGC has an AUC of 0.684 with greater than 0.068 decrease in mean difference between preTACE and postTACE values has a sensitivity and specificity of 72.7% and 70% respectively for correctly identifying complete response lesions. In literature, no studies were found comparing preTACE and postTACE values of IAUGC in HCC patients.

In summary, mean values of Ktrans, Kep, IAUGC were decreased significantly in complete responders as expected but Max slope values were not decreased significantly and there was only a slight nonsignificant increase in mean Ve values. In nonresponders, no significant changes were noted in all the parameters. This is expected in residual or viable lesions as persistent or increased neoangiogenesis and same or increased cellular density occurs. The comparison was made between mean preTACE values in group 1 and group 2 lesions which showed no significant difference between the two groups indicating that preTACE values may not predict the future response after TACE. Kep has the highest AUC with a sensitivity and specificity of 77.27% and 60% respectively. Ktrans has a sensitivity and specificity of 77.27 % and 80% respectively. Ktrans has the highest sensitivity and specificity.

IVIM

In tumors or liver pathology, altered diffusion or perfusion characteristics can be detected by using the IVIM technique. D or Dslow measured at high b value measures the diffusion of free protons giving tissue cellularity (different from ADC calculation in that ADC is calculated from the assumption of monoexponential fit). D*(pseudodiffusion coefficient) measures the velocity of protons in the microcapillaries perfusing the tissue and f (perfusion fraction) measures the tissue blood volume. For IVIM to be used in clinical settings, accuracy, and reproducibility in different settings is needed. Accurate quantification is also challenging because of limited sampling and low signal to noise ratio for fast data acquisition of the liver. There is no standard consensus on the actual values of D fast and f in normal liver and liver tumors. There is also no standard consensus on the protocol and the number of b values to be used(67). So assessment of response to TACE or other treatments without using contrast injection is feasible by the IVIM technique. However, there are only a few articles published evaluating the post TACE response assessment by IVIM imaging.

ADC (apparent diffusion coefficient)

ADC represents an apparent diffusion coefficient which is usually expected to increase after TACE due to tumor necrosis. Of 22 complete responded lesions 18 lesions showed an increase while 4 lesions showed a minimal decrease in ADC after TACE. The mean percentage changes from baseline values of

ADC was 29% after TACE. In 10 residual enhancing lesions, 2 lesions showing minimal decrease and 8 lesions showing a minimal increase ADC. This increase may be due to some necrosis that happened after TACE. Multiple studies hows varying results of ADC changes postTACE. Park YS et al showed no significant change of ADC between the LGU(Lipiodal good uptake) and LPU(Lipiodal poor uptake) groups; similar results were shown by Wagner et al(68),. Kakite et al(66) found significantly higher values of ADC in HCC when compared to the liver. Between ADC and tumor necrosis, there was a significant correlation. Peng et al(69) showed a significant increase in the values of ADC(0.94+/- 0.17 vs 1.23+/-0) after TACE. Post TACE ADC values were significantly higher in responders compared to the residual lesion. Our study also showed a statistically significant increase in mean ADC **(1.37 X$10^{-3}m^2/s$ vs 1.65X$10^{-3}m^2/s$; p-value- 0.016)**after TACE in completely responded lesions whereas there was no statistical difference in non rsponders. PostTACE difference between ADC values between responders and non responders was significant (1.65X$10^{-3}m^2/s$ vs 1.366X$10^{-3}m^2/s$ p-value 0.02). In ROC curve analysis, ADC has an AUC of 0.645 with greater than 0.23 increase in mean difference between preTACE and postTACE values has a sensitivity and specificity of 54.55 % and 90 % respectively for correctly identifying complete response lesions

D (D slow or true diffusion coefficient)

D is usually expected to increase after TACE due to tumor necrosis. Of 22 complete responders, 18 lesions showed an increase, 4 lesions showed a decrease in mean values of D after TACE. The mean percentage changes from baseline values of D were 43%. Park YS et al(73) showed that D was not significantly different between lipoidal Good uptake(LGU) and lipiodol poor uptake(LPU) groups. In a study by Wagner et al(68), IVIM parameters were calculated and compared between viable, necrotic, and fibrotic regions of HCC. D slow showed significant difference between viable and fibrotic tumor tissue regions(1.16x10-3mm2/sec and 1.48x 10-3 mm2/sec)and between viable and necrotic tumor tissue regions(1.7 x10-3mm2/sectumor. Among all diffusion IVIM parameters, D had the highest area under curve for predicting complete tumor necrosis. Peng et al(69) found a significant increase in the values of D(0,72+/- 0.14 vs 0.91 +/- 0,14; p-value- <0.01). Post TACE values of responsive and nonresponsive groups were compared and found that D slow values didn't differ significantly between the groups. Our study results in true diffusion coefficient is also in concurrence with the above mentioned studies with a statistically significant increase in mean D values **(1.208 vs 1.560; p-value- 0.0207)** after TACE positive correlation (r= 0.2865) between preTACE and postTACE values completely responded lesions. ROC curve analysis, D(D slow) has an AUC of 0.714 with greater than 0.04X$10^{-3}mm^2/s$

increase in mean difference between preTACE and postTACE values has a sensitivity and specificity of 77.27% and 60% respectively for correctly identifying complete response lesions. tumor.

Comparison between D and ADC in complete responders

D slow appears to be better than ADC for assessing necrosis as ADC contains combined information of tissue cellularity and perfusion(microcirculation) in the tumor tissue. These have opposite effects in measuring ADC resulting in decreased sensitivity and specificity(5).In our study, mean ADC was higher than mean D in both preTACE and postTACE values. When compared to ADC, D has the highest AUC and also significant cutoff values for sensitivity and specificity of 77.27% and 60%(P-value 0.026). D derived IVIM parameter(D or D slow) appears to be better than ADC for assessing necrosis. This is because ADC contains information that is a combination of both tissue cellularity and perfusion (microcirculation) in the tumor tissue. This will have opposite effects while measuring ADC value resulting in decreased sensitivity and specificity. There was good correlation between D and ADC values(r= 0.834). In completely responded lesions, of the four lesions showing a decrease in ADC after TACE in complete response lesions 3 lesions also showing a corresponding decrease in D values and one lesion showing an increase in D value.

D* (Dfast or pseudodiffusion coefficient)

D* represents perfusion related diffusion of tumor vasculature. Of the 20 lesions which showed complete response, 18 showed a decrease, 2 lesions(fig 60-62) showed an increase in mean values of D* after TACE. The mean percentage changes from baseline values of D* was 28% with statistically significant decrease in mean D* (33.7 vs 23.75; p-value – 0.0005)after TACE and good positive correlation (r= 0.506) between preTACE and postTACE values. These results are similar to Park YS et al(73) who showed D* significantly higher in LGU group than LPU group. Wagner et al(68), divided the lesion into viable, necrotic and fibrotic regions and found that D* did not differ significantly among the three regions. Peng et al(69) found a significant decrease in the values of D*(37.14 +/- 7.96X$10^{-3}m^2/s$ vs 28.94+/- 7.24X$10^{-3}m^2/s$) after TACE..They also compared post TACE values of responsive and nonresponsive groups and found that D* values were significantly lower in responsive than those of non-responsive groups. In our study, D* did not differ significantly between group 1 and group 2 lesions(23.75X$10^{-3}m^2/s$ vs 31.5$10^{-3}m^2/s$), p-value 0.11) in postTACE values. In ROC curve analysis, D* has an AUC of 0.691 with greater than 2.4 X$10^{-3}mm^2/s$ decrease in mean difference between preTACE and postTACE values has a sensitivity and specificity of 81.8 % and 60% respectively for correctly identifying complete response lesions

Comparison between D* and Ktrans & Kep

Since D*, Kep, and Ktrans are parameters of perfusion but using different sequences, we tried to correlate them. There was a weak positive correlation between D* and Ktrans(r= 0.076). Of 18 lesions that showed a decrease in Ktrans after TACE, 17 lesions showed a decrease in D* also . Of 17 completely responded lesions which showed a decrease in Kep value, 16 lesions showed a decrease in D*. No study to date in our search has compared these two values. There was a weak correlation between D* and Kep(r= 0.057). Two lesions with increased Ktrans and Kep were correctly identified by D* and other IVIM parameters (fig 52-55). However, the correlation is weak because the calculation of D* needs assessment of blood flow in microcirculation which depends on the number and density of microcapillaries while K trans in a highly vascular tumor depends on the permeability and inflow.

f (perfusion fraction)

In our study, there was a statistically significant decrease in mean 'f' (19.92% vs 12.9%; p-value – 0.012) after TACE in compete responders with mild correlation (r= 0.365) between preTACE and postTACE values in group 1(r= 0.365) and also in group 2 lesions(r= 0.211). Post TACE values of responsive and nonresponsive groups were compared and found that f values didn't differ significantly between the responsive and nonresponsive groups (12.9% vs 18.6%, p-value 0.2). In ROC curve analysis, f has an AUC of 0.655 with greater than 6% decrease in mean difference between preTACE and postTACE values has a sensitivity and specificity of 59.09% and 70% of 95.4 % for correctly identifying complete response lesions. Combined sensitivity and specificity of D and f is 45.65% and 90% respectively and combine sensitivity and specificity of D and D* is 63.2% and 84%. By this, we can identify the response with more specificity. In a study by Park YS et al(73), 'f' was not significantly different between two lipoidal good uptake(LGU) and poor uptake(LPU) groups. In a study by Wagner et al(68), perfusion fraction(f) was significantly lower in necrotic tissue (14% +/- 6) than in viable tissue(21%+7). In the study by Peng et al(69), no significant change in values of perfusion fraction(f)(15.52 +/- 3.33 vs 15.45 +/- 3.84 ; P-value- 0.928) was observed in postTACE values.

To summarise lesions showing complete response showed a significant decrease in D* (33.7 vs 23.75; p-value – 0.0005) and f (19.92 vs 12.9; p-value – 0.012) values and significant increase in ADC((1.37 vs 1.65; p-value- 0.016) and D(1.208 vs 1.560; p-value- 0.0207) values. Between pre and post TACE values, there was a good correlation in D*(r=0.506), weak to moderate correlation in D(r=0.2865), moderate correlation in f, and ADC values noted. No IVIM parameters showed significant changes in residual lesions. In complete response lesions, as expected due to the increase in cell necrosis by cytotoxic drug injected during TACE procedure, ADC and D values were significantly increased after TACE(fig 45 &47). After TACE, vessels get blocked and partially damaged by embolization. So D* which represents the capillary density decreased after TACE and f which represents the percentage volume

of blood in the tumor tissue also decreased after TACE. As expected no significant changes were observed in the values of IVIM parameters in residual/viable lesions group.

To conclude of perfusion parameters, Kep has the highest AUC. Ktrans and Kep has the highest sensitivity of 77.27%. Ktrans and max slope has the highest specificity of 80%. The 'Ve'and Kep has less specificity of 60%. Among IVIM parameters, D mean difference has the highest AUC. D* has the highest sensitivity. ADC has the highest specificity. Among these, D and Kep are significant with p values <0.05. Combined D and f have a specificity of 90% which is similar to ADC and combined D and D* had a sensitivity of 63.2% which is higher than ADC.

LIMITATIONS

1. Sample size was only 32 which is less for generalization of the obtained values
2. Histopathological confirmation of necrosis was not done. Only the absence of arterial contrast enhancement and delayed washout was taken as the gold standard for assessing the MR perfusion and IVIM parameters.
3. Left lobe lesions were also affected by cardiac pulsations artifacts and stomach gas susceptibility artifacts (fig65 A). Seg VI lesions were also sometimes affected by bowel gas artifacts.
4. Due to the motion artifacts, images analyzed before and after TACE treatment may not be at the same levels, which may be a potential source of error. Breathing motion artifacts (fig 65B) may affect the image quality and also the values of IVIM and MR perfusion parameters. Therefore good breath-hold training before imaging may decrease the respiratory motion artifacts.
5. The relationship between the prognosis and changes of IVIM and MR perfusion parameters after TACE treatment was not investigated in this study.
6. In IVIM, we used only 7 b values. Using more b values especially less than 200 s/mm^2 may give more accurate measurements of D* and f parameters. As IVIM parameter value mainly depends on b value, the selection of b values needs to be further optimized and standardization of the protocol has to be done.
7. In further studies, an increased number of cases should be studied for standardizing the cutoff values.

Summary &Conclusion

Summary

1. We conducted this study to assess the feasibility and efficacy of imaging sequences like MR perfusion, Intravoxel incoherent motion (IVIM) imaging in post trans-arterial Chemoembolization(TACE) response evaluation of HCC and to compare the changes in HCC between preTACE and postTACE values in MR perfusion and Intravoxel incoherent motion (IVIM) imaging
2. BCLC A or BCLC B patients selected for TACE after exclusion criteria underwent preTACE MRI one week before and postTACE MRI after 6weeks of TACE. Total of 26 patients with 32 lesions was selected
3. Depending on the response, lesions were divided into group 1 (complete response without any enhancement) and group 2 (with residual or viable or nonresponding lesions showing partial or total enhancement of the lesion)
4. Baseline preTACE values in complete responding lesions and nonresponding lesions showed no significant difference in all parameters.
5. 65% of HCC has alcoholism as etiology with male patients having 90% of total HCC cases BCLC A lesions responded to TACE better than BCLC B lesions However there was no correlation of response rate with the etiology of HCC.
6. In complete responding lesions, significant difference between mean preTACE and postTACE values of Ktrans(0.38min^{-1} vs 0.20$min^{-1,}$ p-value 0.011), Kep(2.09min^{-1} and 0.86min^{-1},p-value 0.007) and IAUGC(0.276 vs 0.154, p-value 0.006) were noted
7. There was no significant differences between preTACE and postTACE values of Ve (0.23% and 0.29%, p-value- 0.207) and max slope(0.024mmol/s vs 0.020mmol/s, p-value 0.48).
8. In complete responding lesions significant differences between preTACE and postTACE values of D(1.208 X $10^{-3}mm^2/s$ vs 1.560 X $10^{-3}mm^2/s$; p-value- 0.0207 D*(33.7 X $10^{-3}mm^2/s$ vs 23.75 X $10^{-3}mm^2/s$; p-value – 0.0005), f (19.92% vs 12.9%; p-value – 0.012) and ADC(1.37 X $10^{-3}mm^2/s$ vs 1.65 X $10^{-3}mm^2/s$; p-value- 0.016) were noted.
9. There was a weak positive correlation (r= 0.056) in Ktrans, mild negative correlation (r= -0.248)in kep, no correlation (r= 0.009) in Ve, moderate negative correlation (r= -0.364) in max slope, mild positive correlation (r=0.24) in IAUGC between pre and post TACE values of MR perfusion parameters.
10. There was a good correlation in D*(r=0.506), moderate correlation in D(r=0.2865), moderate correlation in f(), and ADC() values between pre and post TACE values of IVIM parameters.

11. In nonresponding lesions, no significant difference between mean preTACE and postTACE values of MR perfusion and IVIM parameters was noted.
12. In complete responding lesions and nonresponding)lesions mean differences between preTACE and postTACE values of MR perfusion parameters were significant in Kep(1.23 min^{-1} vs 0.15, p – value 0.009)
13. In complete responding lesions and nonresponding lesions mean differences between preTACE and postTACE values of IVIM parameters were significant in D(0.352 $X10^{-3}mm^2/s$ (43%) vs 0.006x $10^{-3}mm^2/s$ (0.4%), p- value 0.02) ,ADC (0.285$X10^{-3}mm^2/s$ vs 0.11X $10^{-3}mm^2/s$, p-value 0.17) and nonsignificant in D*(9.95$x10^{-3}mm^2/s$ vs 0.13X $10^{-3}mm^2/s$), f(7.02% vs 0.07%, p-value 0.14),
14. ROC curve analysis of MR perfusion parameters showed Kep having the highest AUC with greater than 0.038 min^{1} decrease between preTACE and postTACE values having a sensitivity and specificity of 77.27% and 60% respectively with significant P value(0.0073).
15. All other MR perfusion parameters have no significant P-value in ROC analysis.
16. Ktrans with >0.23min^{-1} decrease has the highest sensitivity and specificity of 77.27% and 80%(p-value 0.072)..Ktrans and Kep have the highest sensitivity of 77.27%. Ktrans and max slope have the highest specificity of 80%. The 'Ve' and Kep has less specificity of 60%.
17. D(true diffusion) had the highest AUC with greater than 0.04 $X10^{-3}mm^2/s$ increase between preTACE and postTACE values having a sensitivity and specificity of 77.27% and 60% with significant P value 0.026.
18. D* with > 2.4 $X10^{-3}mm^2/s$ decrease has high sensitivity of 81.8% but less specificity(60%) and ADC > 0.23 $X10^{-3}mm^2/s$ increase has high specificity of 90% but very less sensitivity(54.55%) in post TACE reponders
19. Combined D and f have a specificity of 90% which is similar to ADC and combined D and D* sensitivity have a sensitivity of 63.2% which is higher than ADC.

Conclusions

MR perfusion and IVIM imaging are technically feasible to assess the response in HCC lesion after TACE treatment. .Quantification of perfusion parameters helps us to identify the response better than visual assessment. MR perfusion has adjunct value in assessing the response after TACE. It is the change in the values rather than the absolute values that indicate the response better after TACE. MR perfusion values like Ktrans, Kep, and IAUGC can be used as an adjunct to the visual assessment especially useful in equivocal cases. However, they cannot be used as standalone in the assessment of response because of less sensitivity and specificity. IVIM parameters can be used as an adjunct to contrast enhancement and as standalone in cases where contrast injection is contraindicated. However, as the sample size is less results cannot be standardized for a larger population. Standardization of the b values is also necessary which warrants further research.

References

References

1. Yang JD, Hainaut P, Gores GJ, Amadou A, Plymoth A, Roberts LR. A global view of hepatocellular carcinoma: trends, risk, prevention and management. Nat Rev Gastroenterol Hepatol. 2019 Oct;16(10):589–604.

2. Raoul J-L, Forner A, Bolondi L, Cheung TT, Kloeckner R, de Baere T. Updated use of TACE for hepatocellular carcinoma treatment: How and when to use it based on clinical evidence. Cancer Treat Rev. 2019 Jan;72:28–36.

3. Niu Z-J, Ma Y-L, Kang P, Ou S-Q, Meng Z-B, Li Z-K, et al. Transarterial chemoembolization compared with conservative treatment for advanced hepatocellular carcinoma with portal vein tumor thrombus: using a new classification. Med Oncol Northwood Lond Engl. 2012 Dec;29(4):2992–7.

4. Lammer J, Malagari K, Vogl T, Pilleul F, Denys A, Watkinson A, et al. Prospective Randomized Study of Doxorubicin-Eluting-Bead Embolization in the Treatment of Hepatocellular Carcinoma: Results of the PRECISION V Study. Cardiovasc Intervent Radiol. 2010 Feb;33(1):41–52.

5. Hussein RS, Tantawy W, Abbas YA. MRI assessment of hepatocellular carcinoma after locoregional therapy. Insights Imaging [Internet]. 2019 Jan 29 [cited 2020 Jul 12];10. Available from: https://www.ncbi.nlm.nih.gov/pmc/articles/PMC6352610/

6. Hayano K, Lee SH, Sahani DV. Imaging for assessment of treatment response in hepatocellular carcinoma: Current update. Indian J Radiol Imaging. 2015;25(2):121–8.

7. Donato H, França M, Candelária I, Caseiro-Alves F. Liver MRI: From basic protocol to advanced techniques. Eur J Radiol. 2017 Aug;93:30–9.

8. Global Burden of Disease Liver Cancer Collaboration, Akinyemiju T, Abera S, Ahmed M, Alam N, Alemayohu MA, et al. The Burden of Primary Liver Cancer and Underlying Etiologies From 1990 to 2015 at the Global, Regional, and National Level: Results From the Global Burden of Disease Study 2015. JAMA Oncol. 2017 01;3(12):1683–91.

9. 2019 Update of Indian National Association for Study of the Liver Consensus on Prevention, Diagnosis, and Management of Hepatocellular Carcinoma in India: The Puri II Recommendations - Journal of Clinical and Experimental Hepatology [Internet]. [cited 2020 Jul 12]. Available from: https://www.jcehepatology.com/article/S0973-6883(19)30240-3/abstract

10. Marrero JA, Kulik LM, Sirlin CB, Zhu AX, Finn RS, Abecassis MM, et al. Diagnosis, Staging, and Management of Hepatocellular Carcinoma: 2018 Practice Guidance by the American Association for the Study of Liver Diseases. Hepatol Baltim Md. 2018;68(2):723–50.

11. Thng CH, Koh TS, Collins DJ, Koh DM. Perfusion magnetic resonance imaging of the liver. World J Gastroenterol WJG. 2010 Apr 7;16(13):1598–609.

12. Inchingolo R, Faletti R, Grazioli L, Tricarico E, Gatti M, Pecorelli A, et al. MR with Gd-EOB-DTPA in assessment of liver nodules in cirrhotic patients. World J Hepatol. 2018 Jul 27;10(7):462–73.

13. Huang J, Chen W, Yao S. Assessing diagnostic value of contrast-enhanced ultrasound and contrast-enhanced computed tomography in detecting small hepatocellular carcinoma. Medicine (Baltimore) [Internet]. 2017 Jul 28 [cited 2020 Jul 12];96(30). Available from: https://www.ncbi.nlm.nih.gov/pmc/articles/PMC5627828/

14. Bota S, Piscaglia F, Marinelli S, Pecorelli A, Terzi E, Bolondi L. Comparison of international guidelines for noninvasive diagnosis of hepatocellular carcinoma. Liver Cancer. 2012 Nov;1(3–4):190–200.

15. Johnson PJ. The role of serum alpha-fetoprotein estimation in the diagnosis and management of hepatocellular carcinoma. Clin Liver Dis. 2001 Feb;5(1):145–59.

16. Kudo M, Izumi N, Kokudo N, Matsui O, Sakamoto M, Nakashima O, et al. Management of hepatocellular carcinoma in Japan: Consensus-Based Clinical Practice Guidelines proposed by the Japan Society of Hepatology (JSH) 2010 updated version. Dig Dis Basel Switz. 2011;29(3):339–64.

17. Kinoshita A, Onoda H, Fushiya N, Koike K, Nishino H, Tajiri H. Staging systems for hepatocellular carcinoma: Current status and future perspectives. World J Hepatol. 2015 Mar 27;7(3):406–24.

18. Bolondi L, Burroughs A, Dufour J-F, Galle PR, Mazzaferro V, Piscaglia F, et al. Heterogeneity of patients with intermediate (BCLC B) Hepatocellular Carcinoma: proposal for a subclassification to facilitate treatment decisions. Semin Liver Dis. 2012 Nov;32(4):348–59.

19. Zhou Y, Lei X, Wu L, Wu X, Xu D, Li B. Outcomes of hepatectomy for noncirrhotic hepatocellular carcinoma: a systematic review. Surg Oncol. 2014 Dec;23(4):236–42.

20. Majumdar A, Roccarina D, Thorburn D, Davidson BR, Tsochatzis E, Gurusamy KS. Management of people with early- or very early-stage hepatocellular carcinoma: an attempted network meta-analysis. Cochrane Database Syst Rev. 2017 Mar 28;3:CD011650.

21. Jia JB, Zhang D, Ludwig JM, Kim HS. Radiofrequency ablation versus resection for hepatocellular carcinoma in patients with Child-Pugh A liver cirrhosis: a meta-analysis. Clin Radiol. 2017 Dec;72(12):1066–75.

22. Unek T, Karademir S, Arslan NC, Egeli T, Atasoy G, Sagol O, et al. Comparison of Milan and UCSF criteria for liver transplantation to treat hepatocellular carcinoma. World J Gastroenterol WJG. 2011 Oct 7;17(37):4206–12.

23. Yi P-S, Huang M, Zhang M, Xu L, Xu M-Q. Comparison of Transarterial Chemoembolization Combined with Radiofrequency Ablation Therapy versus Surgical Resection for Early Hepatocellular Carcinoma. Am Surg. 2018 Feb 1;84(2):282–8.

24. Yang D-J, Luo K-L, Liu H, Cai B, Tao G-Q, Su X-F, et al. Meta-analysis of transcatheter arterial chemoembolization plus radiofrequency ablation versus transcatheter arterial chemoembolization alone for hepatocellular carcinoma. Oncotarget. 2017 Jan 10;8(2):2960–70.

25. Duan F, Bai Y-H, Cui L, Li X-H, Yan J-Y, Wang M-Q. Simultaneous transarterial chemoembolization and radiofrequency ablation for large hepatocellular carcinoma. World J Gastrointest Oncol. 2020 Jan 15;12(1):92.

26. Liu L, Chen H, Wang M, Zhao Y, Cai G, Qi X, et al. Combination therapy of sorafenib and TACE for unresectable HCC: a systematic review and meta-analysis. PloS One. 2014;9(3):e91124.

27. Feng F, Jiang Q, Jia H, Sun H, Chai Y, Li X, et al. Which is the best combination of TACE and Sorafenib for advanced hepatocellular carcinoma treatment? A systematic review and network meta-analysis. Pharmacol Res. 2018;135:89–101.

28. Vilgrain V, Pereira H, Assenat E, Guiu B, Ilonca AD, Pageaux G-P, et al. Efficacy and safety of selective internal radiotherapy with yttrium-90 resin microspheres compared with sorafenib in locally advanced and inoperable hepatocellular carcinoma (SARAH): an open-label randomised controlled phase 3 trial. Lancet Oncol. 2017;18(12):1624–36.

29. D'Avola D, Iñarrairaegui M, Pardo F, Rotellar F, Marti P, Bilbao JI, et al. Prognosis of hepatocellular carcinoma in relation to treatment across BCLC stages. Ann Surg Oncol. 2011 Jul;18(7):1964–71.

30. Vande Lune P, Abdel Aal AK, Klimkowski S, Zarzour JG, Gunn AJ. Hepatocellular Carcinoma: Diagnosis, Treatment Algorithms, and Imaging Appearance after Transarterial Chemoembolization. J Clin Transl Hepatol. 2018 Jun 28;6(2):175–88.

31. Vincenzi B, Di Maio M, Silletta M, D'Onofrio L, Spoto C, Piccirillo MC, et al. Prognostic Relevance of Objective Response According to EASL Criteria and mRECIST Criteria in Hepatocellular Carcinoma Patients Treated with Loco-Regional Therapies: A Literature-Based Meta-Analysis. PloS One. 2015;10(7):e0133488.

32. Takada J, Hidaka H, Nakazawa T, Kondo M, Numata K, Tanaka K, et al. Modified response evaluation criteria in solid tumors is superior to response evaluation criteria in solid tumors for assessment of responses to sorafenib in patients with advanced hepatocellular carcinoma. BMC Res Notes. 2015 Oct 26;8:609.

33. Sato Y, Watanabe H, Sone M, Onaya H, Sakamoto N, Osuga K, et al. Tumor response evaluation criteria for HCC (hepatocellular carcinoma) treated using TACE (transcatheter arterial chemoembolization): RECIST (response evaluation criteria in solid tumors) version 1.1 and mRECIST (modified RECIST): JIVROSG-0602. Ups J Med Sci. 2013 Mar;118(1):16–22.

34. Hyun D, Shin SW, Cho SK, Park KB, Park HS, Choo SW, et al. Efficacy of RECIST and mRECIST criteria as prognostic factors in patients undergoing repeated iodized oil chemoembolization of intermediate stage hepatocellular carcinoma. Acta Radiol Stockh Swed 1987. 2015 Dec;56(12):1437–45.

35. Choi MH, Park GE, Oh SN, Park MY, Rha SE, Lee YJ, et al. Reproducibility of mRECIST in Measurement and Response Assessment for Hepatocellular Carcinoma Treated by Transarterial Chemoembolization. Acad Radiol. 2018;25(11):1363–73.

36. Mitchell DG, Bruix J, Sherman M, Sirlin CB. LI-RADS (Liver Imaging Reporting and Data System): summary, discussion, and consensus of the LI-RADS Management Working Group and future directions. Hepatol Baltim Md. 2015 Mar;61(3):1056–65.

37. Kloeckner R, Otto G, Biesterfeld S, Oberholzer K, Dueber C, Pitton MB. MDCT versus MRI assessment of tumor response after transarterial chemoembolization for the treatment of hepatocellular carcinoma. Cardiovasc Intervent Radiol. 2010 Jun;33(3):532–40.

38. Hunt SJ, Yu W, Weintraub J, Prince MR, Kothary N. Radiologic monitoring of hepatocellular carcinoma tumor viability after transhepatic arterial chemoembolization: estimating the accuracy of contrast-enhanced cross-sectional imaging with histopathologic correlation. J Vasc Interv Radiol JVIR. 2009 Jan;20(1):30–8.

39. Kim S, Mannelli L, Hajdu CH, Babb JS, Clark TWI, Hecht EM, et al. Hepatocellular carcinoma: assessment of response to transarterial chemoembolization with image subtraction. J Magn Reson Imaging JMRI. 2010 Feb;31(2):348–55.

40. Ronot M, Clift AK, Vilgrain V, Frilling A. Functional imaging in liver tumours. J Hepatol. 2016;65(5):1017–30.

41. Yang K, Zhang X-M, Yang L, Xu H, Peng J. Advanced imaging techniques in the therapeutic response of transarterial chemoembolization for hepatocellular carcinoma. World J Gastroenterol. 2016 May 28;22(20):4835–47.

42. Tofts PS, Wicks DA, Barker GJ. The MRI measurement of NMR and physiological parameters in tissue to study disease process. Prog Clin Biol Res. 1991;363:313–25.

43. Brix G, Semmler W, Port R, Schad LR, Layer G, Lorenz WJ. Pharmacokinetic parameters in CNS Gd-DTPA enhanced MR imaging. J Comput Assist Tomogr. 1991 Aug;15(4):621–8.

44. Larsson HB, Stubgaard M, Frederiksen JL, Jensen M, Henriksen O, Paulson OB. Quantitation of blood-brain barrier defect by magnetic resonance imaging and gadolinium-DTPA in patients with multiple sclerosis and brain tumors. Magn Reson Med. 1990 Oct;16(1):117–31.

45. Chou R, Cuevas C, Fu R, Devine B, Wasson N, Ginsburg A, et al. Imaging Techniques for the Diagnosis of Hepatocellular Carcinoma: A Systematic Review and Meta-analysis. Ann Intern Med. 2015 May 19;162(10):697–711.

46. Ippolito D, Inchingolo R, Grazioli L, Drago SG, Nardella M, Gatti M, et al. Recent advances in non-invasive magnetic resonance imaging assessment of hepatocellular carcinoma. World J Gastroenterol. 2018 Jun 21;24(23):2413–26.

47. Chen G, Ma D-Q, He W, Zhang B-F, Zhao L-Q. Computed tomography perfusion in evaluating the therapeutic effect of transarterial chemoembolization for hepatocellular carcinoma. World J Gastroenterol WJG. 2008 Oct 7;14(37):5738–43.

48. Yang L, Zhang X, Tan B, Liu M, Dong G, Zhai Z. Computed tomographic perfusion imaging for the therapeutic response of chemoembolization for hepatocellular carcinoma. J Comput Assist Tomogr. 2012 Apr;36(2):226–30.

49. Braren R, Altomonte J, Settles M, Neff F, Esposito I, Ebert O, et al. Validation of preclinical multiparametric imaging for prediction of necrosis in hepatocellular carcinoma after embolization. J Hepatol. 2011 Nov;55(5):1034–40.

50. A F, C A, M V, J R, Aj H, Cr de L, et al. Evaluation of tumor response after locoregional therapies in hepatocellular carcinoma: are response evaluation criteria in solid tumors reliable? [Internet]. Vol. 115, Cancer. Cancer; 2009 [cited 2020 Aug 8]. Available from: https://pubmed.ncbi.nlm.nih.gov/19117042/

51. Chopra S, Dodd GD, Chintapalli KN, Leyendecker JR, Karahan OI, Rhim H. Tumor Recurrence After Radiofrequency Thermal Ablation of Hepatic Tumors. Am J Roentgenol. 2001 Aug 1;177(2):381–7.

52. Chen J, Chen C, Xia C, Huang Z, Zuo P, Stemmer A, et al. Quantitative free-breathing dynamic contrast-enhanced MRI in hepatocellular carcinoma using gadoxetic acid: correlations with Ki67 proliferation status, histological grades, and microvascular density. Abdom Radiol N Y. 2018;43(6):1393–403.

53. Wang J, Chen L-T, Tsang Y-M, Liu T-W, Shih TT-F. Dynamic Contrast-Enhanced MRI Analysis of Perfusion Changes in Advanced Hepatocellular Carcinoma Treated with an Antiangiogenic Agent: A Preliminary Study. Am J Roentgenol. 2004 Sep 1;183(3):713–9.

54. Zhu AX, Sahani DV, Duda DG, di Tomaso E, Ancukiewicz M, Catalano OA, et al. Efficacy, safety, and potential biomarkers of sunitinib monotherapy in advanced hepatocellular carcinoma: a phase II study. J Clin Oncol Off J Am Soc Clin Oncol. 2009 Jun 20;27(18):3027–35.

55. Thibodeau-Antonacci A, Petitclerc L, Gilbert G, Bilodeau L, Olivié D, Cerny M, et al. Dynamic contrast-enhanced MRI to assess hepatocellular carcinoma response to Transarterial chemoembolization using LI-RADS criteria: A pilot study. Magn Reson Imaging. 2019;62:78–86.

56. Taouli B, Johnson RS, Hajdu CH, Oei MTH, Merad M, Yee H, et al. Hepatocellular carcinoma: perfusion quantification with dynamic contrast-enhanced MRI. AJR Am J Roentgenol. 2013 Oct;201(4):795–800.

57. Pahwa S, Liu H, Chen Y, Dastmalchian S, O'Connor G, Lu Z, et al. Quantitative perfusion imaging of neoplastic liver lesions: A multi-institution study. Sci Rep. 2018 21;8(1):4990.

58. Pokuri VK, Tomaszewski GM, Ait-Oudhia S, Groman A, Khushalani NI, Lugade AA, et al. Efficacy, Safety, and Potential Biomarkers of Sunitinib and Transarterial Chemoembolization (TACE) Combination in Advanced Hepatocellular Carcinoma (HCC): Phase II Trial. Am J Clin Oncol. 2018;41(4):332–8.

59. Saito K, Ledsam J, Sugimoto K, Sourbron S, Araki Y, Tokuuye K. DCE-MRI for Early Prediction of Response in Hepatocellular Carcinoma after TACE and Sorafenib Therapy: A Pilot Study. J Belg Soc Radiol. 2018 Apr 20;102(1):40.

60. D I, C T, C TF, A C, S L, F V, et al. Dynamic Contrast-Enhanced Magnetic Resonance Imaging With Gadolinium Ethoxybenzyl Diethylenetriamine Pentaacetic Acid for Quantitative Assessment of Vascular Effects on Hepatocellular-Carcinoma Lesions Treated by Transarterial Chemoembolization or Radiofrequency Ablation [Internet]. Vol. 40, Journal of computer assisted tomography. J Comput Assist Tomogr; 2016 [cited 2020 Jul 23]. Available from: https://pubmed.ncbi.nlm.nih.gov/27560010/

61. Chen X, Xiao E, Shu D, Yang C, Liang B, He Z, et al. Evaluating the therapeutic effect of hepatocellular carcinoma treated with transcatheter arterial chemoembolization by magnetic resonance perfusion imaging. Eur J Gastroenterol Hepatol. 2014 Jan;26(1):109–13.

62. Kim KA, Park M-S, Ji H-J, Park JY, Han K-H, Kim M-J, et al. Diffusion and perfusion MRI prediction of progression-free survival in patients with hepatocellular carcinoma treated with concurrent chemoradiotherapy. J Magn Reson Imaging JMRI. 2014 Feb;39(2):286–92.

63. Wang D, Gaba RC, Jin B, Riaz A, Lewandowski RJ, Ryu RK, et al. Intraprocedural transcatheter intra-arterial perfusion MRI as a predictor of tumor response to chemoembolization for hepatocellular carcinoma. Acad Radiol. 2011 Jul;18(7):828–36.

64. Padhani AR, Liu G, Koh DM, Chenevert TL, Thoeny HC, Takahara T, et al. Diffusion-weighted magnetic resonance imaging as a cancer biomarker: consensus and recommendations. Neoplasia N Y N. 2009 Feb;11(2):102–25.

65. Goshima S, Kanematsu M, Kondo H, Yokoyama R, Tsuge Y, Shiratori Y, et al. Evaluating local hepatocellular carcinoma recurrence post-transcatheter arterial chemoembolization: is diffusion-weighted MRI reliable as an indicator? J Magn Reson Imaging JMRI. 2008 Apr;27(4):834–9.

66. Kakite S, Dyvorne HA, Lee KM, Jajamovich GH, Knight-Greenfield A, Taouli B. Hepatocellular carcinoma: IVIM diffusion quantification for prediction of tumor necrosis compared to enhancement ratios. Eur J Radiol Open. 2015 Dec 8;3:1–7.

67. Li YT, Cercueil J-P, Yuan J, Chen W, Loffroy R, Wáng YXJ. Liver intravoxel incoherent motion (IVIM) magnetic resonance imaging: a comprehensive review of published data on normal values and applications for fibrosis and tumor evaluation. Quant Imaging Med Surg. 2017 Feb;7(1):59–78.

68. Wagner M, Doblas S, Daire J-L, Paradis V, Haddad N, Leitão H, et al. Diffusion-weighted MR imaging for the regional characterization of liver tumors. Radiology. 2012 Aug;264(2):464–72.

69. Peng J, Yang C, Zheng J, Wang R, Zhou Y, Wang W, et al. Intravoxel Incoherent Motion Diffusion Weighted Imaging for the Therapeutic Response of Transarterial Chemoembolization for Hepatocellular Carcinoma. J Cancer Ther. 2019 Jan 1;10:591–601.

70. Liu P, Xie S-H, Hu S, Cheng X, Gao T, Zhang C, et al. Age-specific sex difference in the incidence of hepatocellular carcinoma in the United States. Oncotarget. 2017 Jul 12;8(40):68131–7.

71. Acharya SK. Epidemiology of Hepatocellular Carcinoma in India. J Clin Exp Hepatol. 2014 Aug;4(Suppl 3):S27–33.

72. Essig M, Shiroishi MS, Nguyen TB, Saake M, Provenzale JM, Enterline D, et al. Perfusion MRI: The Five Most Frequently Asked Technical Questions. AJR Am J Roentgenol. 2013 Jan;200(1):24–34.

73. Park YS, Lee CH, Kim JH, Kim IS, Kiefer B, Seo TS, et al. Using intravoxel incoherent motion (IVIM) MR imaging to predict lipiodol uptake in patients with hepatocellular carcinoma following transcatheter arterial chemoembolization: A preliminary result. Magn Reson Imaging. 2014 Jul;32(6):638–46.

ANNEXURES

PATIENT INFORMATION SHEET

SREE CHITHRA THIRUNAL INSTITUTE FOR MEDICAL SCIENCES AND TECHNOLOGY – TRIVANDRUM

Study title: "Role of multiparametric Magnetic Resonance Imaging(MRI) in post Transarterial Chemoembolisation (TACE)response evaluation of Hepatocellular Carcinoma(HCC)."

Study number : 32 lesions in 26 patients

This consent form is meant to invite you for the participation in a research study conducting at Sree Chitra Tirunal Institute for Medical Sciences and Technology (SCTIMST) on "Role of multiparametric Magnetic Resonance Imaging (MRI) In post TACE response evaluation of HCC. "

Purpose of the study

MRI is the routine imaging modality used to assess the response after treatment of Hepatocellular carcinoma (HCC) with TACE. The study is to use the MRI (multiple sequences/parameters) in evaluating the response of Hepatocellular carcinoma after performing TACE. These imaging sequences/parameters of the lesion will be assessed before and after `TACE to look for success of procedure and for planning further management. This study does not affect the type of treatment that you may receive.

If you want any more information,we will be glad to discuss further with you.

If you take part, what will you have to do?

Being a participant in the study,you don't have to do anything extra than your routine imaging and follow up.The information that we obtain from this investigation and follow up will help us to better evaluate the lesion characterisation and response of HCC to TACE.

Your consent is taken because your study images are analysed and may be published in some scientific journals. However, if we identify any clinically relevant information, it will be communicated to your treating physician for appropriate decision making. Your participation is entirely voluntary and decision will in no way influence your current treatment at SCTIMST. Absolute confidentiality of data shall be maintained.

No additional cost will be incurred /no additional drugs will be used and there are no additional risks as a part of the research.

Can you withdraw from this study after it starts?

Your participation in this study is entirely voluntary and you are also free to decide to withdraw

permission to participate in this study. If you do so, this will not affect your usual treatment at this hospital in any way.

What will happen if you develop any study related injury?

This study only analyzes the results of your investigation and treatment details and thus we do not expect any injury to happen to you but if you do develop any side effects or problems due to the study, these will be treated at this institute by the experienced team of medical professionals. We are unable to provide any monetary compensation, however.

Will you have to pay for the study?

The study will only analyze the results of the investigations and treatment which you will undergo in natural process of your treatment at this institute and no extra cost will be borne by you for this particular study.

What happens after the study is over?

You may or may not benefit from this study, after the study we will be able to better assess the use of MRI (many sequences) in evaluating the response of Hepatocellular carcinoma after TACE.

it may thus benefit other patients with similar illness.You may be asked to follow up with the hospital only as per routine treatment protocol.

Will your personal details be kept confidential?

The results of this study may be published in a medical journal but you will not be identified by

name in any publication or presentation of results. However, your medical notes may be reviewed by people associated with the study, without your additional permission, should you decide to participate in this study.

If you have any further questions, please ask Dr. Bursupalle Mahesh Reddy (tel: 8328520801) or email: maheshreddy@sctimst.ac.in or contact IEC member secretary (tel: 0471-2524263)

Name of the Researcher : Dr. Bursupalle Mahesh Reddy

Mobile no.- 8328520801

Email id – maheshreddy@sctimst.ac.in

ശ്രീ ചിത്ര തിരുനാൾ ഇൻസ്റ്റിറ്റ്യൂട്ട് ഫോർ സയൻസ് ആന്റ് ടെക്നോളജി, തിരുവനന്തപുരം

ട്രേസ് പ്രതികരണത്തിന്റെ അപഗ്രഥനത്തിൽ വിവിധപരിമാണങ്ങളുള്ള എംആർഐ യുടെപങ്ക് വിലയിരുത്തുന്നതിന് രോഗികൾക്കുള്ള വിവരണപത്രം

പഠനശീർഷകം.

ഹെപ്റ്റാസെല്ലുലാർ കാർസിനോമയിലെ (എച്ച് സിസി) ട്രാസ്ആർട്ടീരിയൽ കീമോമൊബിലൈസേഷൻ (ട്രേസ്) പ്രതികരണത്തിന്റെ അപഗ്രഥനത്തിൽ വിവിധപരിമാണങ്ങളുള്ള എംആർഐ യുടെപങ്ക്

പഠനനമ്പർ

ശ്രീ ചിത്ര തിരുനാൾ ഇൻസ്റ്റിറ്റ്യൂട്ട് ഫോർ സയൻസ് ആന്റ് ടെക്നോളജിയിൽ ഹെപ്റ്റാസെല്ലുലാർ കാർസിനോമയിലെ (എച്ച് സിസി) ട്രാസ്ആർട്ടീരിയൽ കീമോമൊബിലൈസേഷൻ (ട്രേസ്) പ്രതികരണത്തിന്റെ അപഗ്രഥനത്തിൽ വിവിധപരിമാണങ്ങളുള്ള എംആർഐ യുടെ പങ്ക് പരിശോധിക്കുന്ന ഗവേഷണ പഠനത്തിൽ താങ്കളുടെ പങ്കാളിത്തം ക്ഷണിക്കുന്നതിന് ഉദ്ദേശിച്ചുള്ള സമ്മതപത്രമാണിത്.

പഠനത്തിന്റെ ഉദ്ദേശം

ട്രേസിനുശേഷമുള്ല പ്രതികരണം വിലയിരുത്താൻ ഉപയോഗിക്കുന്ന പതിവ് ചിത്രീകരണ രീതിയാണ് എംആർഐ. ട്രേസിന് ശേഷമുള്ള ഹെപ്റ്റാസെല്ലുലാർ കാർസിനോമയുടെ പ്രതികരണം അപഗ്രഥിക്കുന്നതിൽ എംആർഐയുടെ ഉപയോഗയോഗ്യത (അനേകം പരമ്പരകൾ) പരിശോധിക്കാനാണ് ഈ പഠനം നടത്തുന്നത്. ക്ഷതത്തിന്റെ ചിത്രീകരണ പരിമാണങ്ങൾ ട്രേസിന് മുമ്പും ശേഷവും നടപടികളുടെ വിജയംവലയിരുത്തുന്നതിനായും തുടർ ചികിത്സക്കായും പരിശോധിക്കും. താങ്കൾക്ക് ലഭിക്കുന്ന തരം ചികിത്സയെ ഈ പഠനം ബാധിക്കില്ല.

താങ്കൾക്ക് കൂടുതൽ വിവരങ്ങൾ ആവശ്യമെങ്കിൽ കൂടുതൽ ചർച്ചചെയ്യാൻ ഞങ്ങൾക്ക് സന്തോഷമുണ്ട്.

പങ്കെടുക്കുന്നു എങ്കിൽ താങ്കളെന്ത് ചെയ്യണം

പഠനത്തിലെ പങ്കാളിയെന്നനിലയിൽ താങ്കളുടെ പതിവ് ചിത്രീകരമത്തിനും തുടർ പരിശോധനക്കും പുറമേ അധികമായി ഒന്നും ചെയ്യേണ്ടതില്ല. താങ്കളുടെ പരിശേധനകളുടെയും തുടർപരിശോധനകളുടെയും വിവരങ്ങൾ എച്ചസിസിമുതൽ ട്രേസ് വരെയുള്ള ക്ഷതത്തിന്റെ സ്വഭാവങ്ങളും പ്രതികരണങ്ങളും കൂടുതൽ നന്നായി വിലയിരുത്താൻ ഞങ്ങളെ സഹായിക്കും.

താങ്കളുടെ ചിത്രങ്ങൾ അപഗ്രഥിക്കുകയും ചില ശാസ്ത്രപ്രസിദ്ധീകരണങ്ങളിൽ പ്രസിദ്ധീകരിക്കുകയും ചെയ്യുമെന്നതിനാലാണ് തങ്കളുടെ സമ്മതം ആവശ്യപ്പെടുന്നത്. എന്നിരുന്നാലും വൈദ്യശാസ്ത്രപരമായി പ്രസക്തമായ എന്തെങ്കിലും വിവരങ്ങൾ ഞങ്ങൾ കണ്ടെത്തിയാൽ അത് താങ്കളെ ചികിത്സിക്കുന്ന ഡോക്ടറെ വേണ്ടുന്ന തീരുമാനമെടുക്കാനായി അറിയിക്കും. താങ്കളുടെ പങ്കാളിത്തം തികച്ചും സ്വമേധയായാണ്, തീരുമാനം താങ്കളുടെ SCTIMST/യിലെ ഇപ്പോഴത്തെ ചികിത്സയെ ഒരുവിധത്തിലും ബാധിക്കില്ല. വിവരങ്ങളുടെ പരിപൂർണ്ണ രഹസ്യ സ്വഭാവം നിലനിർത്തും. പങ്കെടുക്കുന്നതുകൊണ്ട്. താങ്കൾക്ക് ഒരു അധിക ചിലവുമുണ്ടാകില്ല/ അധികമായി മരുന്നുകൾ ഉപയോഗിക്കുകയോ അധികം അപായംഗവേഷണത്തിന്റെ ഭാഗമായി ഉണ്ടാവുകയോ ഇല്ല.

പഠനം ആരംഭിച്ചശേഷം താങ്കൾക്ക് പിൻമാറാമോ

പഠനത്തിന്റെ ഏത് ഘട്ടത്തിലും താങ്കൾക്ക് സമ്മതം പിൻവലിക്കാം, അത് താങ്കളുടെ ഈ ആശുപത്രിയിലെ സാധാരണ ചികിത്സയെ ഒരു വിധത്തിലും ബാധിക്കില്ല.

ബന്ധപ്പെട്ട് താങ്കൾക്ക് എന്തെങ്കിലും പരുക്കുണ്ടായാലെന്ത് സംഭവിക്കും ?

പഠനത്തിൽ താങ്കളുടെ പരിശോധനകളുടെയും ചികിത്സയുടെയും വിശദാംശങ്ങൾ അപഗ്രഥിക്കുക മാത്രം ചെയ്യുന്നതിനാൽ ഞങ്ങളുടെ പഠനം കൊണ്ട് താങ്കൾക്ക് പരുക്കുണ്ടാകുമെന്ന് ഞങ്ങൾ പ്രതീക്ഷിക്കുന്നില്ല.പക്ഷേ താങ്കൾക്ക് എന്തെങ്കിലും പാർശ്വഫലങ്ങളോ പ്രശ്നങ്ങളോ പഠനസംബന്ധമായി ഉണ്ടായാൽ അവ വിദഗ്ധരായ ഡോക്ടർമാരുടെ സംഘം ഈ ആശുപത്രിയിൽ ചികിത്സിക്കും. ഈ പ്രത്യേക പഠനത്തിനായി താങ്കൾക്ക് അധികച്ചിലവുണ്ടാകില്ല.

പഠനത്തിനായി താങ്കൾ പണം ചിലവാക്കണോ?

പഠനത്തിൽ ഈ ആശുപത്രിയിലുള്ള താങ്കളുടെ സ്വഭാവികമായ പരിശോധനകളുടെയും ചികിത്സയുടെയും വിശദാംശങ്ങൾ അപഗ്രഥിക്കുകമാത്രം ചെയ്യുന്നതിനാൽ ഈ പ്രത്യേക പഠനത്തിനായി താങ്കൾക്ക് അധികച്ചിലവുണ്ടാകില്ല.

പഠനം കഴിഞ്ഞ ശേഷം എന്ത് സംഭവിക്കും.

പഠനഫലങ്ങൾ ഒരു വൈദ്യശാസ്ത്ര ജർണ്ണലിൽ പ്രസിദ്ധീകരിച്ചേക്കാം. റ്റോസിന് ശേഷമുള്ള ഹെപ്റ്റോസെല്ലുലാർ കാർസിനോമയുടെ പ്രതികരണം എംആർഐ ഉപയോഗിച്ച് അപഗ്രഥിക്കുന്നത് ഞങ്ങൾക്ക് മെച്ചപ്പടുത്താനായേക്കും. സമാനമായ രോഗമുള്ല മറ്റാളുകൾക്ക് അത് നേട്ടമുണ്ടാക്കിയേക്കും. ആശുപത്രിയുടെ ചികിത്സാ നടപടിക്രമമനുസരിച്ചു മാത്രമേ താങ്കളുടെ തുടർചികിത്സനടത്താനാവശ്യപ്പെടുകയുള്ളു.

താങ്കളുടെ വ്യക്തി വിവരങ്ങൾ രഹസ്യമായിരിക്കുമോ?

താങ്കളുടെ വ്യക്തിവിവരങ്ങൾ രഹസ്യമായി സൂക്ഷിക്കും. പഠനഫലങ്ങൾ ഒരു വൈദ്യശാസ്ത്ര ജേർണലിൽ പ്രസിദ്ധീകരിക്കുമെങ്കിലും താങ്കളെ വ്യക്തിപരമായി തിരിച്ചറിയാനിടയാക്കുന്നതൊന്നും പ്രസിദ്ധീകരണത്തിലോ, പഠനഫലങ്ങളുടെ പ്രദർശനത്തിലോ ഉണ്ടാവില്ല. എന്നിരുന്നാലുംതാങ്കൾ ഈ പഠനത്തിൽ പങ്കെടുക്കുകയാണെങ്കിൽ താങ്കളുടെ ചികിത്സാവിവരങ്ങൾ താങ്കളുടെ പ്രത്യേക സമ്മതമില്ലാതെ പഠനവുമായി ബന്ധപ്പെട്ടയാളുകൾ പരിശോധിച്ചേക്കാം.

താങ്കൽക്ക് കൂടുതൽ ചോദ്യങ്ങളുണ്ടെങ്കിൽ ദയവായി ചോദിക്കുക. ഡോ. ബർസുപള്ളി മഹേഷ് റെഡ്ഡി, (ഫോൺ നമ്പർ. 8328520801) email. maheshreddy@sctimst.ac.in,

ഡോ. മാല രാമനാഥൻ മെമ്പർ സെക്രട്ടറി ഐഇസി (ഫോൺ നമ്പർ 0471-2524234)

INFORMED CONSENT FORM

TITLE OF THE STUDY: Role of multiparametric MRI in post *Transarterial chemoembolisation (TACE)response evaluation of Hepatocellular Carcinoma(HCC)*

Study number:__

Participant's name: Date of Birth / Age (in years):
I_____ _____,
son/daughter of _____ (Please tick boxes).

[ ] Declare that I have read the above information provide to me regarding the study: ***Role of multiparametric Magnetic resonance Imaging (MRI) in post Transarterial chemoembolisation (TACE)response evaluation of Hepatocellular Carcinoma(HCC)*** and have clarified any doubts that I had.

[ ] I also understand that my participation in this study is entirely voluntary and that I am free to withdraw permission to continue to participate at any time without affecting my usual treatment or my legal rights.

[ ] I also understand that as multiparametric MRI is routinely done for HCC , I need not have to pay extra for its use.

[ ] I understand that the study staff and institutional ethics committee members may be not need my permission to look at my health records even if I withdraw from the trial. I agree to this access

[ ] I understand that my identity may be not be revealed in any informatio

Name:	Name of witness:
Signature:	Relation to participant:
Date:	Date:

I attest that the requirements for informed consent for the medical research project described in this form have been satisfied. I have discussed the research project with the participant and explained to him or her in nontechnical terms all of the information contained in this informed consent form, including any risks and adverse reactions that may reasonably be expected to occur. I further certify that I encouraged the participant to ask questions and that all questions asked were answered.

_____ _____
Name and Signature of Person Obtaining Consent

കാര്യബോധത്തോടെയുള്ള സമ്മതപത്രം

പഠനശീർഷകം

ഹെപ്റ്റാസെല്ലുലാർ കാർസിനോമയിലെ (എച്ച് സിസി) ട്രാൻസ്ആർട്ടീരിയൽ കീമോമൊബിലൈസേഷൻ (റ്റേസ്) പ്രതികരണത്തിന്റെ അപഗ്രഥനത്തിൽ വ്യത്യസ്ത അളവുകളിലുള്ള എംആർഐ യുടെ പങ്ക്

പങ്കെടുക്കുന്നയാളുടെ പേര്.....മകൻ/മകൾ..... (ദയവായി (ബോക്സുകളിൽ ശരി അടയാളമിടുക)

- ഹെപ്റ്റാസെല്ലുലാർ കാർസിനോമയിലെ (എച്ച് സിസി) ട്രാൻസ്ആർട്ടീരിയൽ കീമോമൊബിലൈസേഷൻ (റ്റേസ്) പ്രതികരണത്തിന്റെ അപഗ്രഥനത്തിൽ വ്യത്യസ്ത അളവുകളിലുള്ള എംആർഐ യുടെ പങ്ക് എന്ന പഠനസംബന്ധമായി എനിക്കു നൽകിയ വിവരങ്ങൾ വായിച്ചു എന്നും എനിക്കുണ്ടായ സംശയങ്ങൽ ദുരീകരിച്ചു എന്നും ഞാൻ പ്രസ്താവിക്കുന്നു. [ ]

- എന്റെ ഈ പഠനത്തിലുള്ള പങ്കാളിത്തം സ്വമേധയായുള്ളതാണെന്നും, എനിക്ക് ഒരു കാരണവും കൂടാതെ ഏതുസമയത്തും, എനിക്കുള്ള വൈദ്യശുശ്രൂഷയെയോ നിയമപരമായ അവകാശങ്ങളെയോ ബാധിക്കാതെ പിൻവാങ്ങാമെന്നും ഞാൻ മനസ്സിലാക്കുന്നു. [ ]
- എച്ച് സിസിക്കവേണ്ടി വിവിധ പരിമാണങ്ങളിലുള്ള എംആർഐ പതിവാണെന്നും അതിന്റെ ഉപയോഗത്തിന് ഞാൻ അധികം പണം നൽകേണ്ടതില്ലെന്നും മനസ്സിലാക്കുന്നു [ ]
- പഠനം നടത്തുന്നവരും സാഥാപനത്തിലെ എത്തിക്സ് കമ്മിറ്റി അംഗങ്ങളും ഞാൻ പഠനത്തിൽനിന്നും പിൻമാറിയാലും എന്റ ചികിത്സാരേഖകൾ എന്റെ പ്രത്യേകസമ്മതമില്ലാതെ പരിശോധിച്ചേക്കാമെന്നും ഞാൻ മനസ്സിലാക്കുന്നു.
- എന്റെ വ്യക്തിവിവരങ്ങൾ വെളിപ്പെടുത്തുകയില്ലെന്നും ഞാൻ മനസ്സിലാക്കുന്നു. [ ]

- സ്വമേധയാ പഠനത്തിൽ പങ്കെടുക്കാൻ ഞാൻ സമ്മതിക്കുന്നു. [ ]
- സമ്മതപത്രത്തിന്റെ ഒപ്പിട്ട ഒരു പ്രതി എനിക്ക് കിട്ടി. [ ]

പേര് സാക്ഷിയുടെ പേര്

ഒപ്പ്/ രോഗിയുടെ വിരലടയാളം/ ഒപ്പ്

തീയതി തീയതി

രോഗിയുമായുള്ള ബന്ധം

(സമ്മതം വാങ്ങുന്നയാൾ)

മെഡിക്കൽ റിസർച്ച് പ്രോജക്ടിനാവശ്യമായ സമ്മതപത്രത്തിനു വേണ്ടുന്ന എല്ലാ ഘടകങ്ങളും തൃപ്തികരമായി നിർവഹിച്ചിരിക്കുന്നുവെന്ന് ഞാൻ ബോധ്യപ്പെടുത്തുന്നു. പഠനപങ്കാളിയുമായി ഗവേഷണപദ്ധതിയെപ്പറ്റി സാങ്കേതികേതര പദങ്ങളുപയോഗിച്ച് എല്ലാ വിവരങ്ങളെപ്പറ്റിയും ചർച്ച നടത്തുകയും പ്രതീക്ഷിക്കാവുന്ന അപകടസാധ്യതകളും പാർശ്വഫലങ്ങളും വിശദീകരിക്കുകയും ചെയ്തു. പങ്കാളിയെ ചോദ്യങ്ങൾ ചോദിക്കാൻ പ്രേരിപ്പിക്കുകയും എല്ലാ ചോദ്യങ്ങൾക്കും ഉത്തരം നൽകുകയും ചെയ്തു എന്നും ഞാൻ സാക്ഷ്യപ്പെടുത്തുന്നു.

സമ്മതപത്രം വാങ്ങുന്ന ആളുടെ പേരും ഒപ്പും

ഡോ. ബുസുപള്ളി മഹേഷ് റെഡ്ഡി, സീനിയർ റെസിഡന്റ്, (ഡിഎം. കാർഡിയോ വാസ്ക്കുലാർ ഇമേജിംഗ് ആന്റ് ഇന്റർവെൻഷണൽ റേഡിയോളജി) ഐഎസ് ഐആർ ഡിപ്പാർട്ട്മെന്റ്, ശ്രീ ചിത്ര തിരുനാൾ ഇൻസ്റ്റിറ്റ്യൂട്ട് ഫോർ മെഡിക്കൽ സയൻസസ് ആന്റ് ടെക്നോളജി, തിരുവനന്തപുരം

പഠനവുമായി ബന്ധമില്ലാത്ത വ്യക്തിയെ ബന്ധപ്പെടുന്നതിന് ദയവായി സ്ഥാപനത്തിലെ നൈതീക കമ്മിറ്റി മെംബർ സെക്രട്ടറി ഡോ. മാല രാമനാഥനെ ബന്ധപ്പെടാം. ഫോൺ 04712524234, email: iec.mem.sec@sctimst.ac.in

PROFORMA

Title: Role of multiparametric MRI In post Transarterial Chemoembolisation response evaluation of Hepatocellular Carcinoma(HCC).

Anonymized patient key :

CLINICAL:
Age:
Sex:
Etiology:
Date of MRI (pre TACE) :
Date of TACE procedure:
Date of MRI (POST TACE):

Status :
Child Pugh score
BCLC_ stage

Group 1 or 2

MRI (Pre TACE)

T1 W (Inphase and out phase)-Hyper/Hypo/Iso

T2FS -Hyper/Hypo/Iso

Perfusion –contrast enhancing region- size

Ktrans

Kep

Ve

Max slope

IAUGC

IVIM :

D*:

D :

f :

ADC :

MRI (post TACE)

T1 W (Inphase and out phase)-Hyper/Hypo/Iso

T2FS -Hyper/Hypo/Iso

Perfusion –contrast enhancing region- size

Ktrans

Kep

Ve

Max slope

IAUGC

Diffusion: ADC:

D*:

D :

f :

ADC :

MASTER CHART

SL No.	seg inv	CP	BCLC	Gr	age (yrs)	sex	les size(c	etiology	DX10-3m	D*x 10-3n	f %pre	ADCX10-3	Ktransmi	Kepmin-1	Ve %pre	Max slop	IAUGC pre	D x10-3m	D*x10-3m	f%post	ADC x10-3	Ktransmi	Kep min-1	Ve% post	Max slop	IAUGC post
1 II	A	A		1	70 m		2.6	alcoholic	1.197	34	5	1.1	0.452	1.159	0.397	0.0204	0.236	1.34	28	22.9	1.25	0.303	0.845	0.39	0.0286	0.331
2 VI	B	B		1	63 m		5.5	alcoholic	0.63	14	27	1.54	0.321	1.148	0.302	0.059	0.32	2.01	12	9	2.1	0.123	1.301	0.102	0.0084	0.104
3 VI	A	B		1	65 m		5.6	alcoholic	1.15	46	29	1.62	0.21	1.095	0.216	0.0132	0.197	3.1	8.2	27	2.9	0.302	0.939	0.343	0.0129	0.0384
4 II	A	A		1	55 m		3.3	HCV	1.1	39	23	1.3	0.22	1.122	0.213	0.0174	0.249	1.94	24	15	1.73	0.0557	0.567	0.0989	0.0591	0.0621
5 III	A	A		1	56 m		3.4	alcoholic	1.15	29	10	1.44	0.191	1.367	0.142	0.0095	0.144	1.9	26	10	1.84	0.0871	0.752	0.116	0.0647	0.0537
6 IVa	B	A		2	56 m		3	alcoholic	1.03	29	8	1.01	0.284	0.839	0.351	0.0123	0.26	1.07	39	21	1.24	0.448	2.634	0.222	0.0175	0.269
7 VI	B	A		1	54 f		3.8	NASH	1.05	32	13	1.44	0.582	3.132	0.207	0.0413	0.414	1.37	20.2	3.5	1.46	0.112	0.781	0.228	0.0106	0.0534
8 VIII	B	B		1	54 m		2.1	HCV	0.8	31	30	1.02	0.714	4.218	0.203	0.0409	0.478	1.3	28	17	1.5	0.109	0.522	0.232	0.00611	0.0959
9 IVa	B	B		1	54 m		1.8	HCV	1.21	27	20	1.28	0.153	0.928	0.186	0.00707	0.149	1.32	23	19	1.52	0.114	0.99	0.99	0.00562	0.0793
10 III	A	A		1	66 m		3.5	NASH	1.1	57	39	1.58	0.336	1.042	0.368	0.0171	0.204	1.25	44	28	1.53	0.298	1.156	0.392	0.0679	0.232
11 VI	B	B		2	53 m		7.9	alcoholic	1.14	22	14	1.15	0.386	1.227	0.334	0.0297	0.416	1.6	20	8.3	1.63	0.365	1.174	0.389	0.0327	0.333
12 VI	B	A		1	74 m		3.6	alcoholic	1.3	44	33	0.98	0.326	1.245	0.091	0.0357	0.326	1.48	24	27	1.87	0.092	0.92	0.114	0.008	0.24
13 cau	A	A		1	63 m		3.3	alcoholic	3.69	33	13	3.5	0.482	1.46	0.352	0.0279	0.285	2.34	9	3	2.36	0.893	0.595	0.184	0.00766	0.0496
14 VI	A	A		1	56 f		2.5	HCV	0.8	16	6.3	0.65	0.394	1.246	0.344	0.0282	0.351	1.06	10.6	3.5	1.07	0.593	1.807	0.405	0.0385	0.365
15 VII	A	B		1	59 m		3.5	Hbsag	1.06	30	13	1.21	0.163	0.641	0.263	0.00765	0.135	1.77	27.6	5.6	1.86	0.203	1.24	0.27	0.0358	0.159
16 VII	A	B		2	76 m		6.1	alcoholic	1.68	14.4	8.96	1.89	1.052	2.513	0.507	0.0775	0.644	1.5	34	20	1.68	0.578	2.082	0.399	0.383	0.264
17 VI	B	B		2	66 m		3	alcoholic	1.3	37	23.1	1.47	0.363	2.154	0.18	0.0169	0.288	1.55	29.7	14.6	1.68	0.341	2.386	0.169	0.0229	0.383
18 VII	B	B		1	66 m		3	alcoholic	1.58	23	14	1.34	0.196	2.277	0.0948	0.00915	0.14	1.38	18.7	20.4	1.4	0.117	0.773	0.565	0.013	0.0686
19 IVa	B	B		2	66 m		3	alcoholic	1.33	52	29.5	0.94	0.223	2.972	0.0729	0.0137	0.178	1.07	18	12	1.1	0.273	2.961	0.102	0.0176	0.266
20 VI	A	A		1	60 m		3.2	alcoholic	1.12	33.7	19.45	1.1	0.449	2.35	0.23	0.0491	0.297	1.71	14.8	1	1.6	0.0482	0.262	0.4	0.00832	0.0447
21 VI	A	A		1	70 m		1.8	NASH	1.01	32	12.9	1.2	1.198	8.7	0.184	0.0313	0.174	1.26	15.9	8.1	1.3	0.105	0.521	0.236	0.0115	0.106
22 VI	A	A		1	53 m		2.7	alcoholic	1.21	54	30	1.7	0.421	2.323	0.207	0.0316	0.419	1.15	52	38	1.66	0.079	0.917	0.111	0.00657	0.791
23 VI/VII	B	B		2	65 m		12	alcoholic	1	46	19	1.1	0.535	1.114	0.508	0.034	0.462	1.26	36.9	14.1	1.16	0.143	0.748	0.223	0.0113	0.0855
24 VI	A	B		1	60 m		5	alcoholic	1.01	22.6	19.1	1.16	0.467	0.962	0.493	0.0333	0.542	1.97	10.8	5	2.07	0.0261	0.24	0.423	0.00524	0.0125
25 VI	A	A		1	48 f		2.5	Hbsag	0.93	32.3	15.5	1.03	0.415	2.951	0.163	0.0186	0.328	0.95	44.6	3.3	1.1	0.551	2.024	0.313	0.0285	0.386
26 VI	A	A		1	48 f		2.4	Hbsag	1.49	34	9.1	1.64	0.269	1.445	0.163	0.0145	0.328	0.92	42.3	13.8	1.12	0.0826	0.669	0.138	0.00716	0.0379
27 VIII	B	B		2	61 m		2.3	NASH	1.21	38	22	1.33	0.393	3.89	0.107	0.019	0.26	0.92	42	38.6	1.34	0.387	4.29	0.104	0.0204	0.229
28 VIII	B	B		1	61 m		3.28	NASH	1.14	34	12	0.98	0.237	4.069	0.051	0.016	0.158	1.38	24	2.8	1.82	0.03	0.32	0.289	0.00856	0.0321
29 VII	B	B		2	61 m		4.24	NASH	1.49	32	24	1.25	0.265	3.156	0.08	0.0141	0.166	1.25	40	34.8	1.42	0.37	2.55	0.172	0.02	0.253
30 IVa	B	B		2	61 m		2.9	NASH	1.39	19	22	1.45	0.422	2.987	0.15	0.0218	0.284	1.1	46	21.6	1.28	0.483	2.024	0.25	0.0211	0.347
31 III	A	A		1	62 m		1.5	alcoholic	0.85	44	45	1.34	0.248	1.146	0.222	0.0132	0.21	1.43	15	1	1.37	0.0767	0.77	0.102	0.00264	0.0646
32 VI	A	A		2	62 m		2.3	alcoholic	0.84	26.9	14.7	0.99	0.427	1.491	0.297	0.0241	0.265	1.15	9.4	1	1.13	0.753	3.067	0.287	0.062	0.624

KEYS TO MASTER CHART

SL No.- serial number

Seg inv- segments involved

CP- Child-pugh score

BCLC - BCLC staging

Gr- Group

Age(yrs)- age in years

M-male

F-female

Les size(cm)- lesion size in centimetres

D X$10^{-3}m^2/s$ -pre- True diffusion coefficient in preTACE MRI

D* X$10^{-3}m^2/s$ -pre-pseudodiffusion coefficient in preTACE MRI

f %- pre- perfusion fraction in preTACE MRI

ADC $10^{-3}m^2/s$ pre- Apparent diffusion coefficient in preTACE MRI

Ktransmin-1 pre –Ktrans in preTACE MRI

Kepmin-1 pre- kep in preTACE MRI

Ve %pre- Ve in preTACE MRI

Max slope mmol/s pre- max slope in preTACE MRI

IAUGC pre- IAUGC in in preTACE MRI

D x10-3m2/s post- True diffusion coefficient in postTACE MRI

D*x10-3m2/s post- pseudodiffusion coefficient in postTACE MRI

f% post- perfusion fraction in postTACE MRI

ADC x10-3m2/s post- Apparent diffusion coefficient in postTACE MRI

Ktransmin-1post - Ktrans in postTACE MRI

Kep min-1post – Kep in postTACE MRI

Ve% post- Ve in postTACE MRI

Max slope mmol/s post – max slope in postTACE MRI

IAUGC post – IAUGC in postTACE MRI

ABBREVIATIONS

ADC- apparent diffusion coefficient

AF- Arterial Fraction

AHBF)-Arterial hepatic blood flow

BCLC- Barcelona clinic liver cancer

CLD- Chronic liver disease

D- D slow or true diffusion coefficient

D*- pseudodiffusion coefficient

DCE-Dynamic contrast enhancement

DV-distribution volume

EASL- European Association for the Study of the Liver

EES- Extravascular extracellular space

f- perfusion fraction

HCC-Hepatocellular carcinoma

IAUC -initial area under curve

k2=transfer constant from the tissue to the central vein,

ka=transfer constant from the arterial plasma to the surrounding tissue,

kp=transfer constant from the portal venous plasma to the surrounding tissue,

IAUGC- Initial area under Gadolinium concentration curve

LGU- Lipiodal good uptake

LPU- Lipiodal poor uptake

LR- liver resection

LT-liver transplantation

MTT- mean transit time

mRECIST- modified Response Evaluation Criteria in Solid Tumors

OATP - organic anionic transporting polypeptide

PHBF- portal venous hepatic blood flow

RECIST- Response Evaluation Criteria in Solid Tumors

ROI-region of interest

Signal to noise ratio(SNR)

Signal intensity(SI)

श्री चित्रा तिरुनाल आयुर्विज्ञान और प्रौद्योगिकी संस्थान, त्रिवेन्द्रम
तिरुवनन्तपुरम - ६९५०११, केरल, इंडिया
SREE CHITRA TIRUNAL INSTITUTE FOR MEDICAL SCIENCES AND TECHNOLOGY, TRIVANDRUM
Thiruvananthapuram - 695 011, Kerala, India
(An Institute of National Importance under Govt. of India)
Grams : Chitramet, Phone : +91-471-2443152, Fax : +91-471-2550728 / 2446433, E-mail : sct@sctimst.ac.in, Website : www.sctimst.ac.in

Institutional Ethics Committee
(IEC Regn No. ECR/189/Inst/KL/2013/RR-16)

07.09.2018

SCT/IEC/1243/AUGUST-2018

Dr. Bursupalle Mahesh Reddy
Senior Resident
Department of IS & IR
SCTIMST, Thiruvananthapuram

Dear Dr. Bursupalle Mahesh Reddy,

The Institutional Ethics Committee reviewed and discussed your application to conduct the study entitled "ROLE OF MULTIPARAMETRIC MRI IN POST TRANSARTERIAL CHEMOEMBOLISATION RESPONSE EVALUATION OF HEPATOCELLULAR CARCINOMA (HCC) (IEC/1243)" on 17th August, 2018.

The following documents were reviewed:

Original submission

1. *Covering letter addressed to the IEC, SCTIMST dated 19.07.2018 with checklist*
2. *TAC Approval Letter*
3. *IEC Application Form*
4. *Project Proposal*
5. *Patient Information Sheet and Consent Form in English and Malayalam*
6. *CV of Principal Investigator and Co- Principal Investigators*

Revised submission

1. *Covering letter addressed to the IEC, SCTIMST dated 30.08.2018 with checklist*
2. *TAC Approval Letter*
3. *IEC Application Form*
4. *Project Proposal*
5. *Data Collection Chart*
6. *Patient Information Sheet and Informed Consent Form in English and Malayalam*
7. *CV of Principal Investigator and Co- Principal Investigators*

The following members of the Ethics Committee were present at the meeting held on 17th August, 2018 at G. Parthasarathi Board Room, AMCHSS, SCTIMST

SL. No.	Member Name	Highest Degree	Gender	Scientific /Non Scientific	Affiliation with Institution(s)
1.	Dr. R V G Menon	M Tech, PhD	Male	Lay Person (Chairman)	No
2.	Dr. V. Raman Kutty	M D, M Phil, M P H	Male	Health Sciences Expert/Clinician	Yes
3.	Dr. K R S Krishnan	M.E., Ph.D.	Male	Medical Technology	Yes
4.	Dr. Rema M. N	MD	Female	Basic Medical Scientist	No
5.	Dr. Mala Ramanathan	PhD	Female	Social Scientist (Member Secretary)	Yes

IEC Decision

The IEC approved the conduct of the study in the present form.

Remarks:
The Institutional Ethics Committee expects to be informed about the progress of the study, any SAE occurring in the course of the study, any changes in the protocol and patient information/informed consent and asks to be provided a copy of the final report.

There was no member of the study team who participated in voting / decision making process. The ethics committee is organized and operated according to the requirements of Good Clinical Practice and the requirements of the Indian Council of Medical Research (ICMR).

Sincerely,

Mala Ramanathan
Member Secretary, IEC

urkund

Document Information

Analyzed document	for plagirism check .docx (D78245476)
Submitted	8/27/2020 6:07:00 PM
Submitted by	Jineesh
Submitter email	jineesh174@sctimst.ac.in
Similarity	4%
Analysis address	jineesh174.sctims@analysis.urkund.com

Sources included in the report

SA	**Ssc_ HCC report 02112017.docx** Document Ssc_ HCC report 02112017.docx (D31977954)	2
W	URL: https://www.spandidos-publications.com/10.3892/or.2017.5420 Fetched: 8/27/2020 6:08:00 PM	9
W	URL: https://www.karger.com/Article/Fulltext/485471 Fetched: 8/27/2020 6:08:00 PM	4
W	URL: https://www.researchgate.net/publication/285929086_An_Introduction_to_MR_Perfusion ... Fetched: 8/27/2020 6:08:00 PM	3
W	URL: https://www.ncbi.nlm.nih.gov/pmc/articles/PMC4811854/ Fetched: 2/24/2020 5:57:09 PM	5
W	URL: https://www.researchgate.net/publication/23301589_Computed_tomography_perfusion_in ... Fetched: 11/3/2019 10:38:12 AM	2
J	**Post Locoregional Therapy Treatment Imaging in Hepatocellular Carcinoma Patients: A Literature-based Review** URL: 2bdee978-8e76-406e-acdb-6072295b97c3 Fetched: 3/27/2019 10:03:34 AM	4
W	URL: https://www.ncbi.nlm.nih.gov/pmc/articles/PMC6435275/ Fetched: 8/27/2020 6:08:00 PM	2
W	URL: https://www.researchgate.net/publication/285362424_The_Role_of_Diffusion-Weighted_ ... Fetched: 2/26/2020 10:29:23 AM	2
J	**Oncology Letters** URL: dc4866d2-8773-4b13-9ef9-e5649cb889e5 Fetched: 4/7/2019 10:56:17 AM	1
W	URL: https://www.ncbi.nlm.nih.gov/pmc/articles/PMC3593114/ Fetched: 8/27/2020 6:08:00 PM	1
W	URL: https://www.dovepress.com/predictive-values-of-diffusion-weighted-imaging-and-perf ... Fetched: 2/19/2020 11:31:23 AM	3